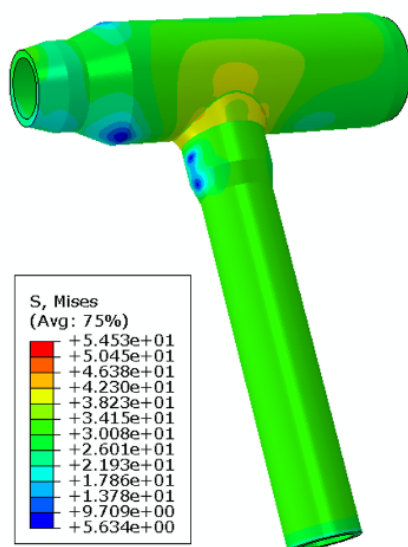


VERIFICATION OF CREEP ANALYSES OF A STEAM PIPE SYSTEM

REPORT 2019:636

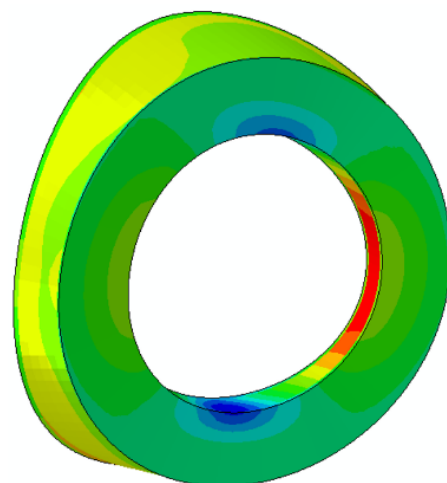


BRÄNSLEBASERAD EL-
OCH VÄRMEPRODUKTION



S, Mises
(Avg: 75%)

+	5.453e+01
+	5.045e+01
+	4.638e+01
+	4.230e+01
+	3.823e+01
+	3.415e+01
+	3.008e+01
+	2.601e+01
+	2.193e+01
+	1.786e+01
+	1.378e+01
+	9.709e+00
+	5.634e+00



Verification of Creep Analyses of a Steam Pipe System

DANIEL ANDERSON, JAN STORESUND, HENRIK C.M. ANDERSSON-ÖSTLING, FRANS SORSH

ISBN 978-91-7673-636-4 | © Energiforsk January 2020

Energiforsk AB | Phone: 08-677 25 30 | E-mail: kontakt@energiforsk.se | www.energiforsk.se

Foreword

Denna rapport är slutrapportering av projekt M 39205–2 Verifiering av krypanalyser av ett ångledningssystem (Energimyndighetens projektnummer P 39205–2) inom SEBRA, samverkansprogrammet för bränslebaserad el- och värmeproduktion.

Programmets övergripande mål är att bidra till långsiktig utveckling av effektiva miljövänliga energisystemlösningar. Syftet är att medverka till framtagning av flexibla bränslebaserade anläggningar som kan anpassas till framtida behov och krav. Programmet är indelat i fyra teknikområden: anläggnings- och förbränningsteknik, processtyrning, material- och kemiteknik samt systemteknik. Programmet är en samverkan mellan Energiforsk och Energimyndigheten. Ingående projekt finansieras alltså av Energimyndigheten och av de parter som Energiforsk samlar i programmet.

Detta projekt är en fortsättning på två tidigare projekt och har utförts för att förbättra och verifiera metoder för att prediktera kryplivslängd hos ångledningssystem.

Projektet har genomförts av KIWA Inspecta AB med Jan Storesund som huvudprojektledare. Projektet har följts av en referensgrupp bestående av:

Rikard Norling, RISE KIMAB
Tommy Larsson, E.ON,
Per-Åke Binett, Iggesund Bruk, Holmen

Stockholm december 2019

Helena Sellerholm
Områdesansvarig
Termisk energiomvandling, Energiforsk AB

These are the results and conclusions of a project, which is part of a research programme run by Energiforsk. The author/authors are responsible for the content.

Sammanfattning

Ångledningssystem hos kraftvärmeverk har drifttemperaturer där krypning är dimensionerande. Det innebär en tidsberoende deformation. I samband med krypdeformationen utvecklas krypskador som med tiden leder till krypsprickor och haveri om inte kritiska komponenter tas ur drift i tid. Detta sker i regel inom lokala områden av rörledningssystemen, vanligen i svetsar med förhöjda spänningar. Utöver det inre övertrycket beror det på effekter av systemspänningar på grund av den termiska expansionen, egenvikt hos formstycken samt spänningskoncentrationer pga. geometriska faktorer. Erfarenhetsmässigt är det välkänt att knutpunkter i systemen, t.ex. T-stycken, stutsanslutningar, in- och utlopp är känsliga för spänningskoncentrationer pga. systemspänningar och komponentgeometrier. Kryplivslängden kan därför vara förbrukad långt innan designlivslängden (typiskt 100 000 eller 200 000 timmar) vid de kritiska positionerna medan de delar av ångledningen som inte har förhöjda spänningar kan ha betydligt längre livslängd än den dimensionerade.

Elastiska expansionsanalyser av rörsystem används frekvent för tillsyn av spänningsfördelningen och om de finns högre spänningar än tillåtet. Sådana analyser tar dock inte hänsyn till spänningsrelaxation genom krypning, kryptöjning samt töjningsomlagringar. De är därför inte lämpade för analys och bedömning med avseende på krypning och kryplivslängd. Den elastiska analysen kan indikera kritiska positioner för replikprovning* vid drift strax under gränstemperaturen för krypdimensionering (där krypskada och krypsprickor ändå kan förekomma efter lång tids drift) men det kan ifrågasättas om så är fallet vid drift i kryptområdet.

För 15-20 år sedan utvecklades metoder för analys av rörsystem som tar hänsyn till spänningsrelaxation och – omlagringar pga. krypning [3]. Sådana analyser krävde vid den tiden relativt stor datorkraft och de har därför haft mycket begränsad användning sedan dess. Idag är datorkapaciteten avsevärt större och analyser med avseende på krypning kan utföras relativt enkelt. De tidigaste metoderna vidareutvecklades inom Energiforsksprojekten M12-218 och M3905 [1] där bl.a. följande utfördes:

- Koppling av systemanalyser till spänningsanalys av individuella formstycken med detaljerad spänningsfördelning på komponentnivå som även inkluderar effekten av systemspänningar.
- Modellering av rörsystem för krypanalys måste också bli effektivare så att det kan göras tillräckligt snabbt och bli kostnadseffektivt.
- Framtagning av krypdata i svetsar, där kryphållfastheten är reducerad, inklusive värmepåverkade zoner genom miniatyr provning med metoden "Impression Creep (IC)".
- Svetsar inkluderade i modeller av formstycken som analyserades med resultaten från IC provningen. Det har möjliggjort beräkning av återstående livslängd i detalj och identifikation av kritiska positioner för replikprovning.

Föreliggande projektet är en fortsättning av Energiforsksprojekt M12-218 "Livslängdsbedömning av ångledningssystem genom provning och analys" samt det därtill hörande tilläggprojektet M39205. Det fortsatta arbetet går ut på att verifiera provnings- och analysresultaten genom jämförelser med hur krypskador fördelat sig i komponenter som tagits ut från det analyserade systemet. För detta modelleras och analyseras hela ångsystemet i Heleneholmsverket. Till skillnad från [1], där t-stycket modellerades separat med överlagrade systemspänningar inkluderade och bara en del av systemet modellerades, integreras t-stycket i systemmodellen som omfattar hela ångnätet. Det möjliggör en korrekt analys av systemspänningar hos det t-stycke som studerades i [1]. En ytterligare omhändertagen svets verifieras genom i) krypprovning för att generera krypdata, ii) metallografisk kartläggning av krypskador samt ii) modellering av svetsen i syfte att erhålla spännings- och töjningsfördelningar som motsvarar krypskadefördelningen. I M12-218 ingick endast sekundärkryp i modelleringen. Primärkryp implementeras nu i simuleringen av kryprelaxation eftersom det nyligen har visats att detta är nödvändigt för att erhålla fullgod överensstämmelse mellan simulering och verklig kryprelaxation vid kryprelaxationsprovning [3]. Därtill utförs en känslighetsanalys av elastiska parametrar.

Syftet med ovanstående projektaktiviteter är att göra metoden fullt användningsbar. Nedan följer en mer detaljerad beskrivning av de olika projektmomenten:

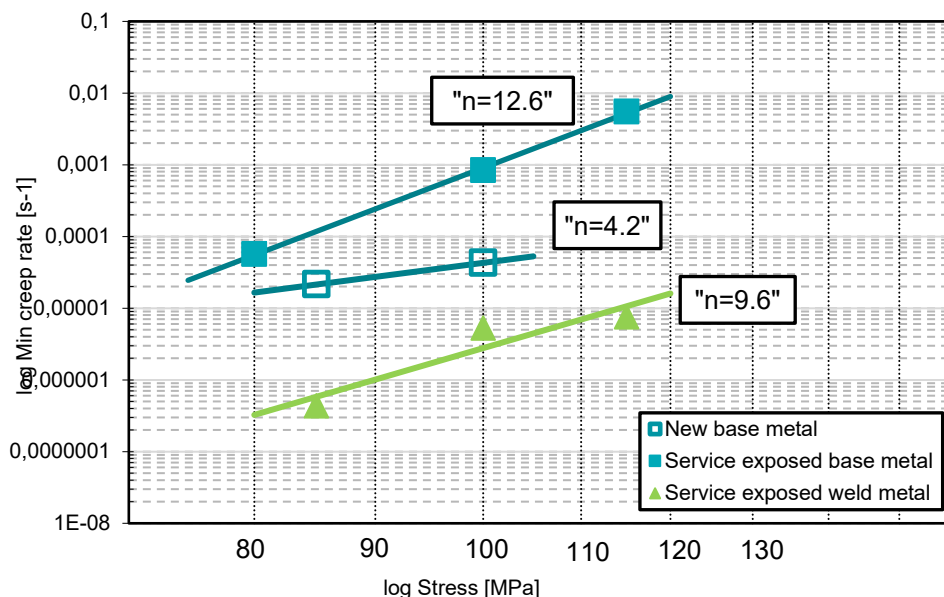
- Modellering och analys av hela ångledningssystemet i Heleneholmsverket. I M12-218 modellerades endast en del av systemet i syfte att kunna verifiera ett script som översätter en Caepipe modell till Abaqus där motsvarande del hade modellerats i Abaqus i ett tidigare projekt (Värmeforskrapport 629). Inspecta 2016-2017.
- Inkludera primärkryp vid kryprelaxation i systemanalyserna och jämföra med tidigare resultat.
- Krypprovning av en rundsvets för att ta fram krypdata för en originaldel av systemet från 1966. Provningen omfattar två serier: grundmaterial och svetsgods och utförs i syfte att ta fram krypdata till simuleringarna. I varje serie utförs provning vid 4 spänningsnivåer och med provtider i spannet 100-10 000 timmar. Provningen avses pågå tills dess att sekundärkrypstadiet har infunnit sig, dvs. kryptöjningshastigheten är konstant. Dessutom utförs kompletterande krypprovning vid de längsta provtiderna på motsvarande sätt av det nya material som provades i [1].
- Kartläggning av krypskador hos krypprovat material, både före och efter krypprovning.
- Kartläggning av krypskador hos två svetsar från Heleneholmsverket i rördelar som har varit i drift sedan 1966.
- Modellering och analys av den rundsvets som har krypprovas. Svetsen integreras i systemmodellen. Tidigare resultat visar ca 0,3 % global kryptöjning vid svetsen. Med kryppmodellen ska det verifieras att det lokalt har uppstått förhöjda töjningar.
- Det T-stycke som modellerades i [1] integreras i den utökade system modellen i syfte att få en fullgod verifikation av observerade krypskador.

- Känslighetsstudier – inverkan elastiska parametrar på resultaten av systemanalyserna studeras i syfte att få kunskap om vilka krav på noggrannhetskrav man måste ställa på indata till modelleringen.

Resultat

Krypprovning

Krypprovningen genomfördes med tider upp till 20 000 timmar och vid spänningar ned till 80 MPa. Resultaten för de tre serierna nytt grundmaterial av 10CrMo9-10, grundmaterial samt svetsgods intill respektive från svets MR15 med 180 000 timmars drift ges i figur S1.



Figur S1. Spänning som funktion av minimum kryphastighet för provserierna.

I figuren plottas spänning mot minsta kryphastighet, där ett linjärt förhållande förväntas i ett log-log diagram. Lutningen utgör exponenten n i Nortons kryplag:

$$\frac{d\varepsilon}{dt} = B\sigma^n$$

I det driftpåkända svetsgodset fanns krypkaviteter som hade bildats innan provningen. Efter provningen observerades ingen utveckling av krypskadorna.

Kartläggning av krypskador hos krypprovd svets

Svets MR15 kartlades även med avseende på kavitetsutveckling på ytan och på tvärsnitt vid positionerna kl. 3, kl. 6, kl. 9 och kl. 12. Krypskadorna klassificerades enligt [5] och resultaten ges i tabell S1 och S2.

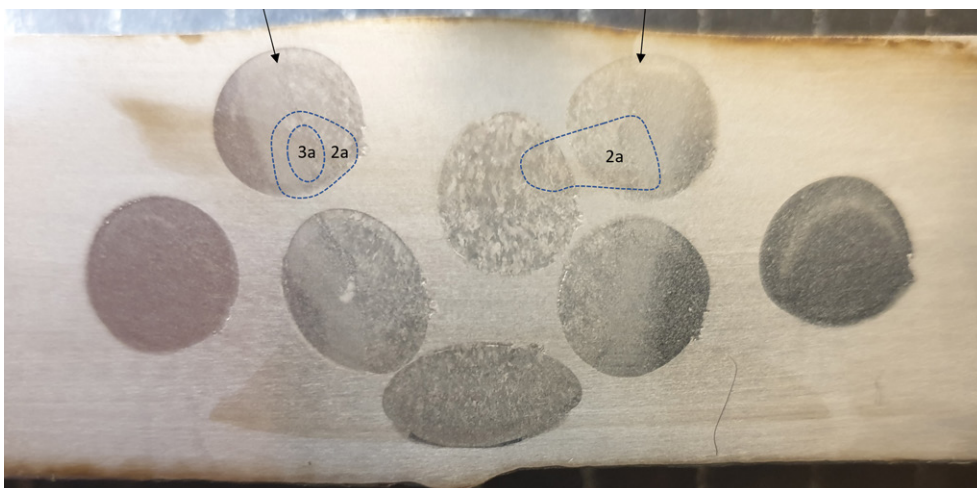
Tabell S1 Svets MR-15 krypskadeklasser för undersökta yttertor.

MR15 - Yta	Kommentar					Kommentar
Position	1	2	3	4	5	
kl.3	1*	2a	1*	1*	1*	*Kaviteter <100/mm ²
kl.6	1*	3a	3a	2a	1*	
kl.9	2a	2a	1	2a	1*	
kl.12	1	2a	1	2a	1	

Table 5 Svets MR-15 krypskadeklasser för undersökta tvärsnitt

MR15 tvärsnitt	Kommentar					Kommentar
Position	1	2	3	4	5	
kl.3	1	1*	1*	2a	1	* Kaviteter <100/mm ²
kl.6	1*	3a	2a	2a	1*	
kl.9	1	2a	2a	2a	1	
kl.12	1	2a	3a	2a	1	

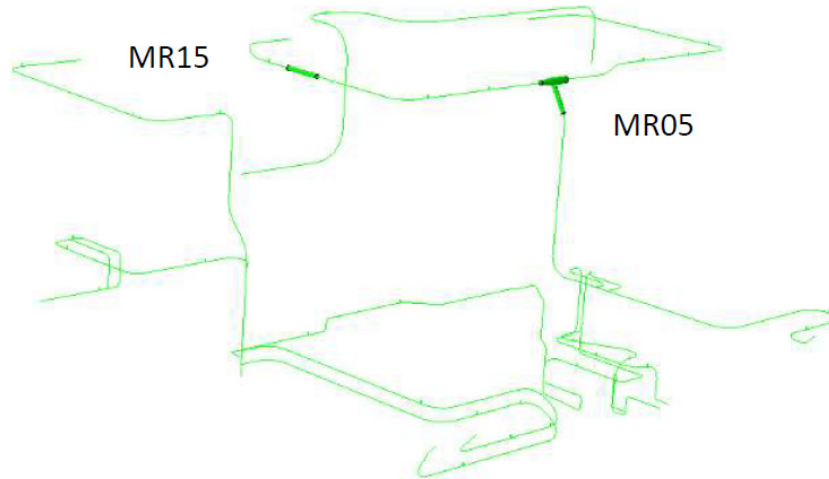
I tvärsnitten fanns det förhöjda krypskador i HAZ och i svetsgods intill HAZ en bit nedanför ytterytan. Dessa skador i något fall högre nedanför ytan. Generellt motsvarades krypskadornas omfattning på ytan med vad som observerades i tvärsnitten. Figur S2 visar krypskadefördelningen vid position kl. 6.



Figur S2. Fördelning av krypskadeklasser hos tvärsnitt av MR15 vid kl. 6.

Numerisk analys

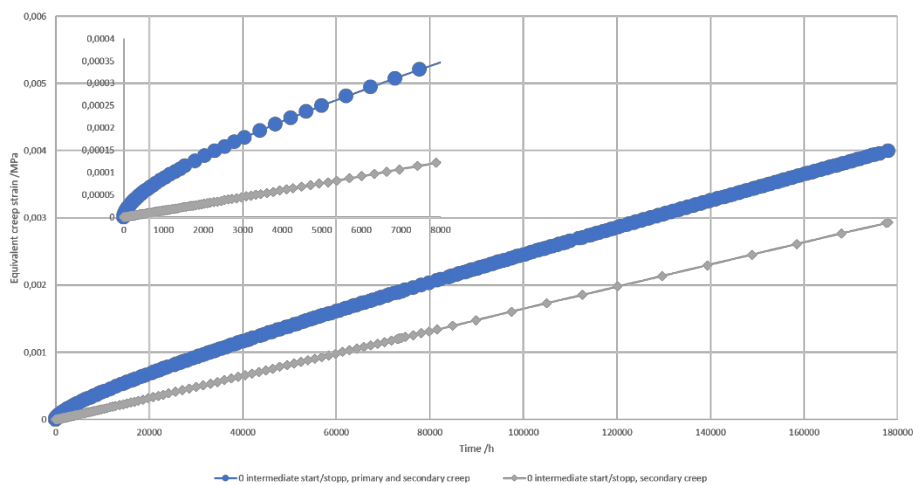
Den resulterande Abaqus-modellen med det analyserade t-stycket och dess stutssvets (MR05) och analyserad rörsvetsen (MR15) integrerade ges i figur S3.



Figur S3. Modell av ångnätet i Heleneholmsverket med studerade komponenter med svetsar M05 och M015 integrerade i modellen.

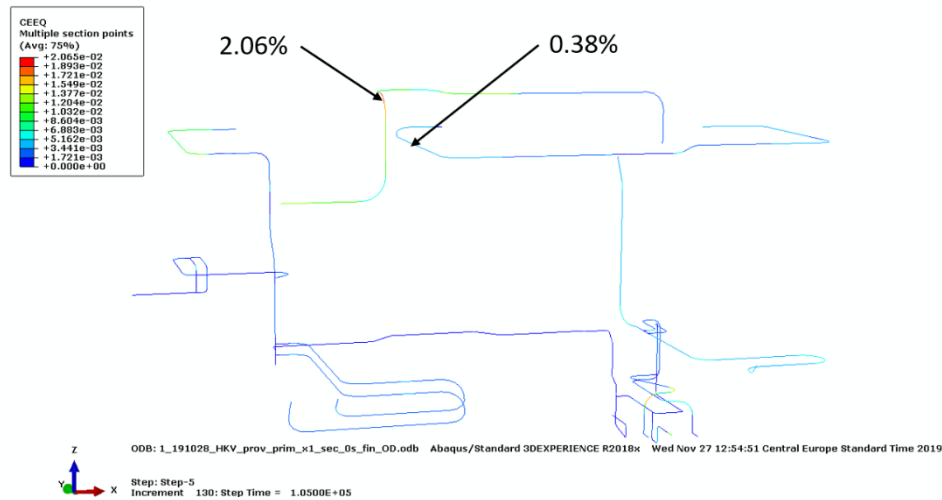
Från kryptöjningskurvorna av nytt grundmaterial beräknades materialkonstanter för en modell för primärkryp som Abaqus använder. Materialkonstanter för sekundärkryp beräknades från data för material 10CrMo9-10 i EN10028-2, krypprovat nytt och driftpåkänt material (grundmaterial och svetsgods). Även simuleringar med materialdata från krypprovning av t-styckets stutssvets från [1] genomfördes.

Resultaten visar att det finns en effekt av primärkryp särskilt i början av krypförloppet som med tiden vidmakthålls, se figur S4. Starter och stopp simulerades också och resultaten pekar på att de inte har inverkan på fördelning och nivå av spänningar och töjningar i systemet.



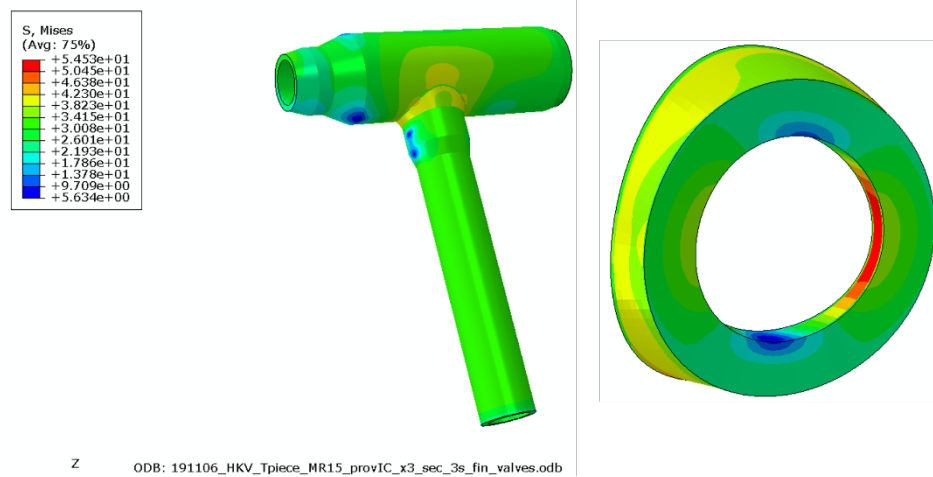
Figur S4. Utvärdering av von Mises spänning vid analyserad rörsvets MR15 med primär och sekundärkryp samt med endast sekundärkryp.

Töjningsfördelningen i systemet som sin helhet visar förhöjda töjningar på 0,5 - 1,0 % i delar av systemet och som högst 2,06 % i en av böjarna, se figur S5. Töjnings-nivån vid svets MR15 är 0,38 %.

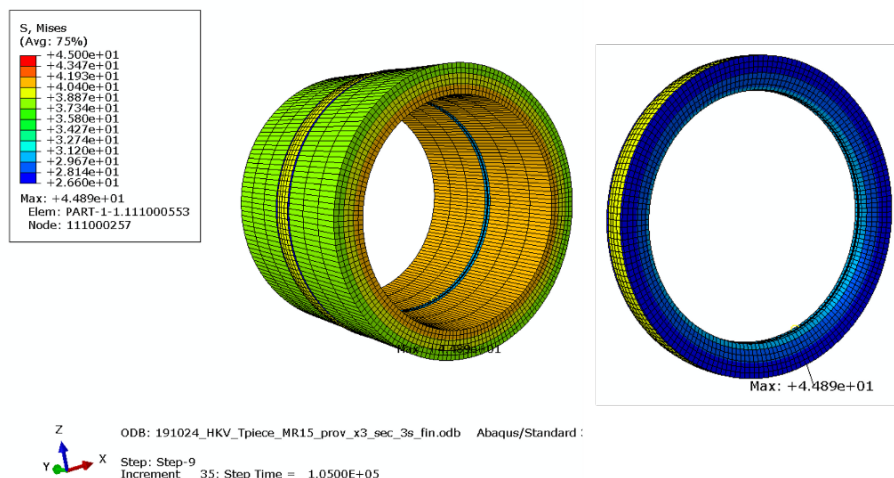


Figur S5. Fördelning av ekvivalent kryptöjning efter 180 000 timmar där både primär- och sekundärkryp är med i beräkningen.

Spännings- och töjningsfördelningarna i stutssvets M05 och rundsvets MR15 analyserades, se figur S6 respektive S7.



Figur S6. Von Mises spänningsfördelning hos MR05 efter 73 000 timmar med krypdata från krypprovning av svetsen i fråga [1].



Figur S7. Von Mises spänningsfördelning hos MR05 efter 180 000 timmar med krypdata från krypprovning av nytt material av 10CrMo9-10

Spännings- och töjningsfördelningarna för M05 stämmer väl överens med fördelningen av krypskador som undersöktes i [1]. För rundsvetsen MR15 visar resultaten högst spänningar och töjningar på insidan. Det motsvarar inte observerad krypskadefördelning.

Tabell S1 visar beräknade töjningar för olika klockpositioner runt svets M05. Olika kombinationer av krypdata har använts i analyserna där resultat från indentorkrypprovning (IC test) av MR05 från [1] har använts. HAZ med 3x grundmaterialets kryphastighet var ett resultat från denna provning medan HAZ med 6x grundmaterialets kryphastighet togs med för att studera effekten av en dubbelt så hög kryphastighet i HAZ. Dessutom genomfördes analyser med tabellerade krypdata (EN10028-2) samt provresultat av nytt grundmaterial där effekterna av kryphastighet i HAZ och inkluderat primärkryp har tagits med.

Det är små skillnader mellan tabellerade krypsdata och provresultat av nytt material. Effekten av fördubblad kryphastighet i HAZ är relativt liten, det samma gäller då primärkryp tas med. Data för IC test av driftpåkänt material gav i storleksordningen dubbelt stora töjningar jämfört med nytt. Överlag är det relativt låga nivåer på kryptöjningarna i förhållande till observerade krypskador, klass 3b.

Tabell S1. Beräknad max kryptöjning vid olika klockpositioner för M05 med olika uppsättningar av materialdata.

Material data	12 o'clock	3 o'clock	6 o'clock	9 o'clock
IC test HAZ-x3	0,34%	0.25%	0.59%	0.18%
IC test HAZ-x6	0.40%	0.30%	0.71%	0.24%
EN10028-2 HAZ-x3	0.17%	0.10%	0.24%	0.08%
Nytt grundmaterial HAZ-x3	0.18%	0.17%	0.30%	0.08%
Nytt grundmaterial HAZ-x6	0.20%	0.19%	0.34%	0.12%
Nytt grundmaterial HAZ-x6 primärkryp	0.19%	0.20%	0.39%	0.13%

Tabell S2 visar beräknade töjningar för olika klockpositioner runt svets M15. Här har krypdata för krypprovt driftpåkänt material från svetsen, tabellerade data och krypprovt nytt material samt effekten av kryphastighet i HAZ och inkluderat primärkryp analyserats.

Resultaten visar väsentligt lägre kryptöjningar för data från provat driftpåkänt material jämfört med provat nytt och tabellerade data. Skadefördelningen runt svetsen är jämn, vilket med observerade krypskador. Töjningsnivåerna är förefaller vara förhållandevis låga med tanke på att krypskador, om än i måttliga nivåer, observerades. Effekterna av fördubblad kryphastighet i HAZ samt att primärkryp inkluderas är små även här.

Tabell S2. Beräknad max kryptöjning vid olika klockpositioner för M15 med olika uppsättningar av materialdata.

Material data	12 o'clock	3 o'clock	6 o'clock	9 o'clock
Driftpåkänt material, HAZ-x6	0.015%	0.014%	0.014%	0.014%
EN10028-2 HAZ-x3	0.17%	0.17%	0.18%	0.18%
Nytt grundmaterial HAZ-x3	0.26%	0.24%	0.23%	0.24%
Nytt grundmaterial HAZ-x6	0.29%	0.25%	0.24%	0.25%
Nytt grundmaterial HAZ-x6 primärkryp	0.31%	0.26%	0.24%	0.26%

Diskussion

Abaqus använder von Mises spänning som kriterium för krypberäkningar. Ser man till maximum huvudspänning finns de största spänningarna i svetsgods i den övre delen av svetsen, vilket stämmer väl överens med observerade krypskador. Töjningsberäkningen tar även hänsyn till maximum huvudspänning men eftersom de högsta töjningarna uppträder vid insidan av svetsen är det tydligt att von Mises dominerar. Det är därför angeläget för fortsatt forskning att ta fram underlag för att kunna bestämma och implementera en riktig balans mellan spänningskriterierna för olika geometrier och material.

Anledningen till att driftpåkänt material ger lägre kryptöjningar än nytt i analysen är de höga värdena på Nortonexponenten, n , som erhöles, se figur S1. En knäck på kurvan till lägre n är förväntat med inträffade inte för de driftpåkända materialen trots så låga provspänningar som det praktiskt är möjligt.

Slutsatser

Hela ångledningssystemet i Heleneholmsverket skapades genom modellering i Abaqus och töjningsfördelningen i systemet verifierades med en motsvarande elastisk Caepipe-modell. Nortons kryplag användes vid simuleringarna. Dessutom analyserades primärkryp.

- Effekten av primärkryp på långtidskrypförlopp var signifikant och resultaten visar tydligt på vikten av att inkludera primärkryp i beräkningsmodellen.
- Det finns ingen inverkan av starter och stopp på spännings- och töjningsfördelningen hos systemet under krypning.
- Resultaten av systemanalysen visade förhöjda töjningar upp till 2,1 % i en böj och 0,5 % - 1,0 % i vissa delar av systemet. Fastän replikprovning inte har utförts direkt på böjen, överensstämmer de höga töjningarna så till vida att små krypsprickor har observerats intill böjen. Flera komponenter i systemet har också bytts ut på grund av bildning av krypsprickor.
- Moderata nivåer av krypskador observerades i rörsvetsen. Analysen av gav lägre kryptöjningar än förväntat. Spännings- och töjningsfördelningen överensstämde med högsta huvudspänningen men inte för von Misesspänningen, som Abaqus använder för krypanalyser.
- Analysen av stutssvetsen överensstämde med observerad krypskadefördelning medan den högsta töjningsnivån på 0,71 % förefaller vara låg i förhållande till de omfattande krypskadorna. Lokala inspänningseffekter och fleraxlighet i svetsar leder dock till betydligt lägre krypduktilitet jämfört med enaxlig krypprovning (som skadorna ofta jämförs med). Det gör att överensstämmelsen mellan beräknade töjningar och observerade krypskador blir rimlig.
- Krypprovningen av driftpåkänt material resulterade i relativt hög Norton exponents och ingen knäck på kurvan till lägre värden vid de lägre provspänningarna som förväntat. Det är knappast möjlig att utföra krypprovning vid ännu lägre spänningar och därför resulterade simuleringar vid driftförhållanden i orimligt låga kryptöjningar.

Summary

The project is a continuation of work with creep simulations of the steam pipe system in Heleneholmsverket [1,2,3] in combination of i) creep testing of new and service exposed materials from welded components and ii) characterisation of the creep damage distribution in creep tested welds of the actual piping. The entire system has now been modelled for creep evaluation to make it possible to compare the simulated creep stress and strain distributions with observed amounts of creep cavitation that correlate to the strain development. Creep data for the analyses were produced by creep testing of service exposed base and weld metals from a pipe weld from the system. In addition, the creep tested weld was studied metallographically in purpose to map the creep damage and make it possible to compare the damage development with the resulting creep stress and strain distributions in the weld. In the previous project also a t-piece branch weld was investigated in a similar way and those results were used for verification of the re-analyses in present project with the updated system model. The model of the entire steam pipe system was created in Abaqus and the strain distributions were verified in comparison to a corresponding elastic Caepipe model. The Norton creep law was used for the simulations. In addition, also primary creep was analysed. The following results were achieved:

- The effects of primary creep on the long-term creep behaviour was significant and the results shows the importance of including primary creep in to the model.
- There is no effect of starts and stops on the stress and strain distributions in the system during creep.
- The system analysis results showed enhanced strains up to 2,1 % at one bend and 0,5 % - 1,0 % in some parts of the system. Although replica testing had not been conducted directly at the bend the high strains indirectly agreed with the observations of small creep cracks had been observed in replica testing of in a weld at one of the ends of the actual bend. Furthermore, several components in the system has been exchanged due to creep crack formation.
- Moderate levels creep damage was observed in the pipe weld. The analysis of this pipe weld gave somewhat lower creep strains than expected. The stress and strain distributions agreed for the maximum principal stress criterion but not for the von Mises stress that Abaqus uses for creep analyses by default.
- The analysis of the branch weld agreed well with observed creep damage distributions whereas the maximum strain level of 0,73 % appears to be rather low in comparison to the quite extensive creep damage. However, local constraint and multiaxiality in welds lead to significantly lower creep ductility compared to uniaxial creep and contribute to a reasonable agreement between the strain and the damage levels.
- The creep tests of service exposed material resulted in relatively high Norton creep law exponents and no shift to lower values at the lowest tested stresses. It is hardly possible to perform tests at even lower stresses and therefore the simulations at service conditions resulted in unreasonably low creep strains.

List of content

1	Introduction	16
2	Realisation of the project	19
3	Creep testing	22
3.1	introduction	22
3.2	Material	22
3.3	experimental	24
3.4	results	24
3.4.1	Creep testing	24
4	Metallography of the creep tested material	30
5	Creep damage in analysed welds	31
5.1	Replica test history and service parameters	31
5.2	Characterization of creep damage in weld MR15	33
6	Standard for design and analysis of piping systems	38
6.1	SS-EN 13480-3	38
7	Numerical analysis in Abaqus and analysed cases	39
7.1	Model of the steam pipe system	39
7.2	Models of weld M15 and M05	41
7.3	Analysed cases	43
8	Creep models and creep constants evaluated from creep test and tabled data	44
9	Analysis results	47
9.1	System analyses	47
9.1.1	Abaqus system model	47
9.1.2	Verification of the Abaqus system model	48
9.1.3	System secondary creep strain distribution	51
9.1.4	Effects of primary creep and stress relaxation	52
9.1.5	Effects of starts and stops	56
9.2	Analyses of weld MR05	58
9.3	Analyses of weld MR15	61
10	Discussion	66
10.1	Creep tests	66
10.2	observed creep damage	67
10.3	Creep analysis	67
10.3.1	System analysis	68
10.3.2	Analysis of weld MR05	69
10.3.3	Analysis of weld MR15	69
11	Practical Implementations, recommendations and further work	71
12	Conclusions	72

13	References	73
14	Appendix 1 Micrographs of creep tested material	74

1 Introduction

Main steam pipe systems in conventional power plants as well as combined power and heating plants are typically operating at temperatures where the design criterion is creep. Creep is a time dependent deformation mechanism and therefore, design for creep involves a design life time. The design life is typically 100 000 hours for steam piping built before the 1980's and thereafter 200 000 hours.

The criterion for creep design of steam piping is creep rupture. Creep rupture involves a considerable amount of creep deformation. However, a safety factor of 1.25 and 1.5 on the rupture stress is applied for 200 000- and 100 000-hours design, respectively. The stress dependence on creep life is strong with a power of 3 – 7 at conventional creep design data. This means that the life time for a straight pipe that is fully utilized and built of an average material would be much longer than the design life, typically 400 000 hours or longer. This applies for both 100 000- and 200 000-hours design because of the difference in safety factor.

The safety factor is primarily considered to take account for possible reduction in creep strength in comparison to the average material, which the design stresses are based on. The lower bound in the creep strength scatter for creep resistant steels is typically 20 % lower in rupture stress compared to the average material. Then, there are other factors in a pipe system that may reduce the life time: system stresses, reduced creep strength in welds, stress concentrations in components with complex geometries that are not caught by the design rules, etc. Hence, it is not possible to know the status with respect to consumed creep life in any detail after long-term operation without inspection and monitor of the system.

Many plants operating in the creep range were built in 1960-90's and in most cases the design life started to be reached 15-20 years later. A long time before creep cracks appear there are changes in the material microstructure. For example, the formation of creep cavities, that can be used as a measure of on-going creep deformation. Over time more cavities are formed, they start to orient perpendicular to the principal stress direction, develop to micro-cracks and to finally macro-cracks. By taking replicas on metallographically prepared surfaces at critical positions this damage development can be monitored, proper re-inspection intervals can be set, and components can be exchanged in a safe and controlled way at planned outages.

One problem with replica testing is to find out where the critical positions are. Creep damage and creep cracks typically appear locally where the stresses, and thereby the accumulated creep strains, are enhanced. Up to date, test positions are often selected by experience. However, if not all possible critical components can be included in a testing program, it is often impossible to be sure of that the representative ones are selected only by experience.

Elastic pipe stress analyses are performed on new pipe systems by routine within the design review to check that the stresses due to thermal expansion and dead weight in addition to the internal pressure do not exceed allowed values. After long term operation it is crucial to update the in-data to such analyses since hanger

and support adjustments changes. It is also common that reconstructions of the pipe system are performed during its lifetime. Reconstructions will in most cases change the boundary conditions for the remaining part of the system, too. Therefore, updates of the analysis are needed in accordance with results of inspections (walk downs) of the system hangers and supports (which should be performed at least once a year) and any reconstructions.

Elastic stress analyses can be used to pinpoint areas with enhanced stresses at the start of the operation, but the effect of creep relaxation is not considered. Stress redistribution due to creep relaxation changes the stress levels and may also change or introduce new positions that are critical with respect to creep damage development [1]. Thus, it is possible that the elastic analysis cannot fully determine critical positions for replica testing. The elastic analysis will over-estimate the stress levels at some positions and may under-estimate them at others and can therefore not be used for estimations of creep life.

By introduction of creep deformation in the analysis it would not only be possible to identify critical position. It would also be possible to calculate the creep strain as a function of time at such positions. This would give a straight forward measure of the consumed life time. The remaining life can be estimated with a high precision and the analysis can be verified by replica testing. Creep analyses of complex pipe systems require powerful hard and soft ware. Therefore, it is not until quite recently such analyses can be expected to be performed acceptably readily.

Based on these premises a Värmeforsk project M12-218 and an associated complementary Energiforsk project M392015 were carried out with the purpose develop *i)* analysis methods that can be used for creep life assessment in live steam pipe system components, *ii)* use newly developed methods for miniature creep testing of weld constituents and *iii)* use produced creep data in the analyses and compare with tabled creep data in EN 10028-2. These projects were reported in [1]. Important results were:

- Significant creep cavitation was observed in two butt welds and in a T-piece weld from the main steam pipe from the Helenholmsverket power plant. The damage in the T-piece can be considered as pre-mature.
- Impression creep testing was performed with a new approach on welds of new and service exposed material from the power plant. The HAZ of the investigated was scanned by testing each 0.5 mm from the parent metal, through the HAZ and into the weld metal. The maximum creep rate in the HAZ was in the intercritical part and was 2.6 times higher than in the parent metal.
- Impression creep testing of parent and weld metals with 73 000 hours service exposure showed 3- and 6-times higher creep rates, respectively, than for corresponding materials in a virgin weld.
- The impression creep test results of virgin parent metal showed very good correlation with uniaxial creep testing of the same material.
- The behaviour of the impression creep test was analysed by FEM and strain distributions were calculated.

- Creep analysis of the main steam pipe system showed that significant stress relaxation occurs after a relatively short service period. These effects cannot be covered by an elastic analysis, such as a Caepipe analysis.
- Creep analyses of a main steam pipe system including starts and stops resulted in higher levels of creep strain than without the starts and stops. In addition, the positions where the highest strains occurred were not the same.
- Creep analysis of the main steam piping was carried out with creep data from standards and from the impression creep test results. Creep test results of new material and standard data gives similar creep strains in the system, approximately 0.1 % after 178 000 hours. The same analysis but with use of creep tests results of service exposed material from the T-piece and with lower bound standard data resulted in 0.3 % creep strain.

The importance of the creep relaxation in the results initiated the Energiforsk project M 39197 where the effect of creep relaxation was studied in detail by both testing and modelling of the creep relaxation [2]. The following conclusions were drawn for the P22 material that is used in the studied main pipe system:

- The relaxation behaviour of P22 is independent on the initial plastic strain, since there is no significant hardening and softening effects.
- The Norton model is insufficient for simulating early stages of relaxation, since these include effect of primary creep.
- The combined time hardening model allows reasonably accurate modelling of the resulting stress during relaxation of material not previously exposed to stress relaxation.
- The combined time hardening model allows reasonably accurate modelling of the resulting stress during relaxation of P22 material even when exposed to previous stress relaxation cycles.

By these projects it was clear that continued research would be needed in order to be able to analyse creep in main steam pipe systems as an engineering tool. In order to reach this overall goal verifications of the analysis models by comparison with actual creep damage in welds are necessary. Complementary modelling, creep testing and metallographical examinations have thus to be carried out to complete the basis for such verifications.

2 Realisation of the project

The starting point of the present project as well as for the preceding projects [1] [2] is a model of the center part of the main steam pipe system at Eon Heleneholmsverket that was produced in a Värmeforsk project entitled “Influence of refurbishment of steam piping systems on the remaining life time” by Segle et. al. [3].

This model was produced in Abaqus software which is well suited for creep analysis. However, Abaqus is suited for modelling of components rather than pipe systems, which would take much too long time in practice. One task in [1] was then to produce a script, which in this case would be a program that is able to interpret an elastic model of a pipe system that has been produced in software specialized for pipe systems, and translate it in to a model in Abaqus. Such elastic software cannot handle creep, but a pipe system can be modeled very fast compared to Abaqus.

This was performed successfully. However, since the model of the piping system was not complete the results of a detailed analysis of a t-joint branch weld were not fully satisfactory. The probable reason for this is that the t-joint was placed close to one of the ends of the model, modelled as a fix point. The piping has a long continuation from where the model ends, and it is obvious that a model of the entire system is necessary in order to be able to verify the analyses by observed distribution of creep damage at selected critical positions. Thus, one task in the present project is to create an Abaqus model of the entire steam pipe system or Heleneholmsverket.

Another improvement of the modelling work would be to integrate welded components to the system model instead of, as in the previous projects, model welded components separately and superimpose displacements from the system thermal loads to the component model loaded with internal pressure and dead weight. In the present project the t-joint branch weld that was studied previously was integrated to the pipe system. In addition, a butt weld in an original part of the system from 1966 was modeled. This weld was cut out and the creep damage was characterized at the surface previously. In the present project cross-sections of the weld were cut and the creep damages were mapped also through the wall thickness.

The third task of the present project is to add primary creep to the secondary creep in the creep model. Primary creep was demonstrated to have a crucial role to describe creep relaxation correctly in 10CrMo9-10 steels [2] and the importance of creep relaxation for the creep stress levels and the stress distributions was pinpointed in [1].

The creep testing in [2] was focused on producing creep data for the t-joint branch weld including the HAZ and the weld metal. The testing of the HAZ with an impression creep testing was innovative and gave very interesting results, where e.g. the HAZ creep rate was approximately 3 times higher than the weld metal whereas the weld metal creep rate was 2 times higher. However, the testing was

accelerated to an extent that was not possible to extrapolate to service conditions and the analyses were performed basically by use of tabled design data for 10CrMo9-10.

Since steam pipes likely consist of material from different batches it is important to keep in mind that the creep properties may differ to a certain extent from one batch to another. In the present project creep data of material from the actual steam pipes and welds were produced by creep testing. In order to make the acceleration of the creep testing and thus the extrapolation of the results as little as possible the following creep test parameters were decided:

- Testing at service temperature
- Test series with lower stresses than usual, involving testing only to the entrance of the secondary creep regions for the lower stresses in each test series.
- Four different test series including parent metal and weld metal of new and service exposed material, respectively

In this way, analyses by use of i) tabled data, ii) virgin material data and iii) service exposed data can be compared to each other and compared to replica test results as a verification of the analyses.

The different parts of the project can be described as:

- Creep testing of a butt weld that has been cut from the original part of the main steam pipe at Helenholmsverket. The testing comprises test series of service exposed parent metal and service exposed weld metal of the retired butt weld. Each test is run until the secondary creep stage is reached at 3-4 different stress levels. Testing times in the interval 100-10 000 hours were planned for each series. In addition, two tests of new parent metal are performed in the same way. These tests will be conducted at lower stresses than the test series of new parent metal in [2] and will thus complete the test series of new parent metal with long term testing that is possible to extrapolate to service conditions.
- Mapping of creep damage in the creep tested material, both before and after the creep test.
- Mapping of the through thickness creep damage in the butt weld of the original part of the steam line that also will be creep tested and creep analysed. Four sections at the 3, 6, 9 and 12 o'clock positions are investigated.
- Modelling of the entire steam pipe system at Helenholmsverket.
- Model and include primary creep in the creep analyses.
- Modelling of the examined and creep tested butt weld integrated into the pipe system model. The weld model for creep analysis includes parent metal, HAZ and weld metal.
- Integrate the model of the t-joint, analysed in [2], into the pipe system model.
- Creep analyses of the pipe system, t-joint and butt weld by use of produced creep data and tabled data.
- Comparisons between different types of creep data.

- Sensitivity studies of the influence of elastic parameters on the results – this will result in knowledge of necessary accuracy requirements on input data in the modelling.

3 Creep testing

3.1 INTRODUCTION

Steam pipe systems in power plants run at temperatures where creep deformation is the dimensioning property. Creep is a time and temperature dependant deformation. As the creep progresses creep damage will accumulate, and failure will occur if the component is not taken out of service. The most likely areas of creep damage are at geometrical stress concentrations and in welds. In addition to this the load from the internal pressure, system loads such as the weight of the pipe system and thermal loads yield stress concentrations. At these sites the design life of the component can be seriously underestimated.

Elastic expansion models of the pipe system are commonly used to monitor where stress concentrations occur. Those models are not adjusted for the stress relaxations and stress redistributions that creep deformation cause. They are therefore not suited to analysis and assessment of creep damage. The elastic model can show critical areas where inspection is warranted.

10 to 15 years ago methods that consider stress relaxation and creep induced stress redistribution was developed. At the time the computing power needed was great and the use of the models hence limited. Today, computing power has reached the level where these models can be used without problems in short timeframes.

The present project aims at verifying the calculated creep damage with the results from calculations of the extent of damage.

3.2 MATERIAL

A weld supplied for the testing. The weld had previously been replica inspected at the cardinal points and the creep damage assessed. The weld was cut to leave slices at position 3, 6, 9 and 12, Figure 1. These slices were metallographically tested elsewhere in the project. Specimen blanks were then spark eroded into the weld metal in a tangential position. The base metal specimens came from a part of the supplied weld but were spark machined well away from the weld itself (service exposed base metal). New base metal came from a separated piece. Base metal specimens were taken in the axial direction of the tube.

To allow for inspection of the state of creep damage in the weld specimens before testing a special geometry was used in the spark erosion process, Figure 2. Along the round specimen blank a rectangular piece was cut. This was used for metallographic studies of the creep damage in the weld before testing.



Figure 1. The material received for the testing. In the foreground is the weld, cut up for specimen manufacture. In the back is the material used for new base metal. The material for service exposed base metal came from the rightmost piece, upper part (between clock position 9 and 12).



Figure 2. The special geometry used for the weld metal service exposed specimens. Alongside the sound blank a rectangular piece was cut. This was later polished and studied metallographically to assess the creep damage before testing in the specimen gauge.

3.3 EXPERIMENTAL

Creep testing was conducted in an active creep test rig where the load is measured continuously by a load cell and fed back to the step motor controlling the load. This setup can conduct testing at an accuracy of ± 3 N. The testing was performed according to SS-EN ISO 204:2018 [4]. Temperature was measured using three type S thermocouples along the gauge length of the specimen. The middle thermocouple was used to control the furnace and the two outer ones were used to keep the axial thermal gradient less than ± 1 °C.

The specimens were named as they were started (Insp-01 to Insp-05). The weld specimens were named after the clock position they were taken from. Thus Insp-1-3 was taken from the material between clock position 1 and 3, and Insp-5-3 between clock positions 5 and 3. Insp 10-2 was taken from the material between clock positions 10 and 12.

3.4 RESULTS

3.4.1 Creep testing

The results from the creep testing are given in Table 1. The same information is given in graphical form in Figure 3 and Figure 4. At the end of the project only two specimens had ruptured, but the other six specimens were judged to be close to the minimum creep rate and were thus interrupted.

The Norton exponent, n , in Eq. 1 has been calculated for all three material conditions. The results have been included in Figure 5 and Table 1. The creep curves for all specimens are given in Figure 6 to Figure 8.

$$\frac{d\varepsilon}{dt} = B\sigma^n \quad (1)$$

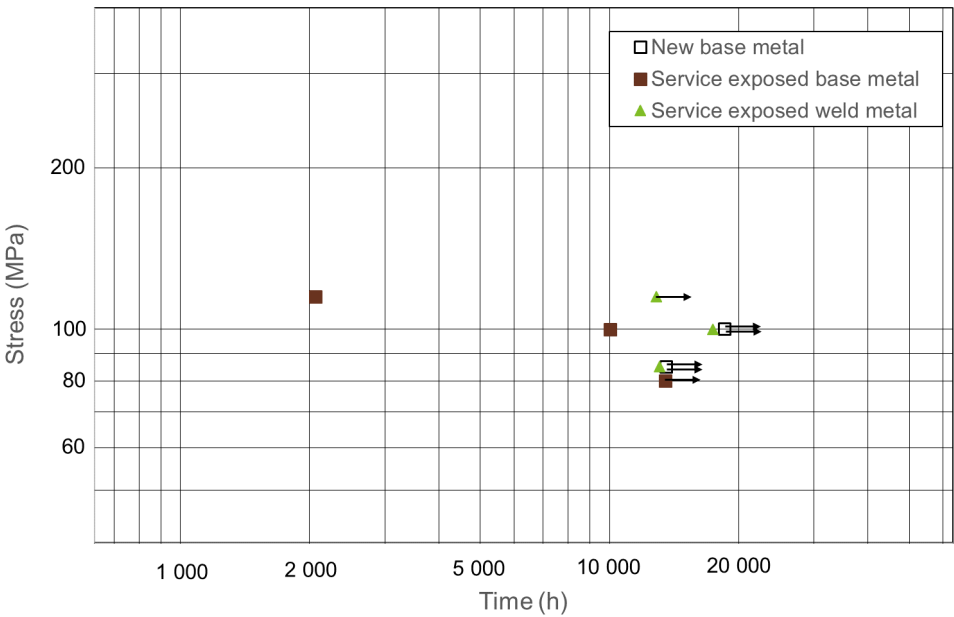


Figure 3. Time to rupture given against applied stress. Arrows denote interrupted specimens.

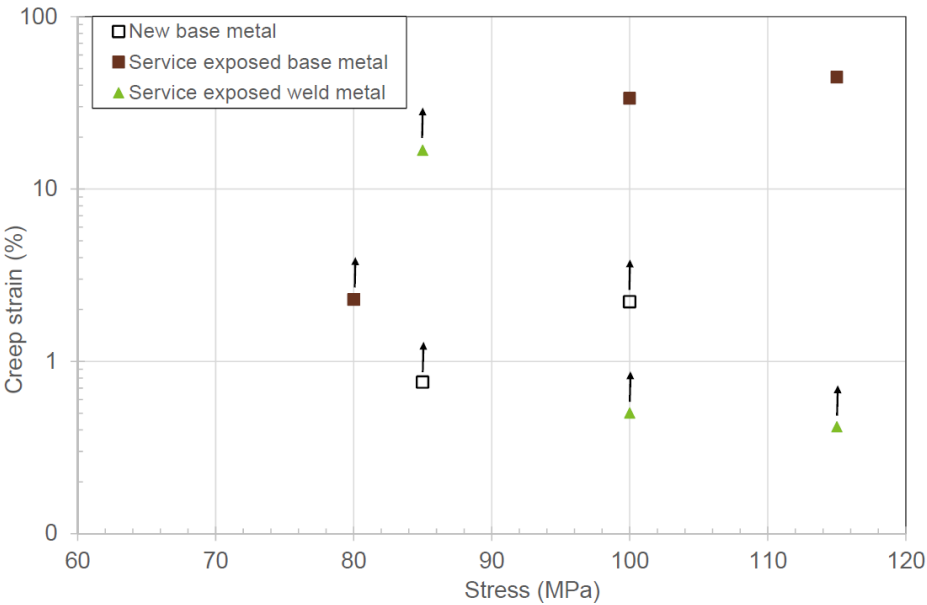


Figure 4. Creep elongation given against applied stress. Arrows denote interrupted specimens.

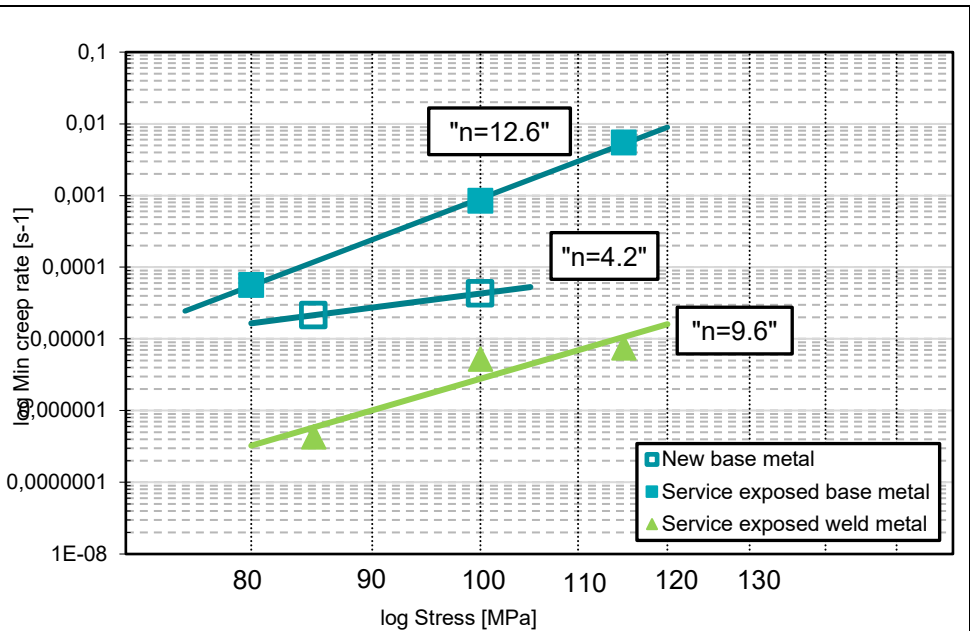


Figure 5. Minimum creep rate vs. stress for the test series.

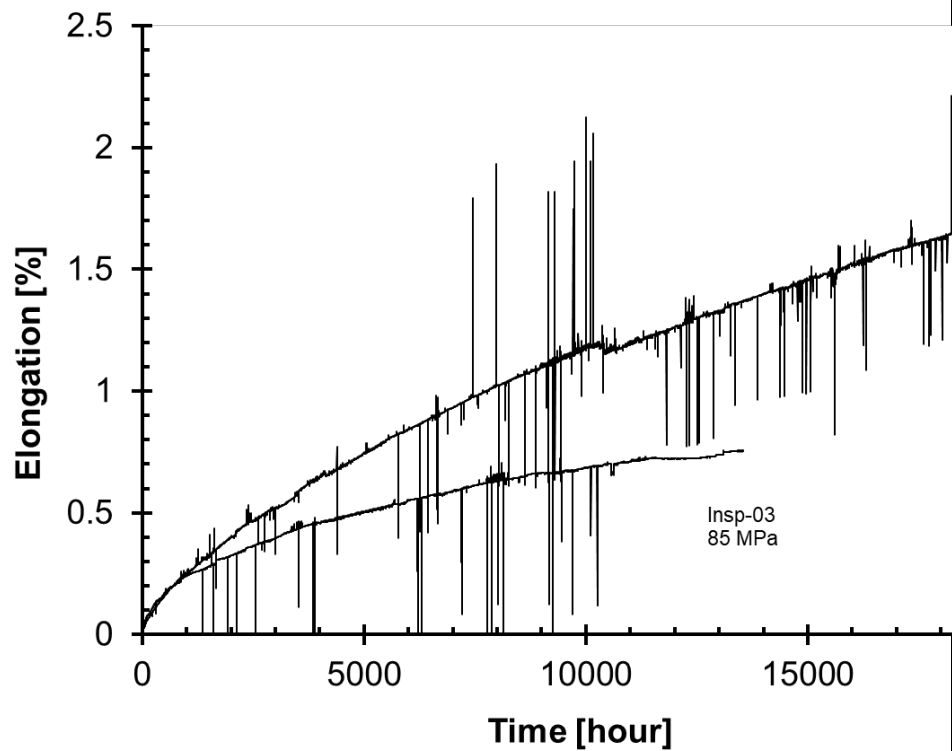
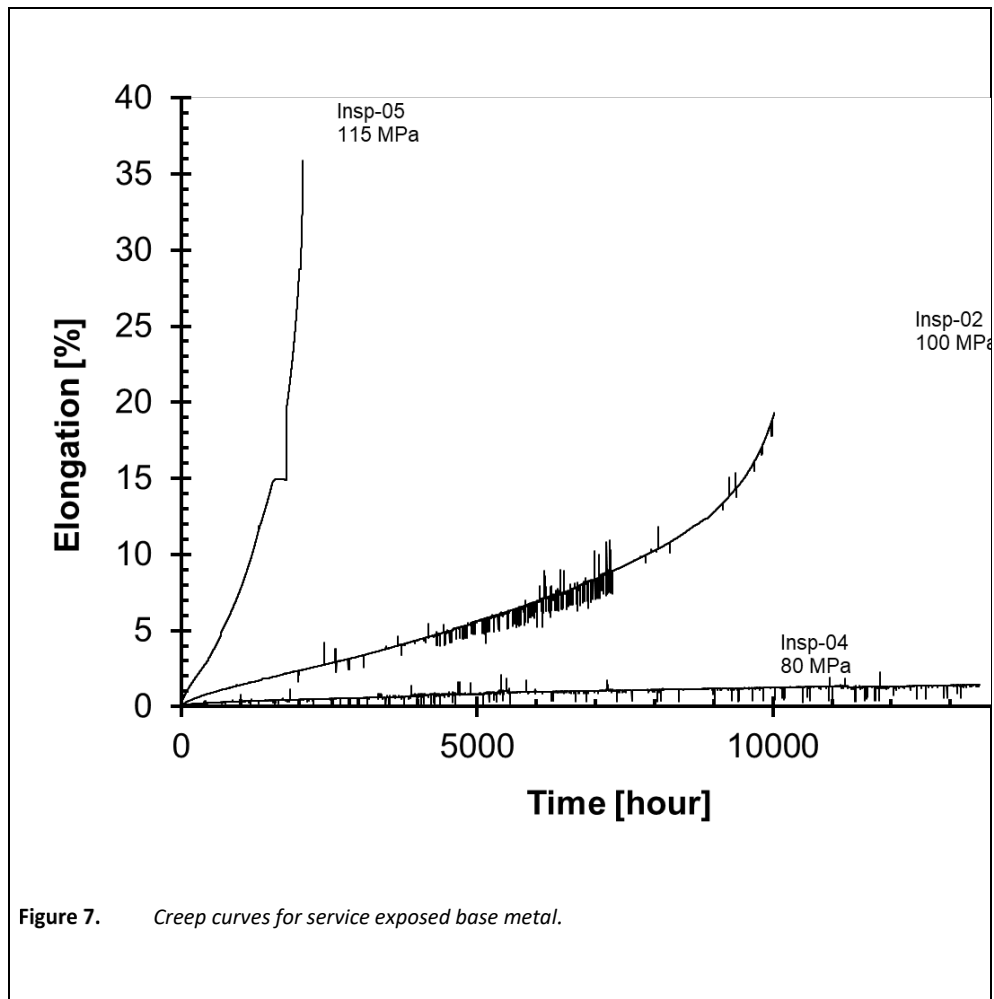


Figure 6. Creep curves for the new base metal.



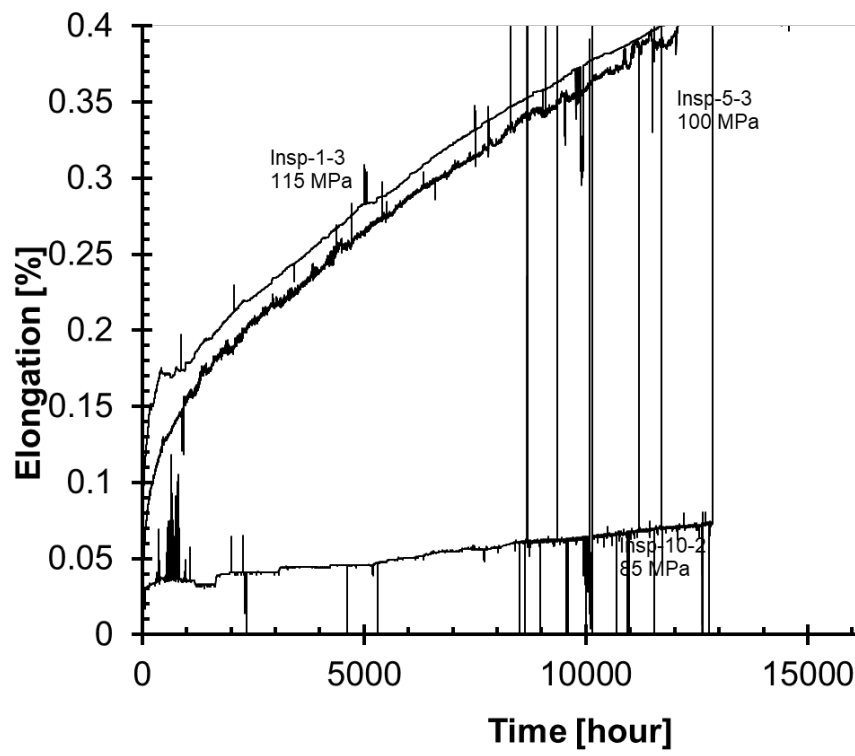


Figure 8. *Creep curves for service exposed weld metal.*

Table 1. Test matrix and results. Creep times and elongation in italics for interrupted specimens.

ID nr	Material	Temp (°C)	Stress (MPa)	Creep time (h)	Loading strain (%)	Creep elongation (%)	Area red (%)	Total strain (%)	Min creep rate* (%/h)	Norton exponent	Notes
Insp-03	New base metal	530	85	<i>13 550</i>	0.39	<i>0.8</i>			<i>0.000021</i>	4.2	Interrupted
Insp-01		530	100	<i>18 563</i>	0.01	<i>2.2</i>			<i>0.000043</i>		Interrupted
Insp-04	Service exposed base metal	530	80	<i>13 502</i>	0.11	<i>2.3</i>			<i>0.000057</i>	12.6	Interrupted
Insp-02		530	100	<i>10 024</i>	0.04	<i>33.5</i>	86.0	33.5	0.000840		Ruptured
Insp-05		530	115	<i>2 063</i>	0.63	<i>44.5</i>	78.9	45.1	0.005500		Ruptured
Insp-10-2	Service exposed weld metal	530	85	<i>13 070</i>	0.58	<i>16.8</i>			<i>0.000000</i>	9.6	Interrupted
Insp-5-3		530	100	<i>17 393</i>	0.15	<i>0.5</i>			<i>0.000005</i>		Interrupted
Insp-1-3		530	115	<i>12 862</i>	0.23	<i>0.4</i>			<i>0.000008</i>		Interrupted

* Minimum creep rate estimated for the interrupted specimens.

4 Metallography of the creep tested material

After the testing was completed selected specimens was cut up and mounted to facilitate the metallographical studies. The selected specimens were all weld specimens and one of the base metal specimens with the longest creep test time. For the ruptured specimens three areas were studied. An area directly adjacent to the rupture, an area far from the rupture but still inside the gauge length and an area of unstressed material in the threaded head of the specimens. For the unbroken specimens only an area in the middle of the gauge length was studied.

The creep damage was classified according to the guidelines in Nordtest NT TR 302 [5]. The assessment of the studied specimens can be found in Table . All observed damage was of the classes 2a or 2b. No damage was assessed to classes 3, 4 or 5 (strings of cavities, microcracks and macrocracks respectively).

As can be seen in Table 2 all weld specimens contain cavities to class 2b. As the weld specimens had been cut with a parallel piece of unaffected weld metal according to Figure 2, untested material was also available for assessment. When material from the gauge length is assessed next to the untested, but service exposed, material it is evident that the same cavity density is present both before and after testing. There might be some increase in cavity density by the testing, but this is difficult to judge in the microscope. In Table 2 the same damage class has been assessed to both the untested and the creep tested weld metal.

The service exposed base metal does not contain any visible creep damage, or very little damage, either before testing or after testing. The new base metal shows creep damage either 2a or 2b after testing. Micrographs of microstructures and observed creep cavitation are given in Appendix 1.

Table 2. Assessed creep damage in the studied specimens according to Nordtest NT TR 302 [5]

Specimen	Position in component	Head of specimen**	Middle of gauge length	Gauge length close to fracture
INSP-01	New base metal	*	2a or 2b	*
INSP-02	Service exposed base metal	0 or 1	0	0 or 1
INSP-1-3	Service exposed weld metal between positions 1 and 3	2b	2b	*
INSP10-2	Service exposed weld metal between positions 10 and 12	2b	2b	*
INSP-5-3	Service exposed weld metal between positions 3 and 5	2b	2b	*

* Position not studied or not available

** Head of specimen or untested weld metal close to the gauge length

5 Creep damage in analysed welds

5.1 REPLICA TEST HISTORY AND SERVICE PARAMETERS

Metallographical investigations are carried out for analysed welds in order to map the amount of creep damage. The damage distribution can then be used as a verification of the analysis results, for example in such way that areas with high local creep strains will be compared to the amount of creep damage in same areas. The steam pipe system of Heleneholmsverket was reconstructed for the first time in 1996 and several components have been replaced over the years as well. An isometry of the pipe system from a Caepipe model of the system from 2014 is seen in Figure 9 [2]. The part of the system that is marked was cut out in at a reconstruction of the system in 2014. A more detailed view of this part is displayed in Figure 10 where the weld MR15 is marked. MR15 has been in operation since 1966 which means the service time was long, approximately 180 000 hours, before it was cut out in 2014. According to the files at Heleneholmsverket of replica test results, micro-cracks were observed, damage rating 4b according to [1] were observed in MR15 at the last testing in 2011. In replica testing 2002 and 2004 damage rating 4a (small amounts of micro cracks) and 3a (small amounts of oriented cavitation) were observed, respectively. MR15 was also replica tested at the outside surface in [1]. A 2.3 mm long creep crack was observed in the weld metal at the 6 o'clock position. At the other test positions, no higher damage than separated creep damage in low amount, damage rating 2a, was observed.

The t-piece that include weld M05 was installed in 1990 and had only been in service for 73 000 hours. In the replica test files, this weld was replica tested in 2001 where damage rating 2.1, separate cavities in a small amount was observed. In [1] damage ratings up to 3b, large amount of oriented creep cavities was observed in the HAZ.

Design and service data are given in Table 3.

Table 3. Design and service data for the main steam pipe

Design pressure	129 bar
Service pressure	105 bar
Design temperature	530°C
Service temperature	530°C (510°C for 8000 h between 1985 and 1987)
Service time	75 000-200 000 hours for different parts of the system

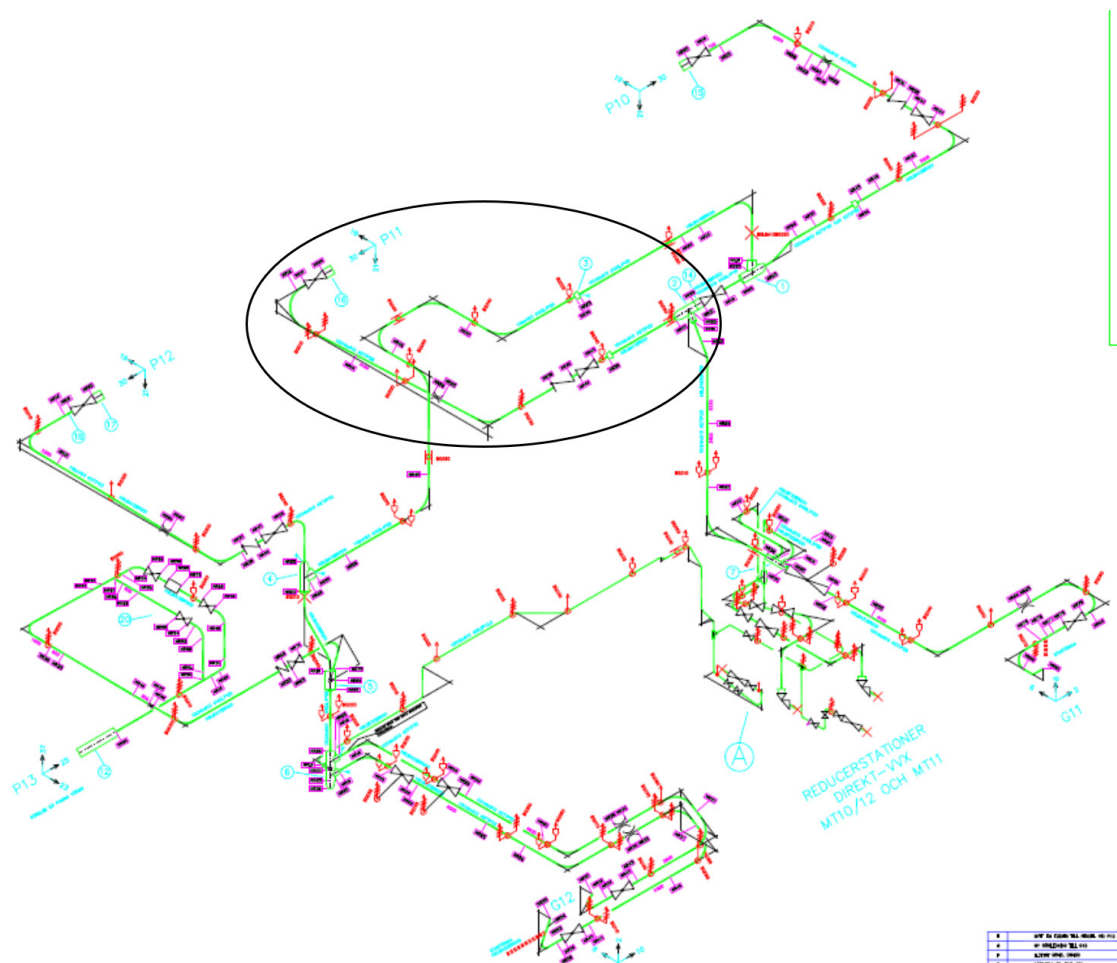


Figure 9. Isometry of the steam pipe system from a Caepipe model before the reconstruction 2014. The marked part was cut out at the reconstruction.

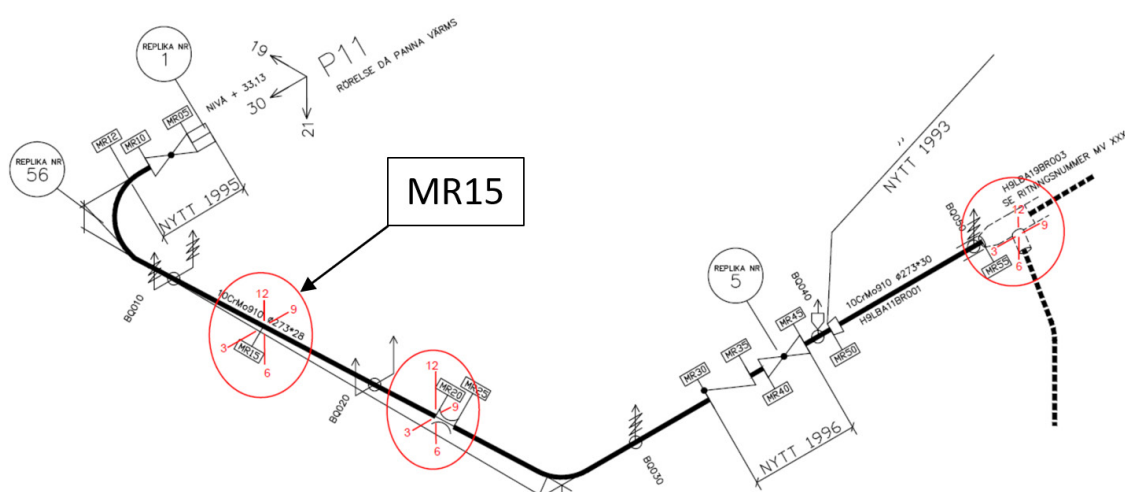


Figure 10. Isometry of cut part of the steam line. The leftmost marked weld, MR15, has been investigated with respect to creep damage in the present project.

5.2 CHARACTERIZATION OF CREEP DAMAGE IN WELD MR15

By replica testing it is possible to examine the microstructure at surfaces of selected positions of power plant components. Weld M15 has previously been replica tested for metallographical characterization of the creep damage in [1]. As a continuation to that project, specimen from four clock positions (3, 6, 9 and 12) of the weld were cut and prepared for metallographical investigation on both the surface and cross-sections of each clock position. Welds and especially the HAZs consist of a laminate of different microstructures which are associated with different creep properties. This results in stress distributions and re-distributions in the weld that are dependent of the creep properties of each constituent of the welded joint and their interrelation to each other. Welds at positions with geometrical stress enhancements as well as possible system stresses can reveal distributions of creep damage in the through-thickness direction that so far has been troublesome to predict. The examined weld and the cut-out specimens are shown in Figure 11.

Each specimen was prepared by grinding an area across the surface and cross-section of the weld with rotating discs of abrasive paper in several stages until a high fineness (400 mesh) is achieved. Electrolytic polishing, which is typically used in replica testing, was used instead of mechanical polishing. The surfaces and cross-sections were polished by use of a portable machine that polished each spot with a diameter of approximately 8 mm. Since this area is relatively small several polishes were performed on base metals and HAZs on both sides of the weld as well as in the weld metal, see Figure 12. Samples were etched by 3 % Nital to reveal the microstructure and replica testing was carried out. The replicas were then examined in a light optical microscope where the observed creep damage was classified according to NT TR 302 [5]. The results of the evaluation are shown in Table 4 for the surface of the weld specimen and Table 5 for the cross-section of the weld specimen. The examined areas are denoted with reference to the steam flow direction: 1 (base metal 1), 2 (HAZ 1), 3 (weld metal), 4 (HAZ 2) and 5 (base metal 2).



Figure 11. The cut-out specimen of MR15 marked with their respective positions.



Figure 12. Tested positions along the surface of the weld. Base metal 1 corresponds to the leftmost polish point and base metal 2 the rightmost point.

The results from the replica testing in Table 4 show that the highest classification of creep damage found were oriented cavities (3a) in the HAZ and weld metal of position 6 o'clock of the weld. Oriented cavities were also detected in the cross-section of positions 6 o'clock and 12 o'clock. All tested positions exhibited isolated cavitation (2a) in both the surface and the cross-section in the HAZs. A notable result is the occurrence of damage rating 3a in the cross-section at 12 o'clock which was not detected on the surface of that position. The weld metal area generally exhibited more creep damage in the cross-sections compared to the surface. Base metal areas exhibited little to no creep damage, only one base metal area with a damage rating over 1 was found in the surface at 9 o'clock. Examples of creep damage is shown in Figure 13.

Table 4. Weld MR-15 creep damage ratings for each tested surface position.

MR15 - Surface	Damage rating					Comment
Position	1	2	3	4	5	
kl.3	1*	2a	1*	1*	1*	*Cavities <100/mm ²
kl.6	1*	3a	3a	2a	1*	
kl.9	2a	2a	1	2a	1*	
kl.12	1	2a	1	2a	1	

Table 5. Weld MR-15 creep damage ratings for each cross-section.

MR15 – Cross-section	Damage rating					Comment
Position	1	2	3	4	5	
kl.3	1	1*	1*	2a	1	*Cavities <100/mm ²
kl.6	1*	3a	2a	2a	1*	
kl.9	1	2a	2a	2a	1	
kl.12	1	2a	3a	2a	1	

Judging from the previous test results, microcracks would be expected in weld metal at the 6 o'clock position. However, higher damage ratings than rating 3a (small amounts of oriented cavitation) were not found as can be seen in Tables 2-3. The reason for this may be explained by the fact that not the same spots were tested. Grinding of the surfaces may also have removed the outermost surface cracks. Such effect could be seen in the replica testing of MR15 when comparing the results from 2003 and 2004, see above.

Comparing the surface replica testing, Table 2, with the one in [1] it is seen that rating 3a was observed in HAZ1 (area 2 in the table) at the 6 o'clock position whereas the same position was rated 2a in [1]. Otherwise, the results agree very well.

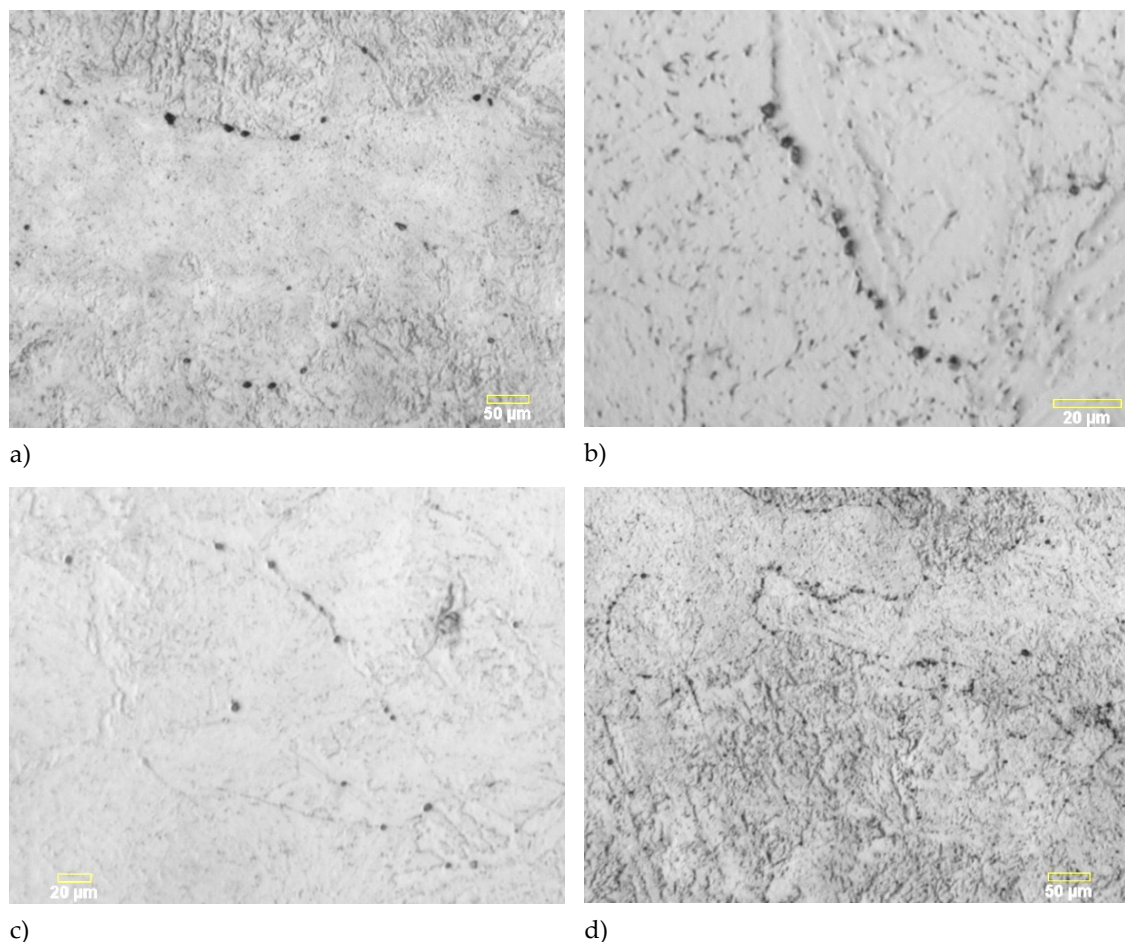


Figure 13. Examples of creep damage in MR 15 a) Surface, 6 o'clock position. Oriented cavities in the weld material, damage rating 3a. b) Cross-section, 6 o'clock position. Oriented cavitation in the HAZ, damage rating 3a. c) Surface, 9 o'clock position. Separate cavities found in the HAZ, damage rating 2a. d) Cross-section, 12 o'clock position. Oriented cavitation in the weld material, damage rating 3a.

Since the stress distribution due to internal pressure is equally distributed in a pipe wall it is common that the creep damage that can be seen at the surface is representative for the creep damage through the thickness. This is true for many geometries but there are exceptions to this. The occurrence of oriented cavities in the cross-section of position 12 o'clock while not observing the same damage rating on the surface for the same position was not expected. The creep damages observed in all four cross-sections was mostly located in the middle-parts towards the outer parts of the thickness of the pipe. Two of the four cross-sections were mapped out in Figures 14-15.

Creep damage is typically concentrated to the HAZs. Sometimes most damage is found in the weld metal. In this case, oriented cavities were detected only in the HAZ at 6 o'clock and in both HAZ and weld metal in the 12 o'clock position. Creep damage rating 2a was observed in the areas in and around the oriented cavities. The rest of the thickness showed isolated cavities but not enough to classify as a rating higher than 1.

It was also observed as can be seen in Figures 14-15 that the creep damages were concentrated around the areas changes of the weld fusions lines curvatures, i.e.

where the top weld bead crosses the one beneath at both sides of the weld sections. This was observed both at the 6 o'clock and the 12 o'clock positions. This may be due to locally enhanced creep stresses in those areas of the weld geometry.

For the modelling of the weld, the width of the HAZ was measured. It is mainly 3,2 mm and 3,8 mm on the left-hand and the right-hand side, respectively, in Figure 14.

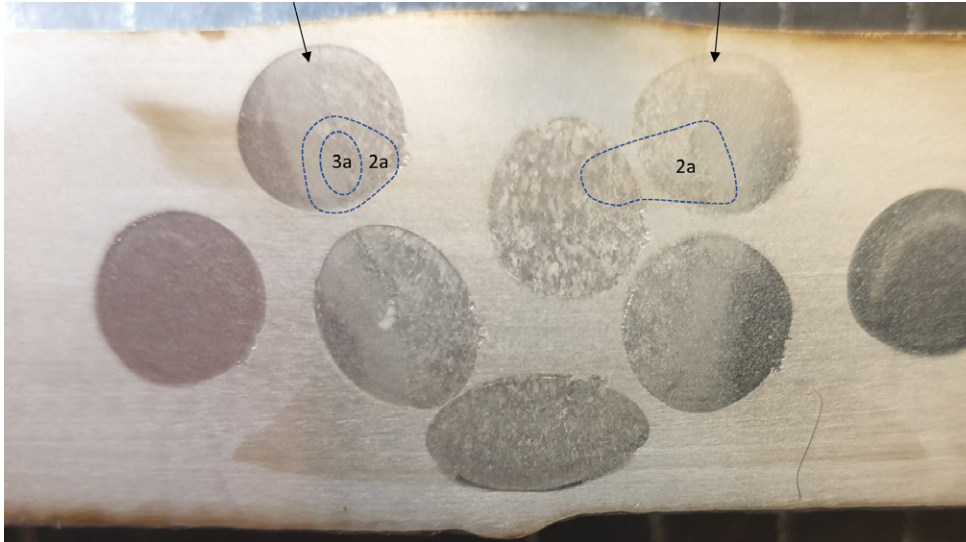


Figure 14. Cross-section of weld MR-15 at position 6 o'clock. The cross-section is etched and the HAZ is visible in the directions of the arrows on both sides of the weld metal. Areas with different creep damage classes are marked according to NT TR 302.

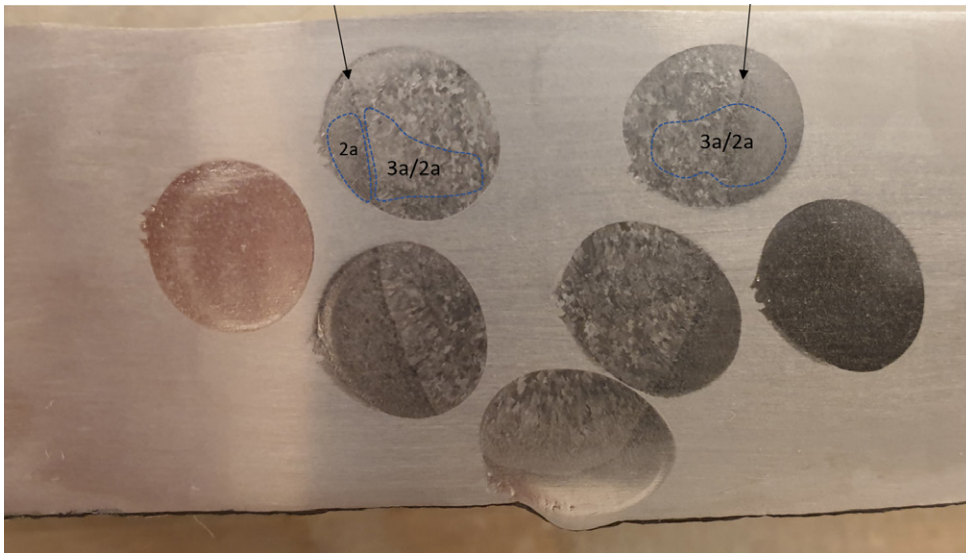


Figure 15. Cross-section of weld MR-15 at position 12 o'clock. The cross-section is etched and the HAZ is visible in the directions of the arrows on both sides of the weld metal. Areas with different creep damage classes are marked according to NT TR 302.

6 Standard for design and analysis of piping systems

6.1 SS-EN 13480-3

Part 3 of the European standard SS-EN 13480 [6] contains rules for design and calculation of metallic piping systems. Section 12 in SS-EN 13480-3 addresses the effects of weight and other loadings as well as the effects of thermal expansion/contraction or similar movements imposed by other sources.

For a piping system, several different criteria should be fulfilled. According to equation 12.3.1-2 in SS-EN 13480, the sum of primary stresses σ_1 due to sustained loads is calculated as

$$\sigma_1 = \frac{p_c \cdot d_o}{4 \cdot e_n} + \frac{0.75 \cdot i \cdot M_A}{Z} \quad (2)$$

where p_c is the calculation pressure, d_o is the outer diameter of the pipe, e_n is the nominal thickness, i is the stress intensity factor ($0.75 \cdot i \geq 1$), M_A is the resultant moment from the sustained mechanical loads and Z is the section modulus of run pipe.

According to equation 12.3.1-4 in SS-EN 13480 the stress range due to thermal expansion and alternating loads can be calculated as

$$\sigma_4 = \frac{p_c \cdot d_o}{4 \cdot e_n} + \frac{0.75 \cdot i \cdot M_A}{Z} + \frac{i \cdot M_C}{Z} \quad (3)$$

where M_C is the resultant moment due to thermal expansion and alternating loads.

In validation of the ABAQUS model of the piping system in Heleneholmsverket, equations (2) and (3) are used for comparison of results from ABAQUS [7] and CAEPIPE [8].

7 Numerical analysis in Abaqus and analysed cases

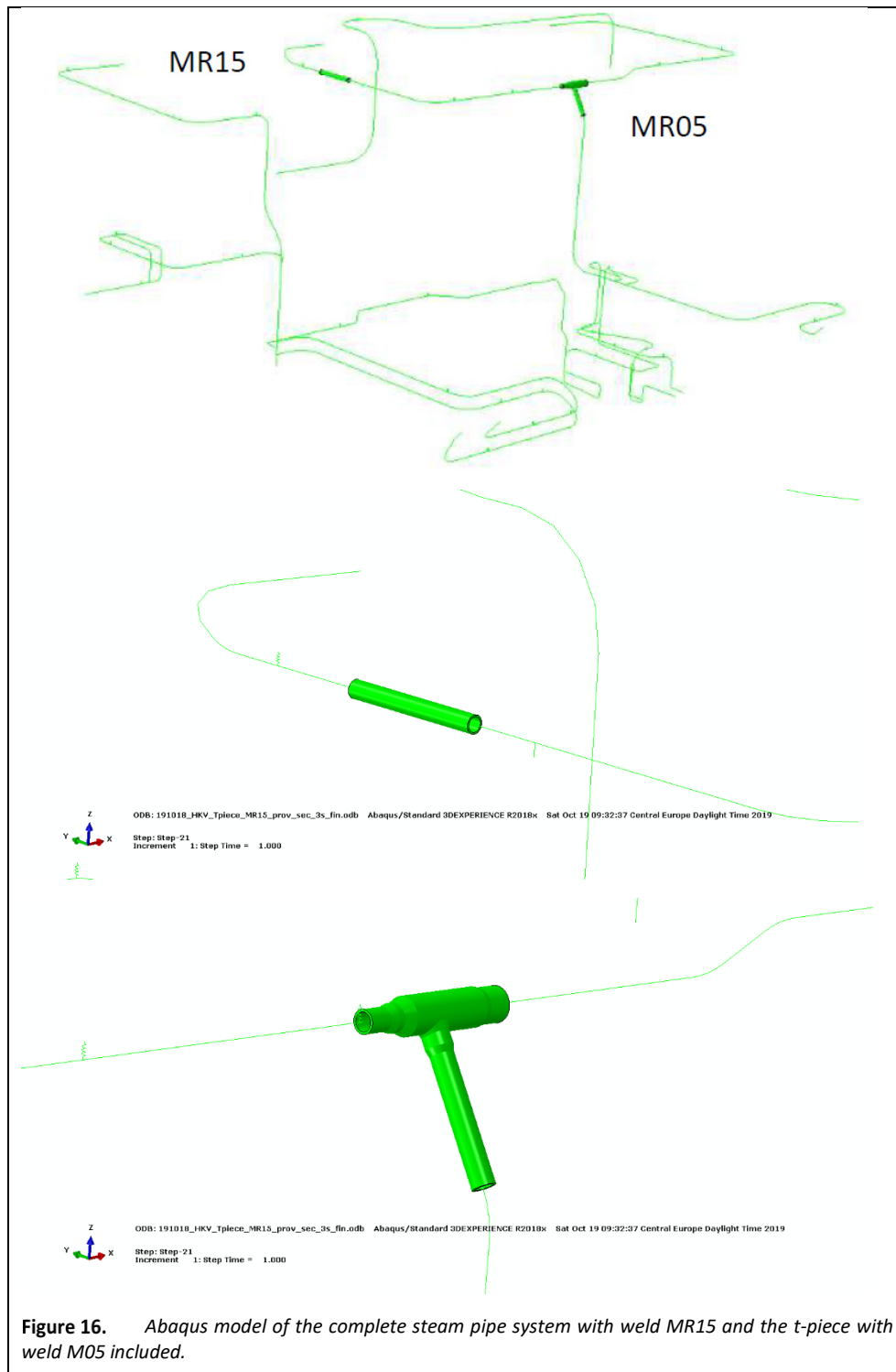
7.1 MODEL OF THE STEAM PIPE SYSTEM

In the previous project [1] an Abaqus model of a part of the system from [3] was used to verify a script that could translate a Caepipe model to Abaqus. Caepipe is a programme for elastic analyses. The modelling work can be done relatively fast in Caepipe and the idea with the script was to make it possible to perform creep analyses of pipe systems by use of Abaqus with minimized modelling in Abaqus since it is suited for creep and modelling of components but is very time consuming for modelling pipe systems.

The results indicated that a model of the entire system would be necessary to be able to verify observed creep damage distributions with the analysed creep strain distributions.

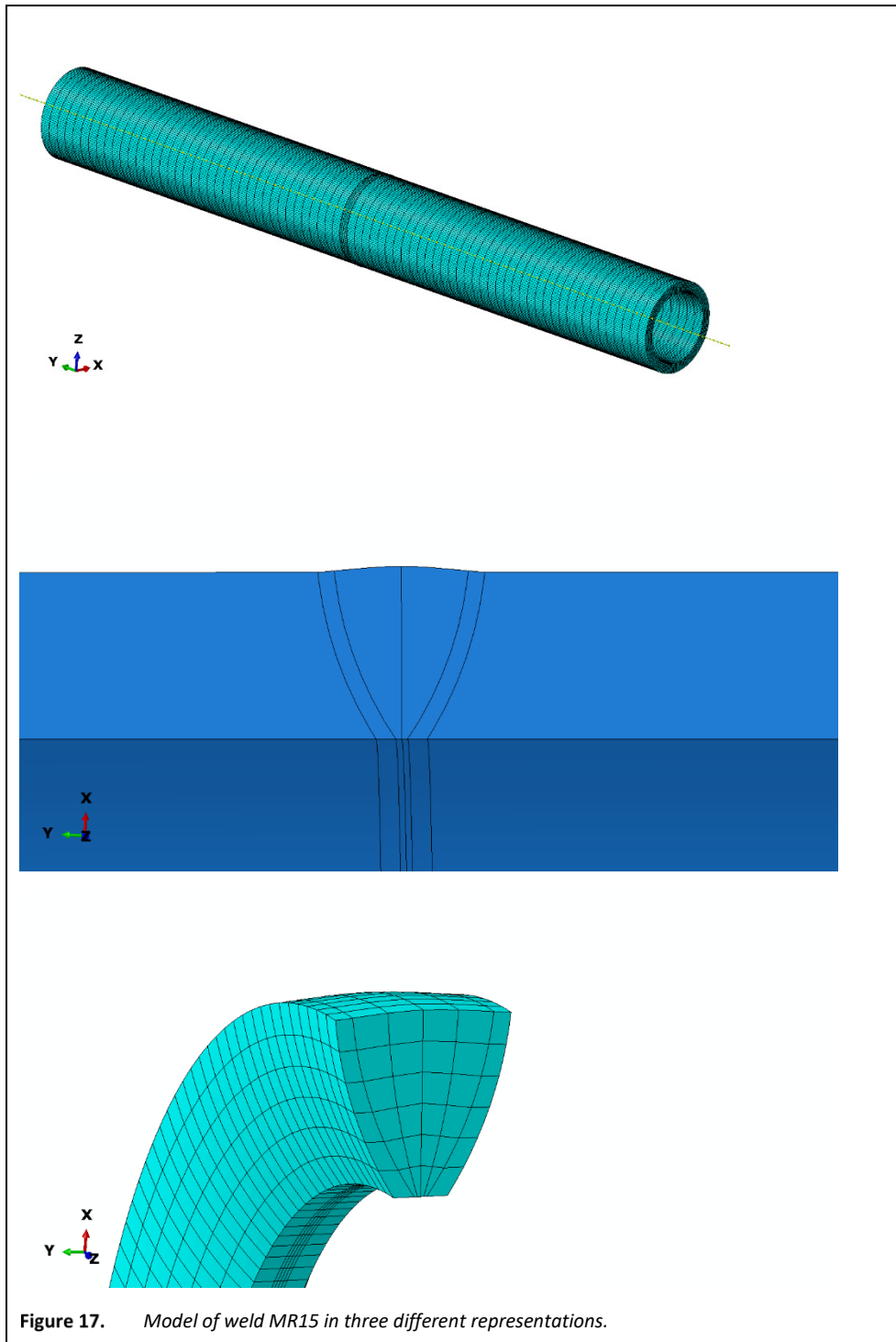
In an examination of the previous models and the script it was found that the only way to complete model with the entire steam pipe system with a desirable frequency of nodes in the model, was to model it directly in text files and subsequently importing it to Abaqus. Although time consuming a very solid model was achieved.

It was also decided to include the weld MR15 as well as the t-joint, including branch weld MR05 that was analysed in [1], into the model of the pipe system. In [1] the t-joint was modelled separately and the system stresses from the pipe model were superimposed to the component analysis. This is an innovative concept, but it may also be sensitive to errors associated to the selection of boundary conditions. By integrating components and welds into the pipe model such possible problems are avoided automatically. Figure 16 shows the complete model with weld MR 15 and the t-joint with weld MR 05 included.

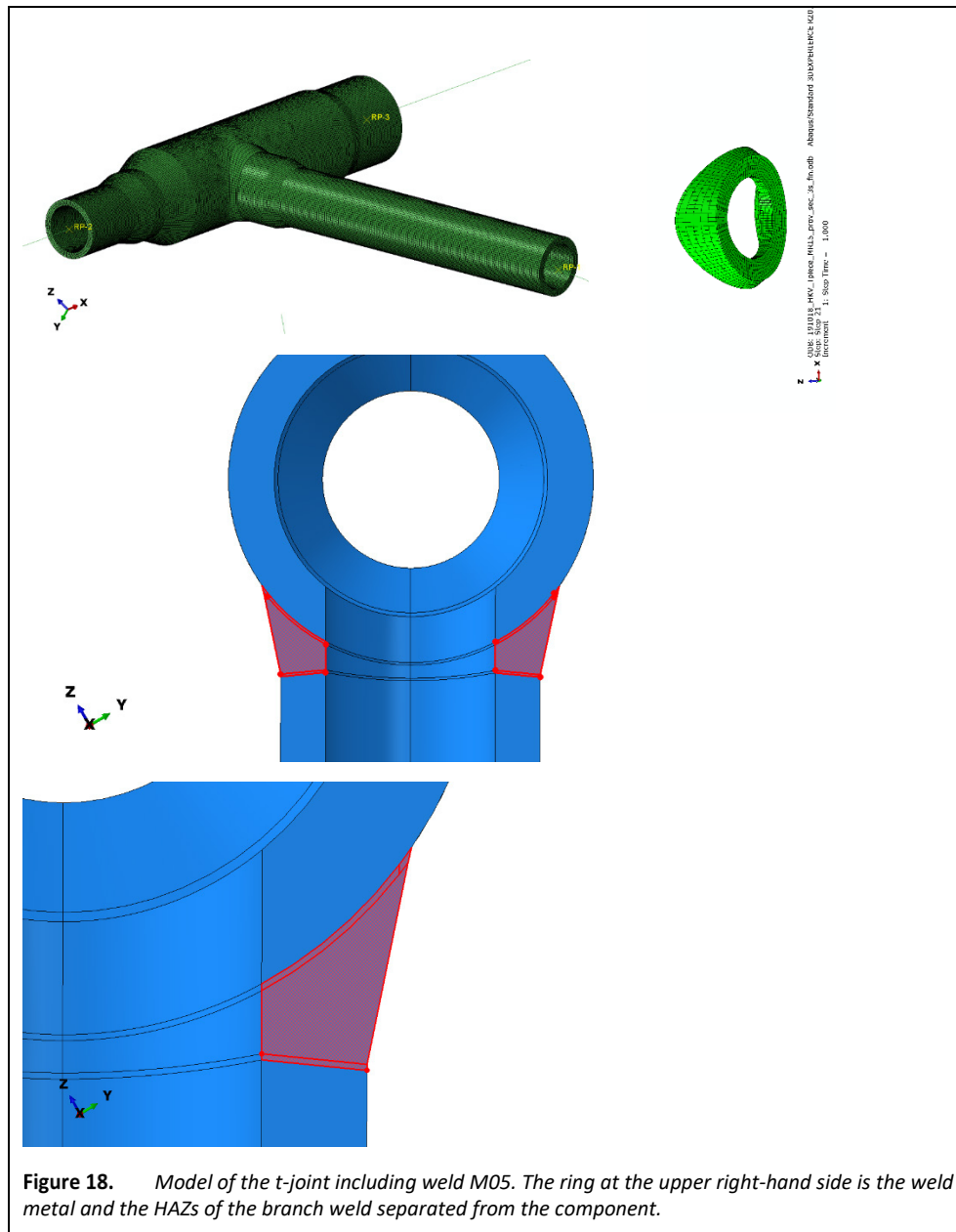


7.2 MODELS OF WELD M15 AND M05

Figure 17 shows the model of weld M015. The width of the HAZ is 3,5 mm in the model. This is the average width according to the measurements in section 5. The modelled dimensions of the weld metal are based on measurements as well as at one of the metallographically prepared sections of the weld.



The t-joint including weld MR05 was modelled in [2]. Figure 18 shows the model including weld region and HAZ.



7.3 ANALYSED CASES

The cases to be analysed include:

- System analyses of secondary creep only. These results can be compared directly to the results in [1] and involves starts and stops.
- System analyses where both primary and secondary creep is included, particularly the effect of stress relaxation when primary creep is introduced is studied.
- Component analyses of weld M015 and the t-joint including weld M05.
- All sets of analysis are compiled with creep data from
 - × Produced data of service exposed parent and weld metals
 - × Produced data of virgin parent metal
 - × Data according to EN 10028-2
- The creep rate in the HAZ was 3 times higher than the parent metal creep rate in [2] as a result of impression creep testing. It was lower than expected since a factor of 10 has been anticipated previously according to creep testing of simulated HAZ microstructures. Therefore, a HAZ/parent metal creep rate ratio of 6 is also analysed for selected cases in order to study the sensitivity of this ratio.
- Sensitivity analyses has been performed on
 - × Elastic Young's modulus.

A matrix of the analysed cases is given in Table 5. All analyses include all the conventional components that develop the stresses and strains: internal pressure, dead weight and thermal expansion.

Table 5. Matrix of analysed cases.

Object	Stress/ strain dist- ribution at 73 000 h	Stress/ strain dist- ribution at 180 000 h	Effect of start and stop	Effect of primary creep	HAZ creep rate 3 times parent metal	HAZ creep rate 6 times parent metal	Virgin creep data	Service exposed creep data	EN 10028-2 creep data
System		x	x	X			x	x	x
MR15		x		X	x	x	x	x	X
MR05	x			x	x	x	x	x	X

8 Creep models and creep constants evaluated from creep test and tabled data

The analyses in [2] were based on secondary creep which is described by the classical Norton creep law:

$$\frac{d\varepsilon_{ij}}{dt} = \frac{(1+\nu)}{E} \left[\left(\frac{d\sigma_{ij}}{dt} \right) - \frac{\nu}{\nu+1} \left(\frac{d\sigma_{kk}}{dt} \right) \delta_{ij} \right] + \frac{3}{2} B \bar{\sigma}^{(n-1)} s_{ij} \quad (4)$$

Where ε_{ij} , σ_{ij} , s_{ij} are the respective strain, stress and stress deviator tensor, $\bar{\sigma}$ is the von Mises effective stress, E and ν is the Young's modulus respective Poisson's number and B and n are the respective constant and exponent in Norton's creep law. The last term in equation (1) describes the creep response of the material.

To be able to define the parameters B and n in the creep law for the pipe system material, the creep law is considered in one dimension, see equation (1).

Equation (1) is integrated, see equation (5)

$$\int_0^\varepsilon d\varepsilon = \int_0^t B \sigma^n dt \rightarrow \varepsilon = B \sigma^n t \quad (5)$$

The parameters B and n can then be solved with an equation pair, equation (6) and (7). By use of tabled values of 10CrMo9-10 in EN 10028-2 [9] at the stresses that result in 1% creep strain at time 10 000 and 100 000 for 10CrMo9-10 at 530°C the equations will read:

$$0.01 = B \cdot 107^n \cdot 10000 \quad (6)$$

$$0.01 = B \cdot 68^n \cdot 100000 \quad (7)$$

The resulting values are $B=4.91 \cdot 10^{-17}$ and $n=5.08$.

In the present project primary creep was included, too. The model for primary creep that was used is the simplest expansion of the regular secondary creep equation. The combined primary and secondary creep model, expressed in creep strain is expressed as:

$$\varepsilon = B_2 \sigma_{vM}^{n_2} t^{m_2} + B_1 \sigma_{vM}^{n_1} t \quad (8)$$

, where the first term on the right-side describes primary creep.

The primary creep constants were evaluated from the primary creep part of the creep curves of new parent metal from the tests at 85 MPa and 100 MPa in Figure 6, by means of curve fitting, see Figure 19.

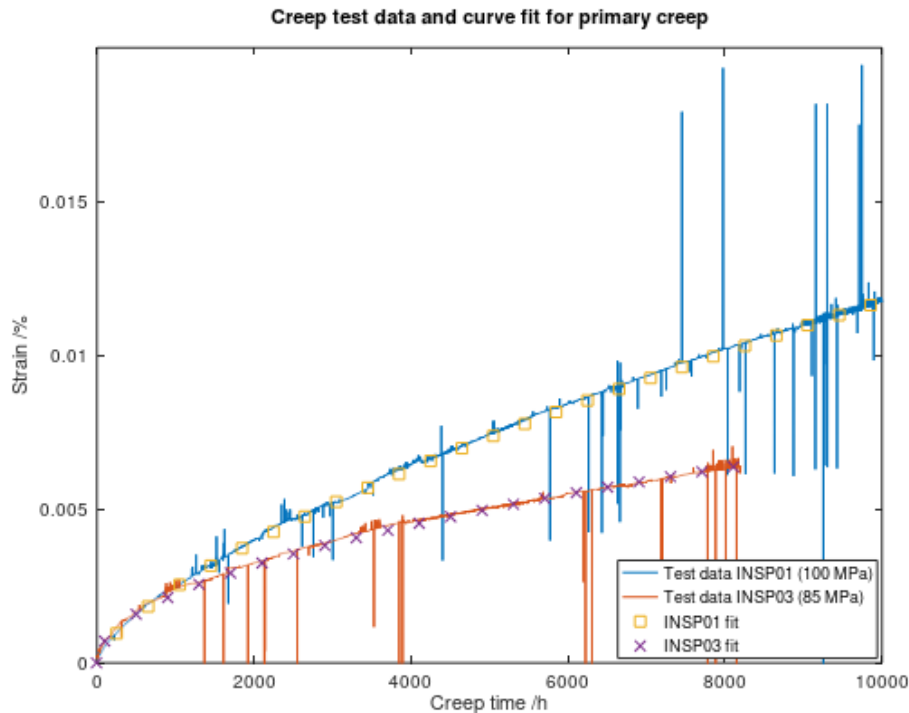


Figure 19. Creep curves for the new base metal, together with fitted curves used to extract primary creep parameters for use in Equation 8.

The constants in the equations above for creep tested material were evaluated and are summarised in Table 6 and 7. Creep constants B1 for weld material and HAZ are calculated from these constants based on creep strain rate for weld material equal to 0.5 times that of base material, and creep strain rate for HAZ equal to 3 times to that of base material. In addition, as mentioned above, creep strain rates of 6 times that in base material is used in HAZ as a sensitivity analysis, in selected analyses.

Table 6. Creep constants for the secondary creep model

	n₁	B₁
New base metal	4.28	1.18E-15
EN10028-2	5.08	4.92E-17
IC test metal (operation 73000h)	5.08	1.64E-16
Service exposed base metal	12.56	7.17E-31
Service exposed weld metal	9.62	1.21E-27

Table 7. Creep constants for the primary creep model

	n₁	B₁	n₂	B₂	m₂
New base metal (INSP03)	4.28	1.18E-15	5.50	1.7E-15	0.50

9 Analysis results

9.1 SYSTEM ANALYSES

9.1.1 Abaqus system model

The model described in section 7.1 was loaded with dead weight, internal pressure and heat load (thermal expansion). Figures 19, 20 and 21 show the resulting von Mises stress distributions after loading (before creep relaxation) for dead weight, dead weight + internal pressure and dead weight + internal pressure + thermal expansion.

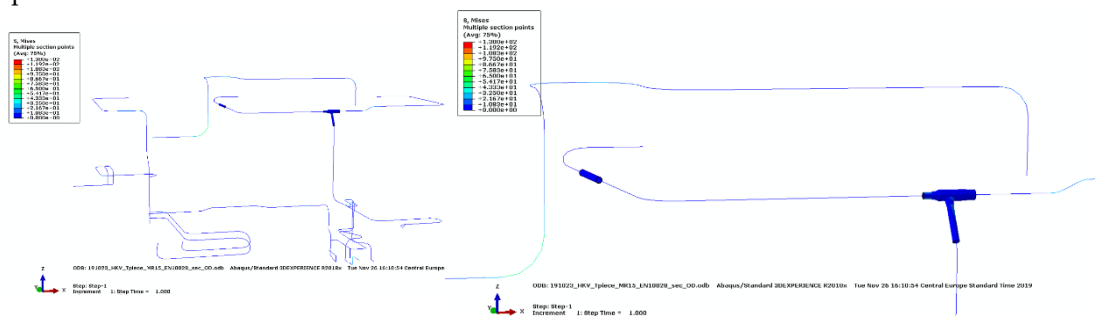


Figure 20. Von Mises stress distribution of dead weight for the entire system and a zoom at the part of the analysed components.

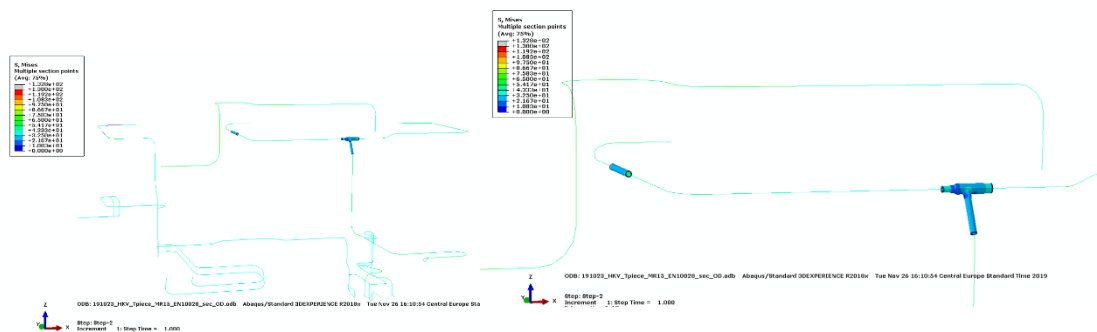


Figure 21. Von Mises stress distribution of dead weight + internal pressure for the entire system and a zoom at the part of the analysed components.

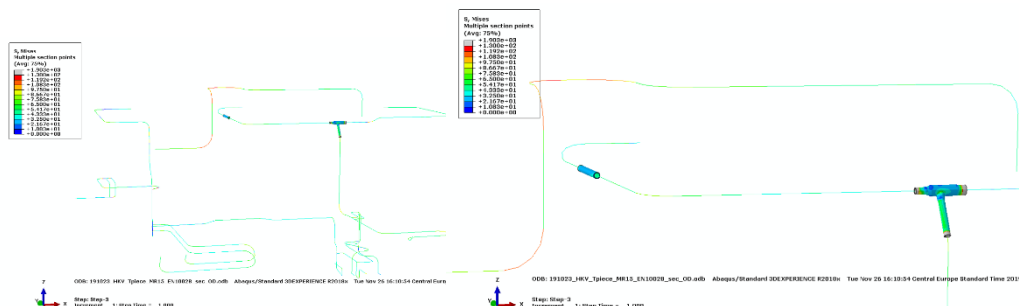


Figure 22. Von Mises stress distribution of dead weight + internal pressure + thermal expansion.

Before stress relaxation the highest total stresses appear at a couple of bends with von Mises stresses of about 110 MPa.

The locally high stress levels seen in the ends of the MR15/MR05 pipe parts arise from the modelling technique used to attach them to the pipe system. These stresses are not affecting the stress distribution and stress levels in the regions where the welds are located and where creep strain is monitored.

9.1.2 Verification of the Abaqus system model

One way to validate the ABAQUS pipework model is to compare elastic results with those from the CAEPIPE model used in [1]. In the following, forces and moments at the rigid end positions of the pipe system model are compared between the two models. Also, deformations of the system are compared.

Table 8 shows a comparison of reaction forces and reaction moments at rigid points of models for the dead weight, pressure and thermal expansion load case. A ratio of 1 (ABAQUS result divided by CAEPIPE result) shows perfect agreement.

Table 8. Reaction forces and reaction moments at rigid points for dead weight, internal pressure and thermal expansion. Ratio equals ABAQUS results divided by CAEPIPE results. Forces in N and moments in Nm.

Node	Rx CAEPIPE	Ry CAEPIPE	Rz CAEPIPE	Mx CAEPIPE	My CAEPIPE	Mz CAEPIPE
10	9,93E+03	-1,31E+04	6,15E+03	1,79E+04	-7,35E+03	9,18E+04
530	-6,34E+03	1,43E+04	2,06E+03	7,23E+03	1,93E+04	4,86E+04
890	-4,74E+02	-3,77E+03	2,41E+03	-7,41E+02	-6,15E+02	-1,63E+03
1000	-6,08E+02	4,00E+03	1,82E+03	6,34E+02	-1,86E+02	1,96E+03
1170	-1,09E+03	1,14E+02	1,31E+04	3,11E+04	-8,34E+02	6,87E+03
1320	4,36E+02	2,24E+02	1,75E+04	5,36E+04	-1,66E+04	-1,27E+03
2180	-3,64E+03	-7,68E+03	6,01E+03	1,43E+04	1,70E+04	-4,21E+04
3330	1,35E+03	-1,78E+04	5,54E+03	1,27E+04	-1,18E+04	7,39E+04
5370	1,27E+04	-1,35E+04	1,01E+04	2,29E+04	-9,49E+03	-4,84E+04
5880	-5,34E+03	1,64E+04	1,10E+04	3,15E+04	5,51E+03	7,90E+04
6080	-2,34E+03	8,60E+03	5,83E+03	2,68E+04	1,68E+04	5,65E+04
Node	Rx Abaqus	Ry Abaqus	Rz Abaqus	Mx Abaqus	My Abaqus	Mz Abaqus
10	8,05E+03	-1,16E+04	7,07E+03	1,39E+04	-3,79E+03	7,29E+04
530	-6,85E+03	1,54E+04	1,34E+03	6,20E+03	1,55E+04	5,42E+04
890	-3,96E+02	-3,11E+03	2,65E+03	-8,96E+02	-4,97E+02	-1,29E+03
1000	-5,59E+02	2,96E+03	2,36E+03	1,12E+03	-1,36E+02	1,58E+03
1170	-1,36E+03	-8,01E+02	1,19E+04	2,16E+04	-2,13E+03	9,35E+03
1320	-1,93E+02	7,13E+02	2,03E+04	4,36E+04	-1,41E+04	2,79E+03
2180	-2,68E+03	-6,45E+03	3,04E+03	9,21E+03	1,15E+04	-3,24E+04
3330	1,36E+03	-1,88E+04	5,24E+03	1,02E+04	-1,59E+04	7,56E+04
5370	1,04E+04	-1,17E+04	4,57E+03	1,71E+04	5,51E+03	-4,29E+04
5880	-6,17E+03	1,91E+04	7,87E+03	2,82E+04	5,66E+03	9,22E+04
6080	-2,68E+03	1,00E+04	3,58E+03	2,24E+04	2,03E+04	6,56E+04
Node	Ratio Rx	Ratio Ry	Ratio Rz	Ratio Mx	Ratio My	Ratio Mz
10	0,81	0,89	1,15	0,78	0,52	0,79
530	1,08	1,07	0,65	0,86	0,80	1,11
890	0,84	0,82	1,10	1,21	0,81	0,79
1000	0,92	0,74	1,30	1,76	0,73	0,80
1170	1,25	-7,03	0,91	0,69	2,55	1,36
1320	-0,44	3,18	1,16	0,81	0,85	-2,20
2180	0,74	0,84	0,51	0,64	0,67	0,77
3330	1,01	1,05	0,95	0,80	1,35	1,02
5370	0,82	0,86	0,45	0,75	-0,58	0,89
5880	1,16	1,17	0,72	0,90	1,03	1,17
6080	1,15	1,16	0,61	0,83	1,21	1,16

Deformations in the pipe system is compared between the models from CAEPIPE and Abaqus, see Figures 23 and 24. The load is dead weight, internal pressure and heat, and the scaling of the deformations with a factor of 10 is done on results from both models. The deformation is very similar in shape, but also in magnitude.

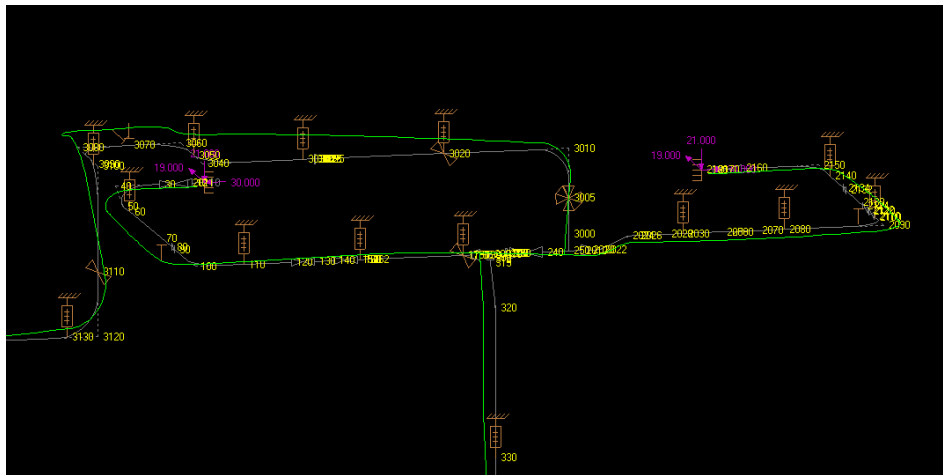


Figure 23. Displacements of the pipe system in CAEPIPE, for when loaded by dead weight, internal pressure and heat.

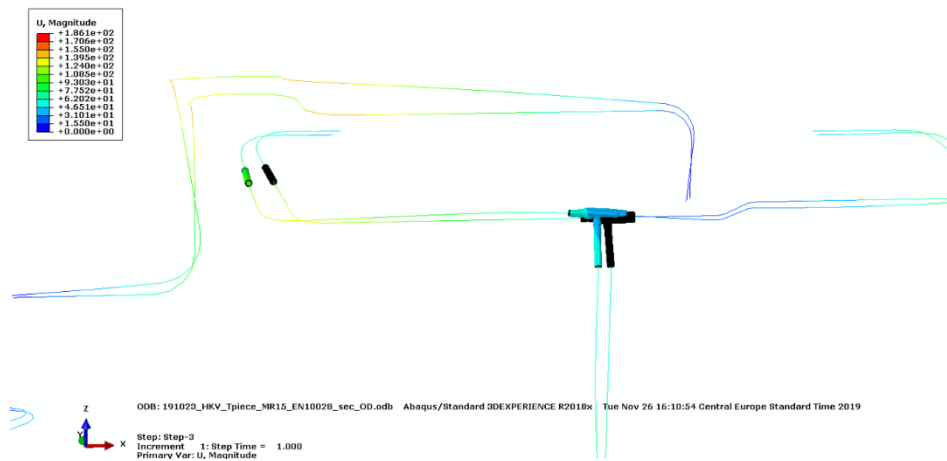


Figure 24. Displacements of the pipe system in Abaqus, for when loaded by dead weight, internal pressure and heat.

Axial stress at the location of MR15 calculated in Abaqus with that of CAEPipe is compared. The stress from Abaqus is equal to 29.6 MPa, and the corresponding stress in CAEPipe (node 60) is 29.62 MPa. A similar comparison close to the location of MR05 gives 23.8 MPa in Abaqus and 23.2 MPa (node 200) in CAEPipe. Locally, but not far from the welds studied in this report, the stresses differ more. This does not however affect the results in the vicinity of the studied welds. Stresses in CAEPIPE and Abaqus are not calculated in similar manners. Stresses in CAEPIPE are calculated for consecutive evaluation according to the standard SS-EN 13480-3. The stress calculated ABAQUS is most physically correct of the two. Thus, a direct comparison of stresses in CAEPIPE and ABAQUS is not expected to give identical results. Better agreement is achieved in straight sections, such as in the MR15 weld region.

In summary, based on the comparison of results from the CAEPIPE and the ABAQUS analysis, the correspondence between the two models is reasonable. To get exact agreement with such a complex pipework cannot be expected.

9.1.3 System secondary creep strain distribution

Investigating the effects from primary creep modelling on the stress relaxation and creep strain evolution in some detail, it is relevant to first show the distribution of creep strain in the system, analysed with secondary creep effects. In figure 25 and 26, the creep strain distribution in the pipe system considering only secondary creep effects is shown. In figure 25 for 73 000 hours of operation, relevant for the t-piece and the MR05 weld. Figure 26 shows the creep strain distribution after 180 000 hours of operation, which is roughly the time in operation for the rest of the system including the MR15 weld. Material data used in these calculations are from testing of new base material, see section 3.

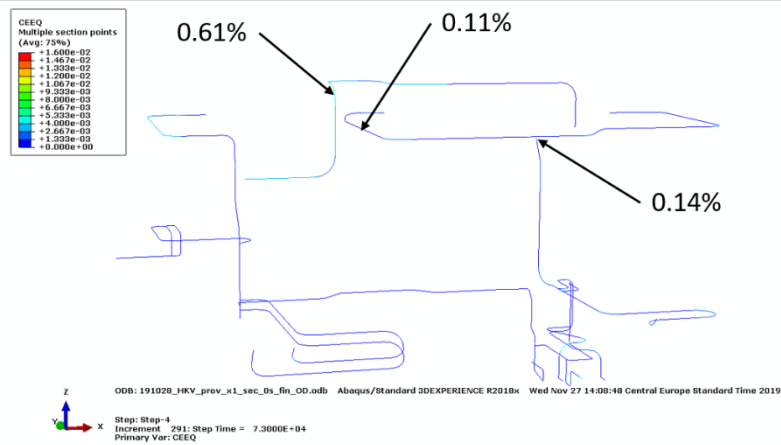


Figure 25. Distribution of equivalent creep strain in the pipe system after roughly 73 000 hours of operation, considering secondary creep effects only.

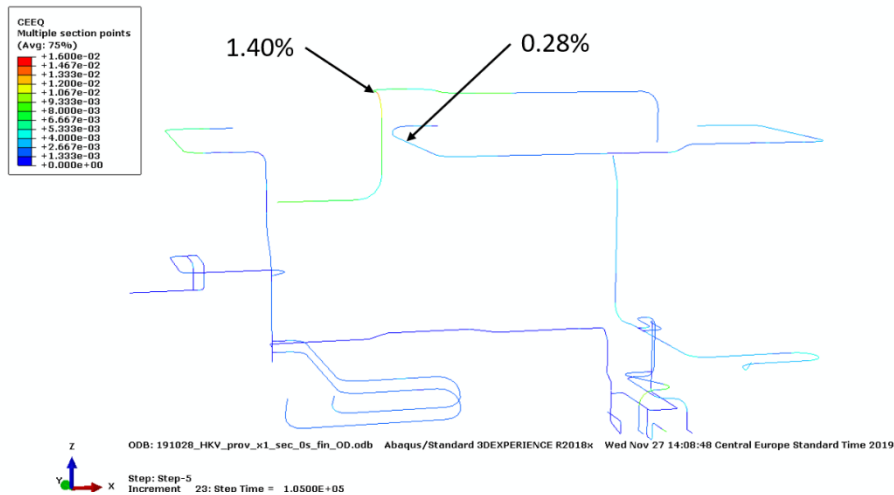
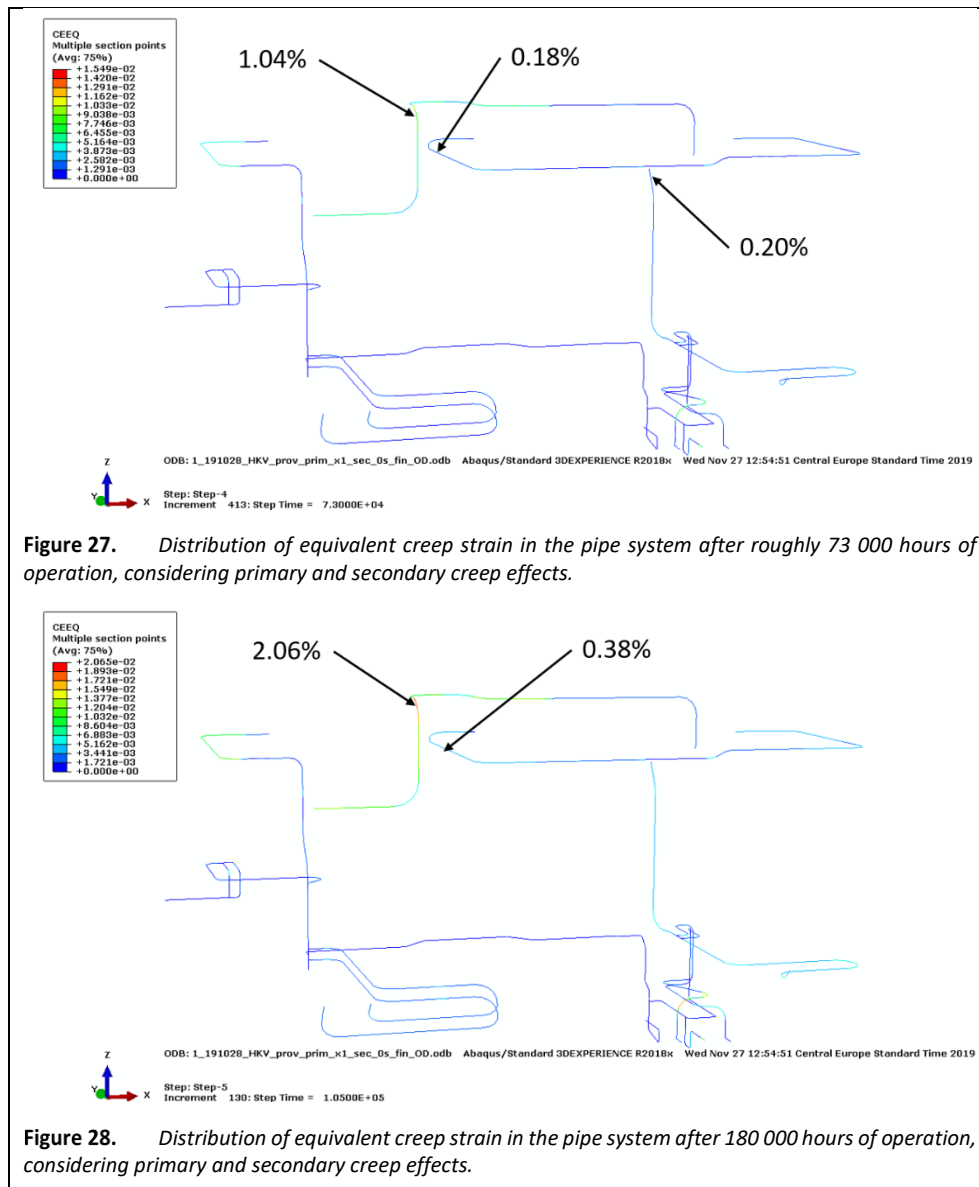


Figure 26. Distribution of equivalent creep strain in the pipe system after 180 000 hours of operation, considering secondary creep effects only.

9.1.4 Effects of primary creep and stress relaxation

Comparing figures 25 and 26 with figures 27 and 28, where corresponding quantities are displayed but where effects from primary creep are considered, it is immediately noticed that the difference is significant. Material data used in these calculations are from testing of new base material, see section 3.

Primary creep has been added to the Norton creep model according to eq. (8). At the beginning of the creep process, primary creep contributes to the developed creep strain after which secondary creep takes over. It is a significant difference in developed creep strain. Adding to the complexity are the facts that a faster relaxation of stress levels slows the creep strain evolution, since the rate of creep strain is dependent on the equivalent stress level.



For a particular location, it is interesting to study the effect from primary creep on the progression of creep damage in some more detail. In figure 29, it is obvious that the addition of primary creep has an initial effect that also remains over long-term creep

This obviously does not consider the complex geometry of the T-piece. This is discussed in some detail in section 9.2.

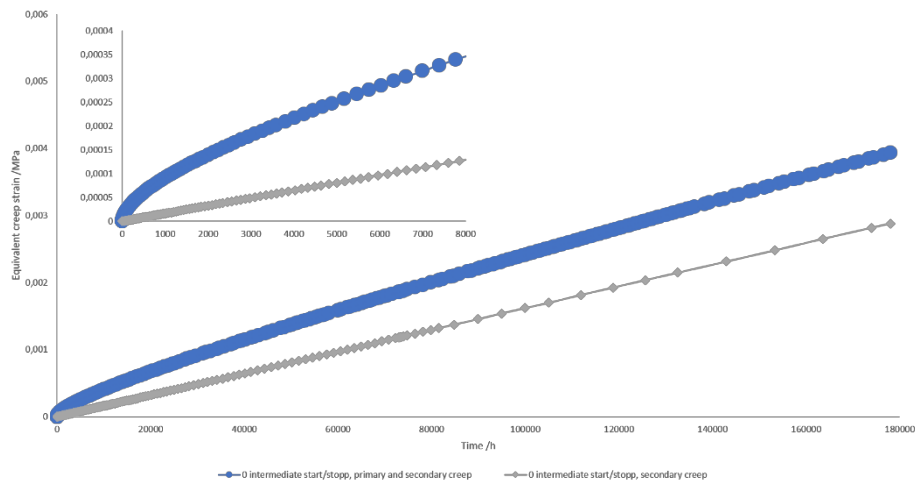


Figure 29. Evolution of equivalent creep strain at a location in the pipe system approximately corresponding to the location of weld MR15.

The stress distributions in the entire steam pipe system after the first start-up, after one year and after 180 000 h are shown in figures 30, 31 and 32, respectively, accounting for primary and secondary creep effects. From these figures, it is clear that in particular the higher stresses in the pipe bends relax significantly during the first year. Straight pipe parts show much less stress relaxation.

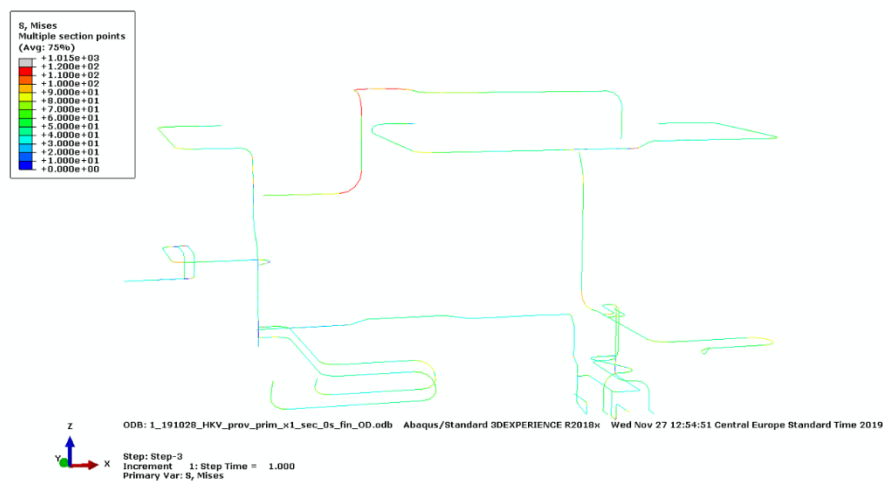


Figure 30. Von Mises stress distribution after the first start up.

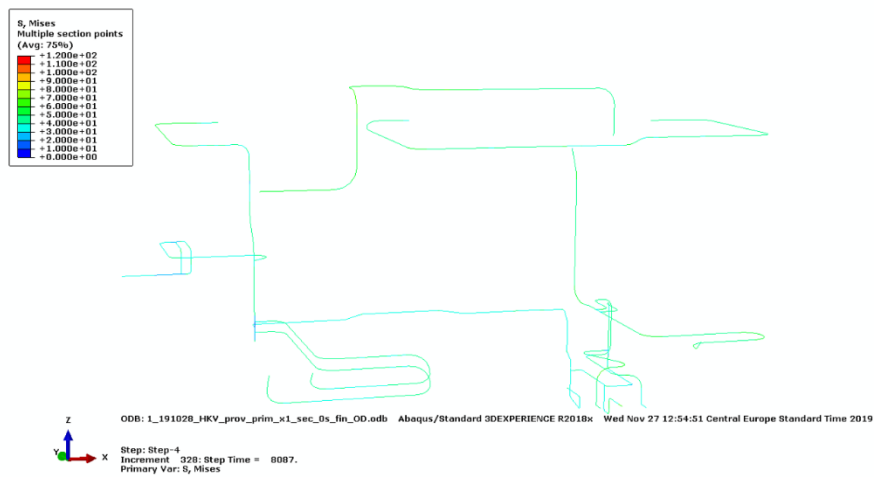


Figure 31. Von Mises stress distribution after one year.

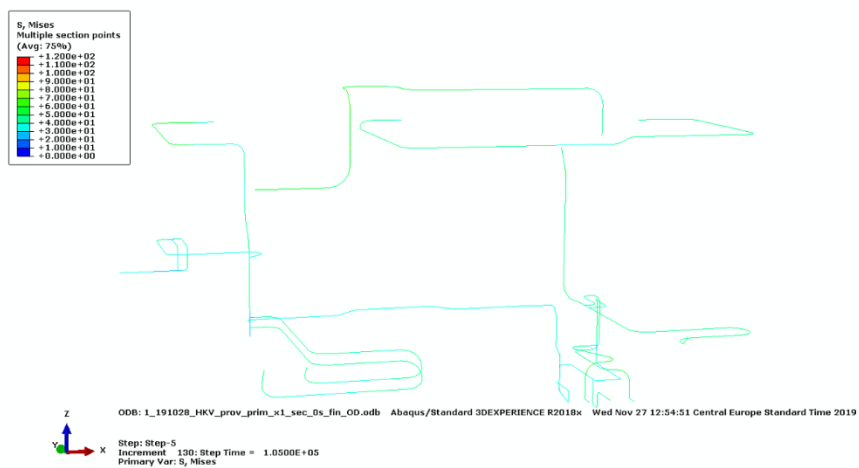


Figure 32. Von Mises stress distribution after 180 000 h.

From the figures on the pipe system, it is clear that in particular, the higher stresses in the pipe bends relax significantly during the first year. Straight pipe parts show much less stress relaxation.

In order to show the influence from considering primary creep in addition to secondary creep, the equivalent stress evolution in a single position in the pipe system calculated. In Figure 33, the evolution of the von Mises stress at the location of the MR15 weld is shown, over 180 000 hours of creep. From figure 33, it is obvious that the addition of primary creep affects the stress relaxation, but also that the effect on stress level is not very significant.

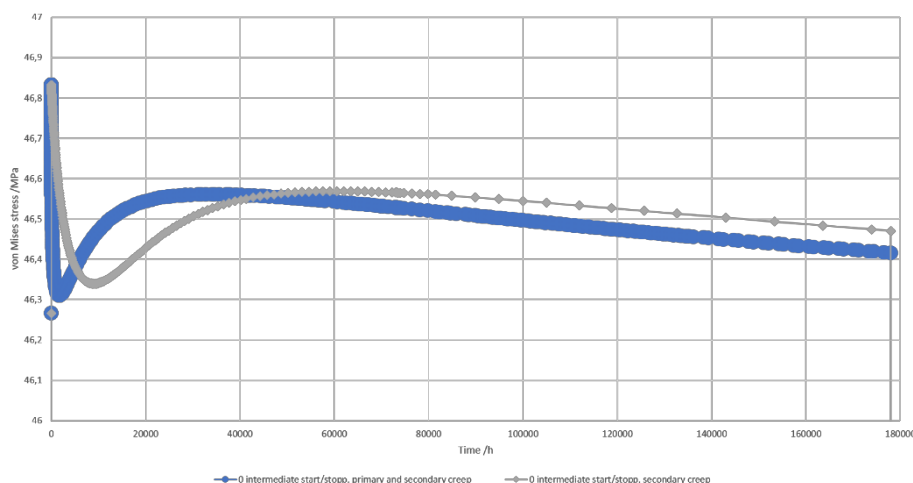


Figure 33. Evolution of equivalent von Mises stress at a location in the pipe system approximately corresponding to the location of weld MR15.

9.1.5 Effects of starts and stops

The stress distribution after 180 000 hours service without stops and the corresponding stress distribution with 10 starts/stops during the 180 000 hours is shown in figure 34 and 35 respectively. In the analysis, the start and stop process is implemented by lowering the pressure to almost zero, lowering the temperature to 20 degrees Celsius, increasing the pressure to operation pressure and lastly increasing the temperature to operation temperature.

The effect from primary creep on the stresses in the system is shown in figures 15, 34 and 35, where it is obvious that start and stops have no influence on the stress distribution in the system. They are identical in the two figures.

In addition, the von Mises stress evolution in an element at the position of MR15 is shown in figure 36, for the cases with and without stops. Exactly during start and stop, the stresses change significantly, as the pressure drops and the temperature drops. Directly when the pressure and temperature is at operational levels again, the stress level and distribution is as it was just before lowering the pressure. It is evident that there is no effect from start and stop on the stress distribution or stress level in the pipe system.

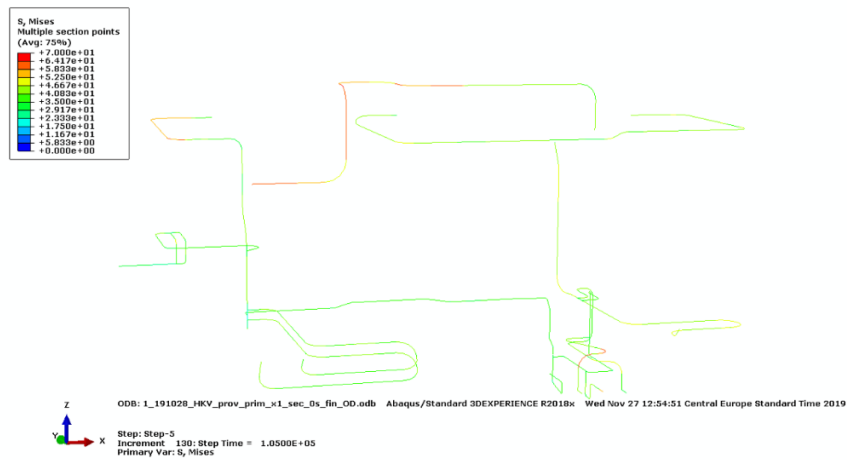


Figure 34. Stress distribution in the system after 180 000 h without intermediate starts and stops.

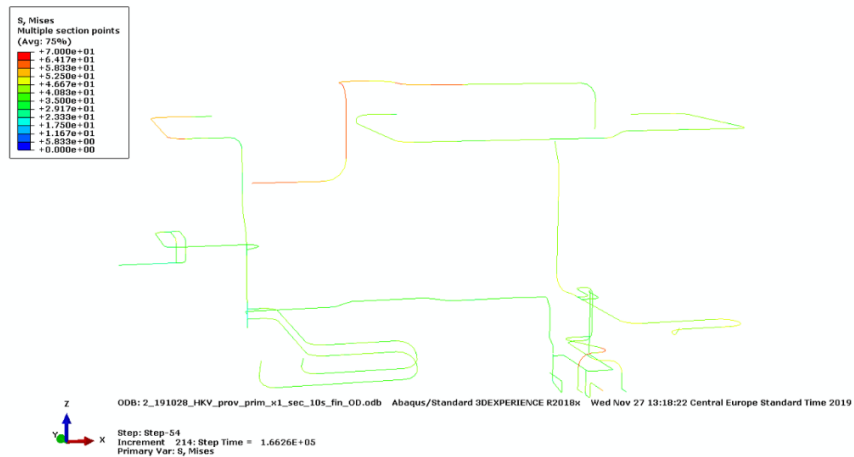


Figure 35. Stress distribution in the system after 180 000 h with 10 intermediate starts and stops.

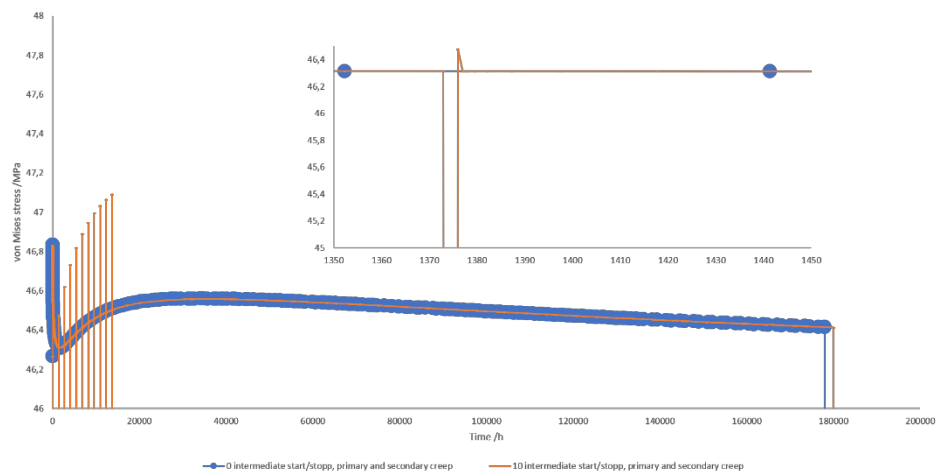


Figure 36. Evolution of equivalent von Mises stress at a location in the pipe system approximately corresponding to the location of weld MR15, with and without start and stops during service.

9.2 ANALYSES OF WELD MR05

The previously analysed weld MR05 [1] was re-analysed with the integrated and the up-dated system model. Figures 37 and 38 show the von Mises stress and creep strain distribution in MR05 after 73 000 h in service, i.e. the service time when the t-joint was cut out. In this case the creep rate in the HAZ was modelled as 3 times the corresponding parent metal creep rate. The width of the HAZ is 3,0 mm in the model and agrees with the measured width of the HAZ at the more critical side of the weld where the creep damage was observed. The creep data for the parent and the weld metal are from the impression creep testing in [1]. The creep strain is enhanced in the HAZ closest to the horizontal pipe at the 3, 6 and 12 o'clock positions. The highest creep strain, 0,59 %, is in the HAZ at one of the saddle points.

For the case when the HAZ strain rate is 6 times higher than the parent metal, the distribution of strain is very similar to the case where the HAZ strain rate is 3 times higher than the parent metal. The result is 0,71 % equivalent strain at the saddle point. In the analyses of the t-piece, the effect from primary creep was analysed with data from test of new base material. In all other analyses secondary creep only was included. Primary creep was included in the HAZ only, and only secondary effects in the other parts of the system. The reason for this is that the inclusion of primary creep is done by using a user sub-routine in Abaqus, which treats creep for a specific material. Abaqus can only use one sub-routine, and therefore only one material use primary creep. In order to see the effect from stress redistribution, different creep data must be used. Starts and stops did not have effect on the strain distribution and therefore, the overall effect of primary creep is quite small in this case. Since analyses that include primary creep are significantly more time consuming than ones of secondary creep only, primary creep has been omitted in these analyses and in those that follows.

Weld MR05 was also analysed with EN10028-2 creep data for 10CrMo9-10. Here the weld metal creep rate was set to 2 times slower than the EN10028-2 data, i.e. the same ratio as for the impact creep test results. This is the same relationship between weld and parent metals the results of the impression creep testing of the weld. For this case the maximum strain is 0,24 %, i.e. 59 % lower compared to the analyses with impression creep test data.

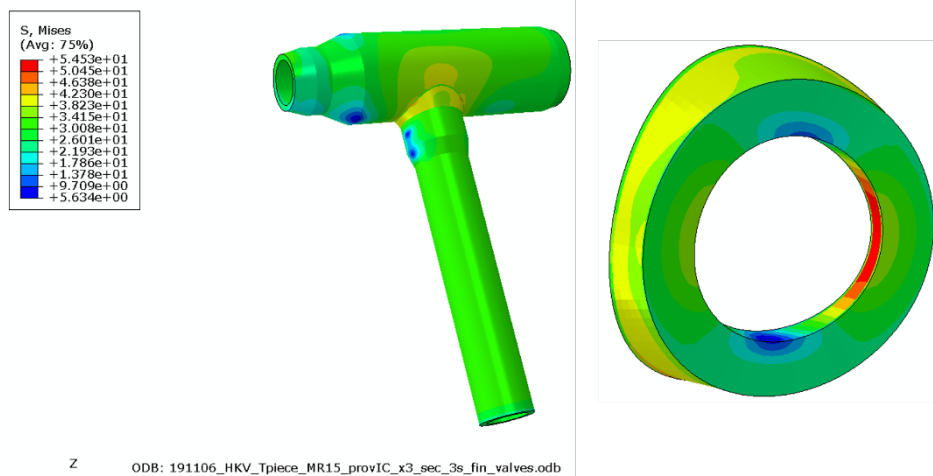


Figure 37. Von Mises stress in weld/HAZ MR05 after 73 000 h in service along with the T-piece base metal is shown. Creep data for Impression test material was used for the simulation.

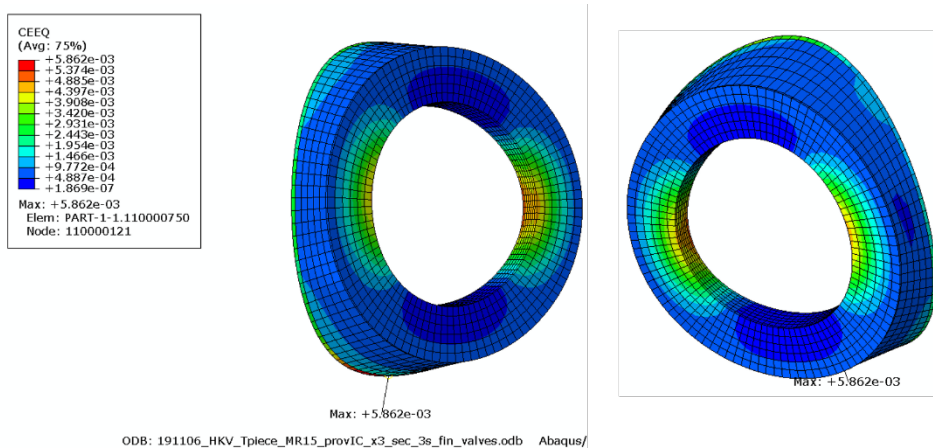


Figure 38. Equivalent strain distribution in weld MR05 with impression creep data of parent metal, HAZ (3x parent metal creep rate) and weld metal.

In order to study the relaxation and evolution of creep strain in the HAZ, where the most strain occur, detailed Figures 39 and 40 demonstrate the behaviour of the model for different material parameters in this region. The results as regards creep strain are summarized in table 9. Plotted in figures 39 and 40 are the values corresponding to the integration points in the FE-model, whereas the values in table 9 correspond to nodal values.

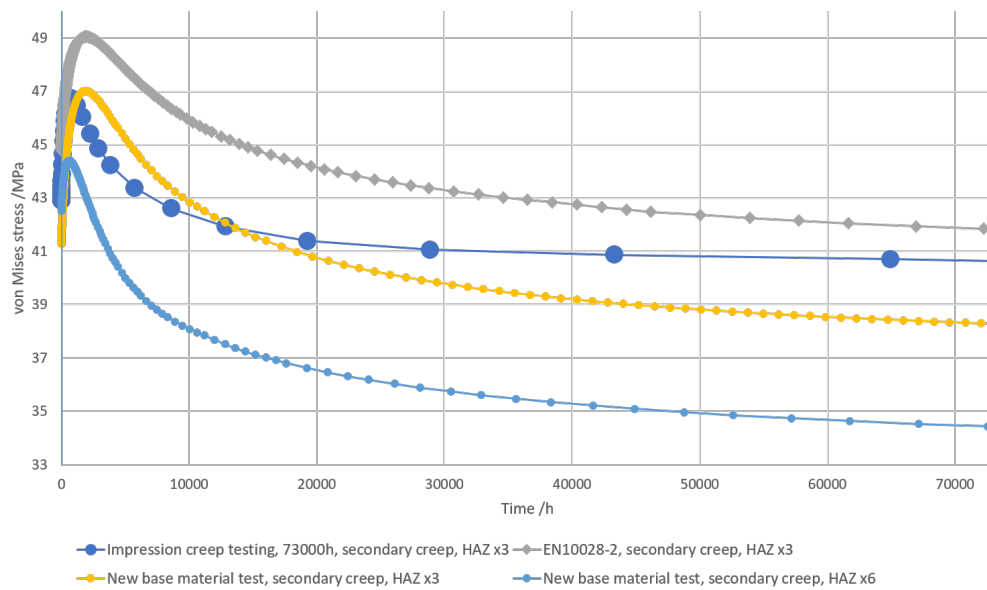


Figure 39. Relaxation of von Mises stress in the HAZ of the MR05 weld, for different material configurations.

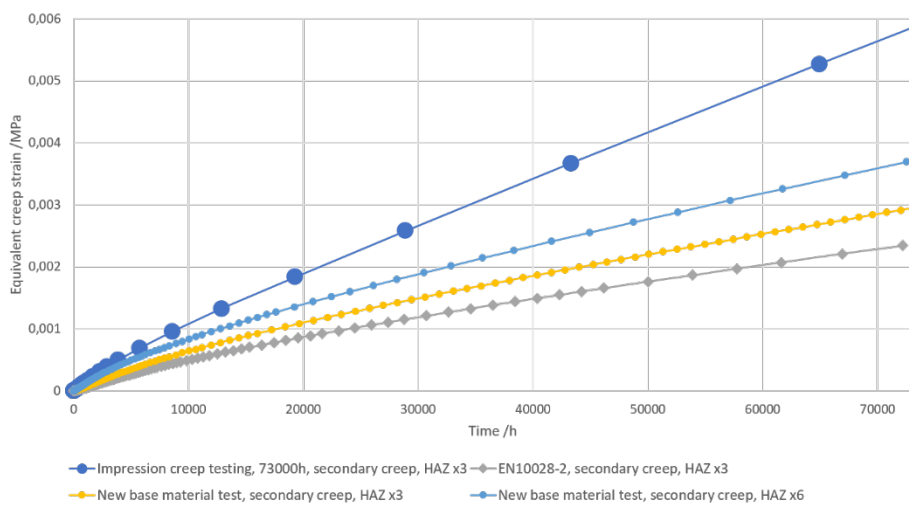


Figure 40. Evolution of equivalent creep strain in the HAZ of the MR05 weld, for different material configurations.

Table 9. Creep strain results for MR05 at 73 000 hours.

Material data	12 o'clock	3 o'clock	6 o'clock	9 o'clock
IC test HAZ-x3	0,34%	0.25%	0.59%	0.18%
IC test HAZ-x6	0.40%	0.30%	0.71%	0.24%
EN10028-2 HAZ-x3	0.17%	0.10%	0.24%	0.08%
New base metal HAZ-x3	0.18%	0.17%	0.30%	0.08%
New base metal HAZ-x6	0.20%	0.19%	0.34%	0.12%
New base metal HAZ-x6 primary creep	0.19%	0.20%	0.39%	0.13%

9.3 ANALYSES OF WELD MR15

Weld MR15 was creep analysed for secondary creep to 180 000 h for the following cases:

- Creep tested new parent metal with weld metal and HAZ where the creep rates are 0,5 and 3 times the creep tested parent metal.
- Creep tested new parent metal with weld metal and HAZ where the creep rates are 0,5 and 6 times the creep tested parent metal.
- Creep tested service-exposed parent metal with weld metal and HAZ where the creep rates are 0,5 and 6 times the creep tested parent metal.
- EN10028-2 creep data for parent metal and HAZ where the creep rates are 0,5 and 3 times the EN10028-2 parent metal creep data.
- Creep tested new parent metal with primary and secondary creep in the HAZ with creep rate 6 times the creep tested parent metal, with weld metal and parent metal where the creep rates are 0,5 and 1 times the creep tested parent metal.

By these cases the difference in creep strains after long term service is demonstrated between tabled creep data, in this case EN10028-2 data and creep test data of new (virgin) material as well as service exposed material for 180 000 h. In addition, the sensitivity of the anticipated creep properties in the HAZ is studied by using the two different creep rates 3 times and 6 times the parent metal creep rate.

Figure 41 shows the stress distribution in MR15 after 180 000 hours service for creep data evaluated from the testing of new base metal, weld metal with 0,5 x base metal creep rate and HAZ with 3 x base metal creep rate.

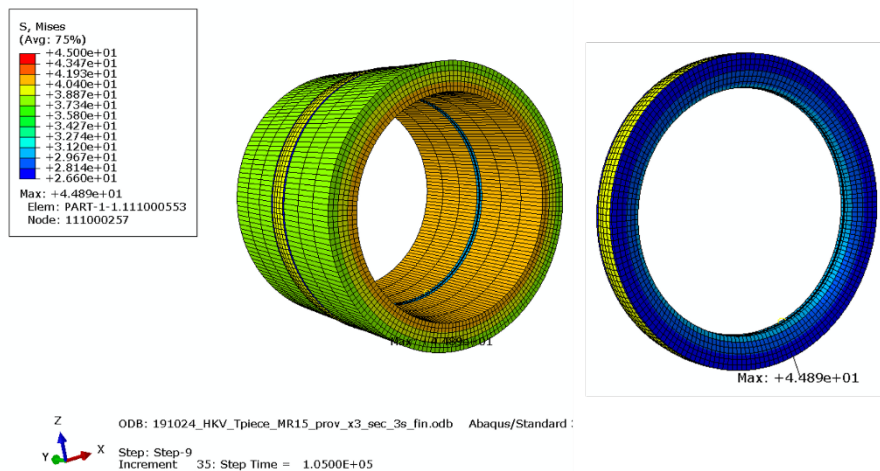
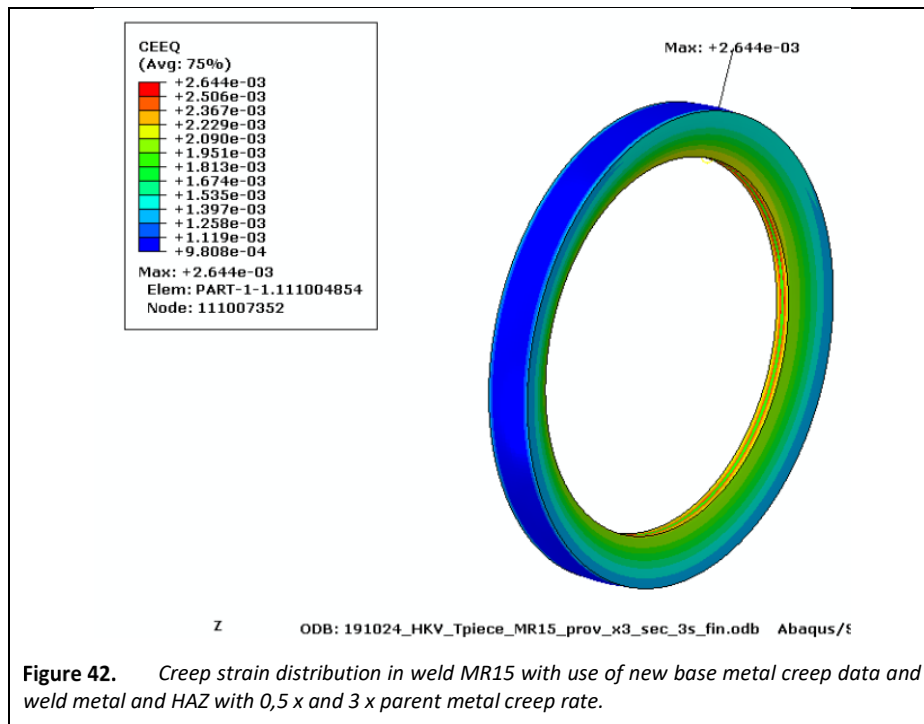


Figure 41. Von Mises stress in weld MR15 after 180 000 h in service where the adjacent pipe base metal is shown to the left and the weld metal and the HAZs alone to the right. Creep data for new base material was used for the simulation.

The highest stresses are in the weld metal where the maximum stress is around 45 MPa. The stress levels in the base metal and the HAZ are 46 and 41 MPa, respectively. During creep the stresses are distributed in such way that the regions with lowest creep rate obtains the highest stress whereas the HAZ, where the strain rate is fastest, is reloaded and obtains lower stress than the surrounding materials. It is also observed that the base metal has a stress distribution where the highest stress is at the inside of the pipe. corresponding creep strains distribution is shown in Figure 42.



The maximum creep strains are formed in the HAZs and are 0,26 % and 0,31 % for the cases with 3 x and 6 x parent metal creep rates in the HAZ, respectively, using material data from test of new base material. A double HAZ creep rate thus results in about 19 % higher creep strain in the HAZ after 180 000 h.

In order to study the relaxation and evolution of creep strain in the HAZ, where the most strain occur, detailed figures 43 and 44 demonstrate the behaviour of the model for different material parameters in this region. The results as regards creep strain are summarized in table 10. Plotted in figures 43 and 44 are the values corresponding to the integration points in the FE-model, whereas the values in table 10 correspond to nodal values.

It can be observed that the stress levels in the HAZ in the solid model is significantly lower as compared to the stress level in the pipe system analysis for the same location (MR15), see figures 33 and 43. This is explained by the redistribution of stresses between HAZ, weld and base material in the solid model, which of course is not considered in the system analysis.

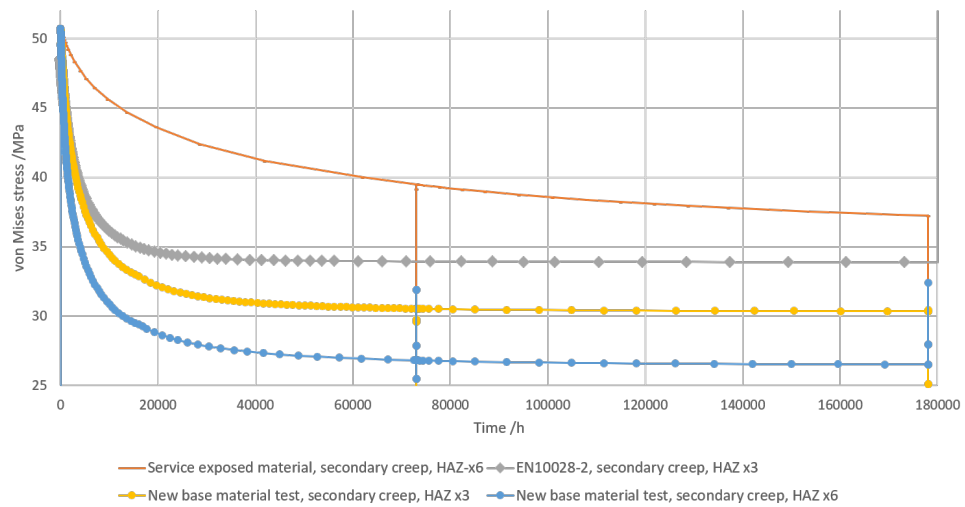


Figure 43. Relaxation of von Mises stress in the HAZ of the MR15 weld, for different material configurations.

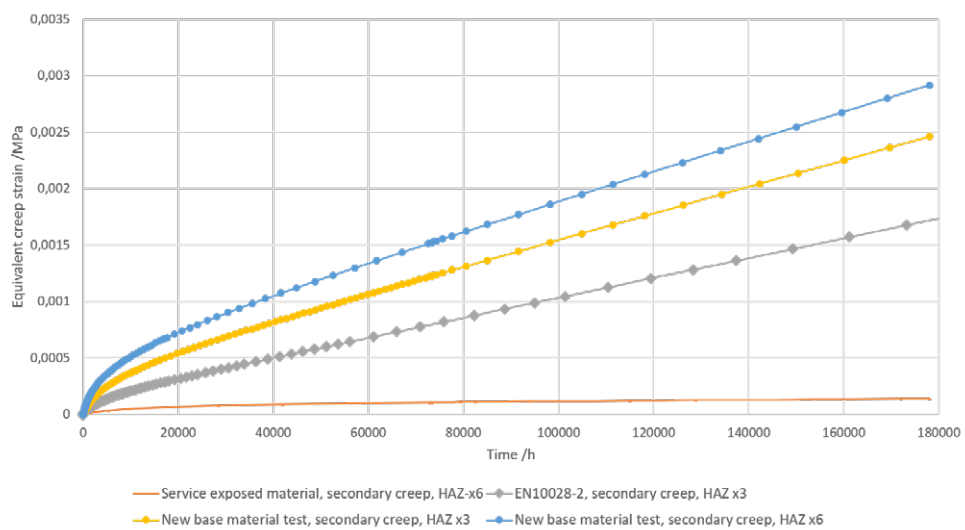


Figure 44. Evolution of equivalent creep strain in the HAZ of the MR15 weld, for different material configurations.

Table 10. Creep strain results for MR05 at 180 000 hours.

Material data	12 o'clock	3 o'clock	6 o'clock	9 o'clock
Service exposed material, HAZ-x6	0.015%	0.014%	0.014%	0.014%
EN10028-2 HAZ-x3	0.17%	0.17%	0.18%	0.18%
New base metal HAZ-x3	0.26%	0.24%	0.23%	0.24%
New base metal HAZ-x6	0.29%	0.25%	0.24%	0.25%
New base metal HAZ-x6 primary creep	0.31%	0.26%	0.24%	0.26%

10 Discussion

10.1 CREEP TESTS

Creep test of the service exposed material showed for both weld metal and base metal Norton creep exponents, $n=9,6$ and $n=12,6$, respectively, that are higher than typical values at creep testing of low alloy at current temperature and stresses. The new material, however, showed a very typical value, $n=4,2$, see Figure 5.

The resulting steady state creep rates were generally significantly higher for the service exposed base metal than for the new base metal, whereas the service exposed weld metal creep rates were much lower than for the new base metal.

These results were extrapolated to service stresses in the analyses. Although the test stresses were as low as possible for creep testing up to as much as almost 20 000 hours (80 MPa for the test with the lowest stress), the service stresses anyhow are significantly lower. The maximum stress during steady state creep was 45 MPa and 58 MPa for the pipe butt weld MR15 and the t-piece branch weld MR05, respectively. For the present results, with higher Norton exponents for the service exposed materials than for the new material and a higher Norton exponent for service exposed base metal than service exposed weld metal, the extrapolation involves changed ranking where the new material obtains the highest creep rate and the service exposed base metal even tends to obtain lower creep rate than the service exposed weld metal. A similar change in order between weld metal and parent metal creep rates has also been observed in creep testing of new welds of a 1Cr0,5Mo steel at stresses between 110 and 145 MPa [10].

The purpose of creep testing of service exposed material is in many cases to obtain an estimate of the remaining creep life. Successful test methods are, for example: Iso-stress creep testing and the Omega method. Unfortunately, it is not possible to establish constitutive equations, like the Norton creep law, with these methods. For constitutive equations, which enables creep analysis, it is necessary to conduct tests at different stress levels at constant temperature. However, extrapolations to service stresses are not straight forward. In addition to differences in Norton exponent values there is typically one or two shifts to a lower value of the Norton exponent at lower stresses [11]. This can be observed when creep data is plotted in stress vs. minimum creep rate diagram, such as figure 5. Such shift has previously been observed to occur at stresses of about 120-140 MPa for some virgin weld metals of low alloy steels [12] but most test series in that study, where the lowest stresses were 90-100 MPa, did not show such behaviour. Nevertheless, for the present new base metal $n = 10,5$ was evaluated when it was creep tested at 140 -180 MPa in [1]. Thus, there is a shift to $n = 4,2$ at about 100 MPa. A shift in n -value did not appear at the present creep testing of service exposed material which would be expected at least for the at the lowest test stress levels. The simulations that use data from these materials then involve extremely low creep rates at service temperatures compared to tabled data and test results from new material, resulting in very low creep strains, see Table 10.

For weld MR05 creep data of impression creep tests of the actual weld were used. These tests were conducted during significantly shorter times than the present creep testing. However, a Norton creep constant n could not be evaluated from these tests and the same value as for EN10028 data was taken. Thus, there is a constant difference in creep rate between impression creep and EN10028-2 at all stresses. According to the impression creep test results the creep rates in the weld metal and the HAZ were 0,5 and 3 times the parent metal. These factors were used also in the analyses with new base metal and EN10028-2 data. The HAZ creep rate is difficult to measure directly. In order to study the effect of relatively higher HAZ creep rates a factor of 6 times the parent metal was chosen. In [10] HAZ strains were measured at cross weld creep tests by strain gauges. The results showed up to 5 times higher strains in the intercritical part of the HAZ compared to the base metal. The stress state is uniaxial in a base metal creep test specimen, but a cross-weld specimen involves multiaxiality. Although the stress state in the cross-weld specimen is not the same as in a pipe weld the results indicate that the chosen factor of 6 is within a relevant range.

10.2 OBSERVED CREEP DAMAGE

The observed creep damage at the surface agrees with the investigation in [1] with exception for weld metal at the 6 o'clock position where micro cracks were observed in [1] whereas not more than damage rating 3a appeared in the present investigation. The most likely explanation for this is that the pipe weld was unaffected in [1] whereas a cut sherd from the actual position was tested recently, see Figure 1. Thus, it is likely that there was a slight displacement between the examined positions between the two investigations.

The creep damage was not much spread out through the wall thickness. Most damage in addition to the surface damage was observed around the fusion line a distance below the surface, at the intersection between two weld beads. Similar behaviour has been observed previously [13]. Local tri-axiality has been suggested to explain the behaviour of enhanced sub surface creep cavitation in the HAZ, particularly leading to type IV cracks (circumferential creep crack in the fine grained and the intercritical regions of HAZs).

10.3 CREEP ANALYSIS

The resulting creep strain calculated using FE-analysis is lower than the creep strain expected considering the damage found in samples.

A comparison of the results from simulation of creep strain formation in Abaqus can be made with formula-based calculation of the estimated creep strain in the HAZ of the T-piece and MR15 weld, as a rough estimate, using the material equation 8, equivalent stress level (calculated with the FE-model) at the point of interest and time in service. Since the bulk of the creep strain seems to come from secondary strain effects, and the fact that the process is unaffected by starts and stops, it could be argued that the simulation and formula-based values of creep strain could be of the same order of magnitude. The calculated stress level used for evaluation of creep strain from secondary effects in the HAZ of the MR15 weld is

33.5 MPa, and the corresponding stress level in the HAZ of the MR05 weld is 40.6 MPa. The stress levels for evaluating creep strain from primary creep effects are 37.5 MPa and 46 MPa respectively.

In the calculations using equation 8, the stress levels used are representative values, during operation, at the point where the creep strain is reported in section 9.2 and 9.3. Values are estimated based on stress plots seen in figures 39 and 43.

The results are summarized in Tables 11 and 12 below. The results are indeed in the same order of magnitude, and very similar in some cases. The differences are explained by the fact that the stresses used in equation 8 are not exactly the same as in the FE-calculation, and also from the fact that in the FE-analysis, the stress deviator are taken into account.

Table 11. Comparison of creep strain results in the MR05 HAZ from FE-simulations with evaluations of the material equation 8, using stress level calculated using FE-analysis.

	FEM (Abaqus)	Eq. 8	Eq. 8 / FEM
IC test HAZ-x3	0,590%	0,494%	0,84
IC test HAZ-x6	0,710%	0,988%	1,39
EN10028-2 HAZ-x3	0,240%	0,148%	0,62
New base metal HAZ-x3	0,300%	0,186%	0,62
New base metal HAZ-x6	0,340%	0,372%	1,09
New base metal HAZ-x6 primary creep	0,390%	0,276%	0,71

Table 12. Comparison of creep strain results in the MR15 HAZ from FE-simulations with evaluations of the material equation 8, using stress level calculated using FE-analysis.

	FEM (Abaqus)	Eq. 8	Eq. 8 / FEM
Service exposed material, HAZ-x6	0,015%	0,000%	0,00
EN10028-2 HAZ-x3	0,170%	0,118%	0,69
New base metal HAZ-x3	0,260%	0,176%	0,68
New base metal HAZ-x6	0,290%	0,353%	1,22
New base metal HAZ-x6 primary creep	0,310%	0,236%	0,76

10.3.1 System analysis

The resulting strain distribution in Figure 28 with both primary and secondary creep after 180 000 hours show enhanced with 0,5 % - 1,0 % creep strain in some parts of the system. The only exception is one bend where maximum strain is 2,1 %. This bend is in a pipe section denoted H9LBA19BR004. In the compilation of replica testing of the system that was received from Eon in association with the previous project [1] replica test results from this section were included. In fact, no

bends, only welds have been replica tested according to these files. There is one pipe weld close to actual bend, demoted MR40 and situated at the upper end of the bend, that was replica tested 2002 with a small amount of creep cracks as a result. This is well supported by the simulation results. The actual Caepipe analysis showed a utilisation factor of 1,02 at the MR40 position. That is slightly higher than allowed but not an obvious indication of severe creep.

In contradiction to results in [1], starts and stops do not influence the stress distribution in the system. In simulations of repeated starts all starts were at the same condition as the first one in the previous analysis. In the present analysis all start conditions were the same as at the nearest stop before the start. This is the correct way to describe the start and stop conditions and gives the present results which certainly are not so surprising as the previous ones. In Figure 34 it is seen that the stop and start time is within a few hours. Thus, the observed absence of start and stop effect appears even when the thermal transients are significantly faster than in the reality.

The effect of primary creep quite significant as indicated in the results in [2]. For the system analysis the case with primary creep gives up to 40 % higher strain than the case with secondary creep only, see Figures 26 and 38 respectively.

10.3.2 Analysis of weld MR05

Significant creep cavitation was observed [1] at the 3, 6 and 12 positions of the HAZ that is closest to the horizontal pipe. The enhancements in strain from the numerical simulations coincide with very well with the creep damaged positions. This is a clear improvement compared to the results in [1] where the highest strain was predicted at the 9 o'clock position. The reason for this is clearly that the model comprises the entire system. In the previous model the branch pipe was cut and fixed after the first bend after the t-piece. Thus, high bending forces were induced that naturally do not exist when the entire system is included since there is no fix point in this area.

The resulting strain levels in the HAZ at the positions of the highest observed creep damage at the 6 and 12 o'clock positions is between 0,17 % to 0,71 % depending on chosen creep rate in the HAZ and experimental or EN10028-2 creep data. The creep damage was rated to damage class 3bC, which is defined as strings of cavities with more than 1600 cavities/mm². Such creep levels of damage may be associated with significantly higher creep strains than the resulting ones from the analysis, especially in comparison with uni-axial creep test results. However, multiaxiality and complex constraint effects occur in the HAZ and they can involve low creep ductility and high levels of local creep damage [14].

10.3.3 Analysis of weld MR15

Weld MR15 showed higher stresses in the inside of the base metal compared to the outside. The typical behaviour is that the highest stresses appear at the inside of a pipe in a creep process but over time the stresses re-distribute and at a certain stage the highest stresses are at the outer part of the wall. This is also true in the present case for the circumferential stress (principally equal to maximum principal stress in

this case). However, in Abaqus, the creep law uses the von Mises stress by default. The distribution of creep damage from metallographical examination of the weld MR15 reveal that the most damage is found slightly below the outer surface of the HAZ. Calculating the von Mises stress in the region, the maximum stress is found on the inside of the pipe, in both the weld material and the HAZ as shown in Figure 41. In Figure 45 the von Mises and the maximum principal stress distributions are compared to each other after 180 000 creep with use of the new base metal creep data. It is obvious that maximum principal stress matches the creep damage distribution in the weld much better.

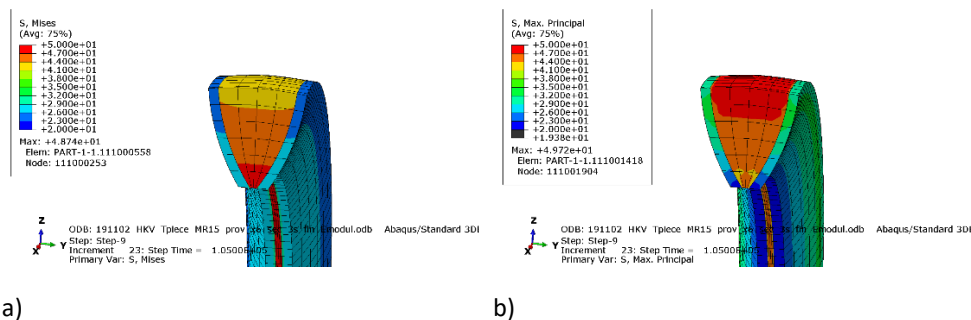


Figure 45. Von Mises (a) and maximum principal stress (b) distributions after 180 000 hours.

Although Abaqus consider maximum principal stress in the calculation of creep strain it is obvious that the von Mises stress criterion dominates as the FE-analysis calculates the maximum creep strain on the inside of the pipe.

Calculating the maximum principal stress in the MR15 region, the maximum values are instead found on the outside of the pipe in both the weld and in the base material. In the HAZ, the maximum stress is found slightly below the outside surface of the pipe. This also correlate well with damage found in the sample of the MR15 weld. This indicate that the use of a dominating influence of the maximum principal stress in the creep law is worth investigating in some detail.

For MR15 the resulting creep strains are lower than what may be expected in comparison to the observed creep damage in the weld. With the nominal service loads, that were used for the analysis, there will not be higher stresses and strains. The effect of increasing the HAZ creep rate from 3 x to 6 x the base metal creep rate was moderate.

11 Practical Implementations, recommendations and further work

Creep testing of service exposed material by iso-thermal creep testing was shown to be difficult to interpret at extrapolations to service stresses. For remaining life purposes, the isostress method, which has been shown to work very well, is preferable.

The new base metal that was creep tested showed similar Norton creep law behaviour as an average material of 10CrMo9-10. Tabled creep data is by tradition evaluated from the average results from several creep test series. There is typically a ± 20 % scatter band in stress in a stress – rupture time diagram that covers all creep test results. In an analysis of a critical part of a system a screening of actual creep rates can therefore be recommended. Semi destructive test methods, such as impression creep and small punch testing that also involve relatively short testing times are well suited for this.

The creep simulations give more precise and more detailed information of stresses and strains than elastic analyses. The analysed strain distribution in the branch weld was well verified by observed creep damage. Severe observed creep damage close to the bend with enhanced creep strain in the simulation is also in agreement. Thus, the creep analysis gives considerably better precision for the selection of positions for replica testing.

However, further work is required with regard to the results of the pipe weld where the maxim principal but not the von Mises strain distributions and strain levels did agree with observed creep damage. Since the creep strain distribution through the wall agreed with the von Mises stresses in this case it must be sorted out some rules for how to choose the accurate stress criterion.

In addition, further studies of the effect of constraint and multiaxiality on creep ductility is needed in order to fully understand correlation between creep strain and creep damage development in welded components.

Nevertheless, the present project has resulted in important steps to enable detailed prediction of remaining creep life of welded components in high pressure steam pipe systems.

12 Conclusions

Creep simulations of the entire steam pipe system in Heleneholmsverket have been conducted. Creep data for the analyses were produced by creep testing of service exposed base and weld metals from a pipe weld from the system. In addition, the creep tested weld was studied metallographically in purpose to map the creep damage and make it possible to compare the damage development with the resulting creep stress and strain distributions in the weld. In a previous project also a t-piece branch weld was investigated in a similar way and the results were used for verification of the re-analyses in present project with the updated system model.

An Abaqus model of the entire steam pipe system was created and verified in comparison to a corresponding elastic Caepipe model. The Norton creep law was used for the simulations. In addition, also primary creep was analysed.

1. The effects of primary creep on the long-term creep behaviour was significant with 40 % higher total strain at the location with the highest strain.
2. There is no effect of starts and stops on the stress and strain distributions in the system during creep.
3. The system analysis results showed enhanced strains up to 2,1 % at one bend and 0,5 % - 1,0 % in some parts of the system. Although replica testing has not been conducted directly at the bend (only welds were included in the replica test programme) the high strains in the simulations indirectly agree with the observations of small creep cracks when performing replica testing in a weld close to the actual bend. Furthermore, several components in the system has been exchanged due to creep crack formation.
4. Moderate levels of creep of damage were observed in the pipe weld. The analysis of this pipe weld gave somewhat lower creep strains than expected. The stress and strain distributions agreed for the maximum principal stress criterion but not for the von Mises stress that Abaqus by default uses for creep analyses.
5. The analysis of the branch weld agreed well with observed creep damage distributions whereas the maximum strain level of 0,71 % appears to be rather low in comparison to the quite extensive creep damage. However, local constraint and multiaxiality in welds lead to significantly lower creep ductility compared to uniaxial creep and contribute to a reasonable agreement between the strain and the damage levels.
6. The creep tests of service exposed material resulted in relatively high Norton creep law exponents and no shift to lower values at the lowest tested stresses. It is hardly possible to perform tests at even lower stresses and therefore the simulations at service conditions resulted in unreasonably low creep strains.

13 References

- [1] J Storesund et.al; Life assessment of high temperature piping, Energiforsk report 2015:187
- [2] R Norling, R Sollander, J Storesund; Effect of stress relaxation on creep of steam pipe systems, Energiforsk 2016:237
- [3] P Segle, P Algotsson, Å Samuelsson; Inverkan av ingrepp i ångledningssystem på dess återstående livslängd, Energiforsk rapport 1999:672
- [4] Metallic materials - Uniaxial creep testing in tension - Method of test, SS-EN ISO 204:2018
- [5] P Auerkari, J Salonen, K Borggreen; Guideline for evaluating in-service creep damage, Nordtest NT TR 302, September 1995.
- [6] SS-EN 13480-3, 2017
- [7] Dassault Systèmes, 2014. Abaqus Analysis User's Manual Volume I-V, Version 6.14, Abaqus INC.
- [8] CAEPIPE, Pipe Stress Analysis Software, Version 7.30.
- [9] SS-EN 10028-2, 2017
- [10] S-T Tu, P Segle, J-M Gong; Creep damage and fracture of weldments at high temperature, Int. J. Pres. Ves. And Piping 81 (2004) 199-209
- [11] R.W. Evans and B. Wilshire. Introduction to Creep. Institute of Materials, London, 1993.
- [12] Rui Wu, Jan Storesund, Kjeld Borggreen and Carl von Feilitzen; Creep properties and simulation of weld repaired low alloy heat resistant CrMo and Mo steels at 540°C Sub-project 2 – Ex-serviced 2.25Cr1Mo weld metal and cross weld repairs, Energiforsk report 2006:980.
- [13] D. J. Abson and J. S. Rothwell; Review of type IV cracking of weldments in 9– 12%Cr creep strength enhanced ferritic steels, International Materials Reviews, November 2013, 58(8), 437-473.
- [14] Francis et al, Type IV cracking in ferritic power plant steels, Mat. Sci. and Technology 2006 Vol. 22, no 12, 2006 pp. 1388-1395.

14 Appendix 1 Micrographs of creep tested material

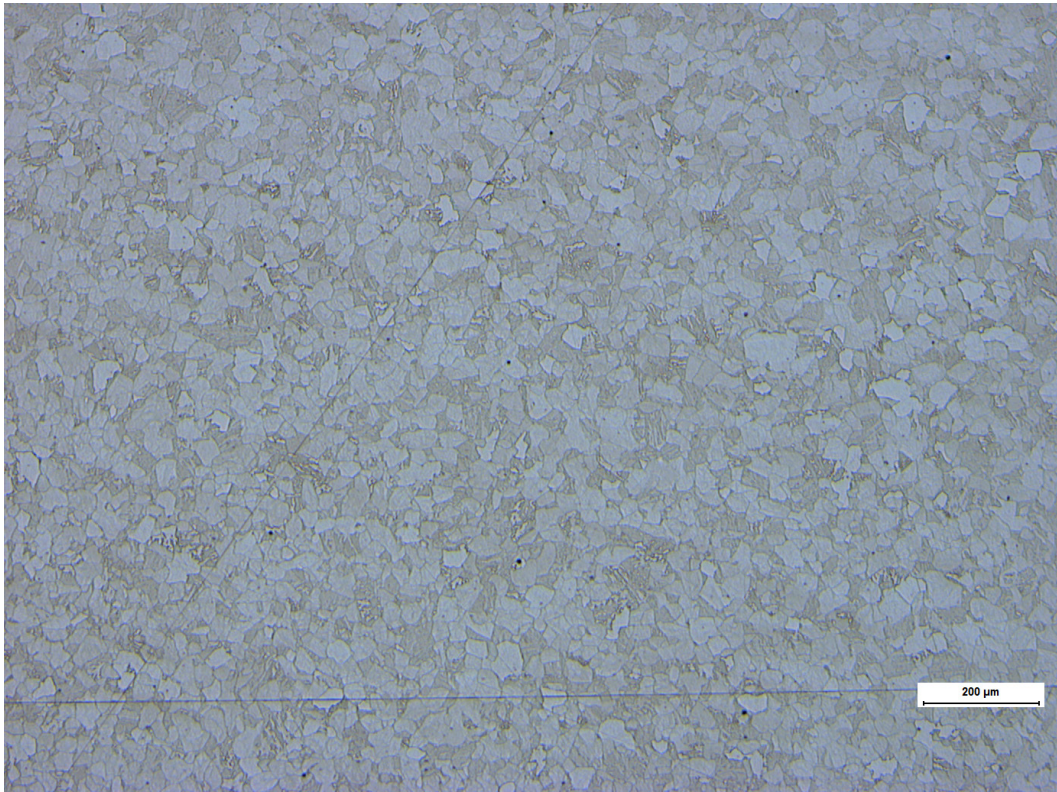


Figure m INSP-01 Middle of gauge length. 50x.

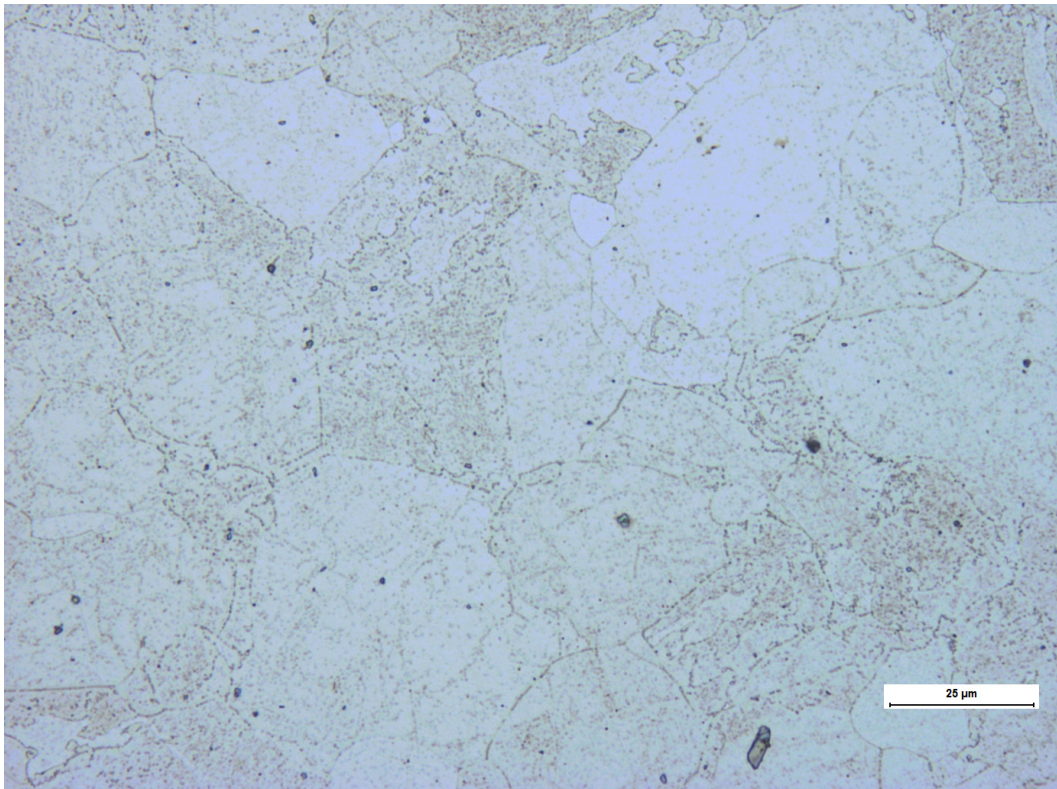


Figure o INSP-01 Middle of gauge length. Separate cavities class 2a or 2b. 500x.

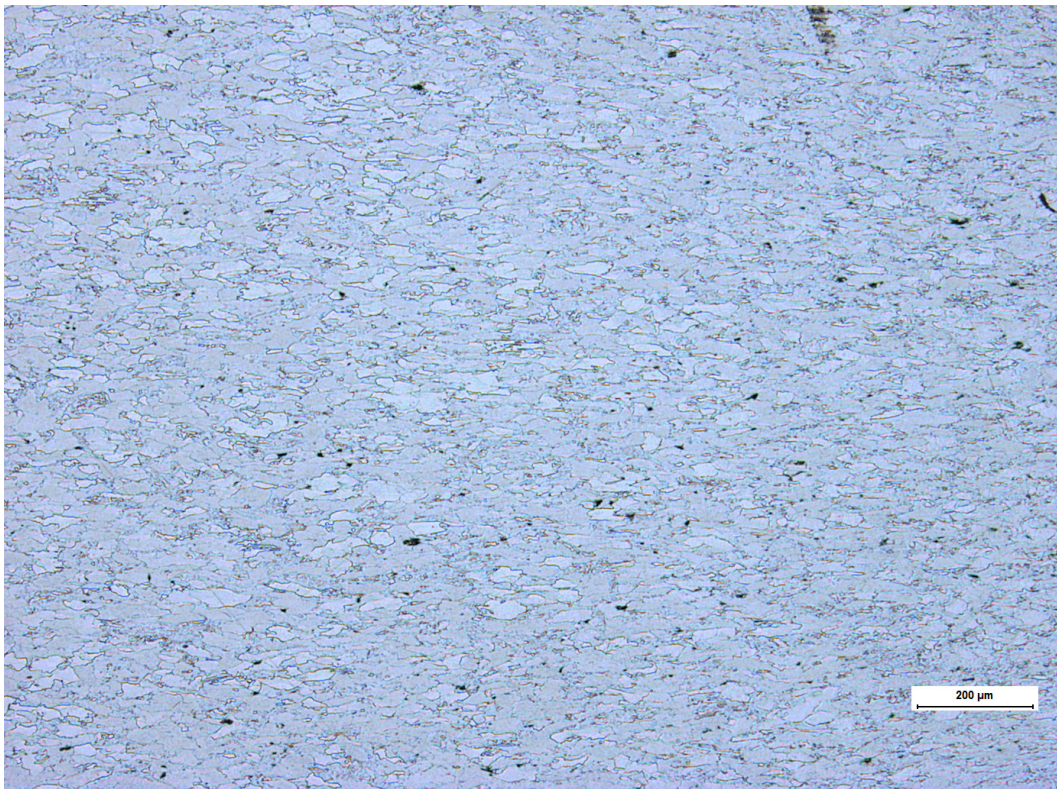


Figure 1 INSP-02 close to fracture. 50x.

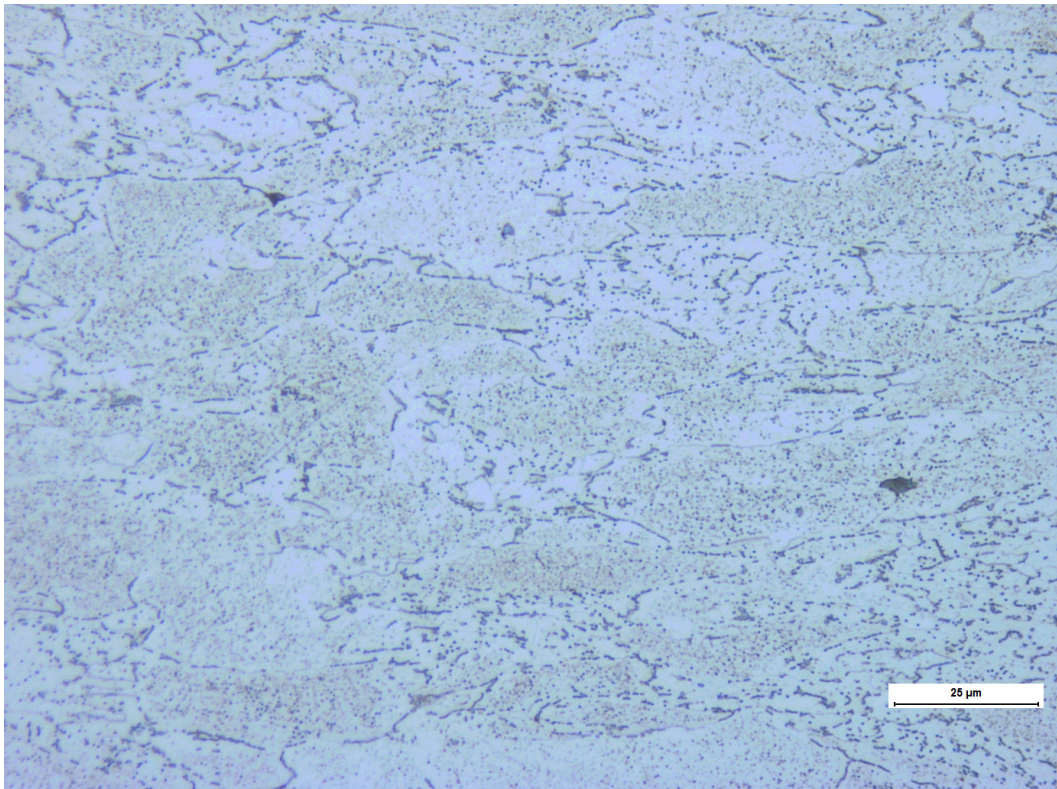


Figure 2 INSP-02 close to fracture. 500x. Damage class 0 or 1.

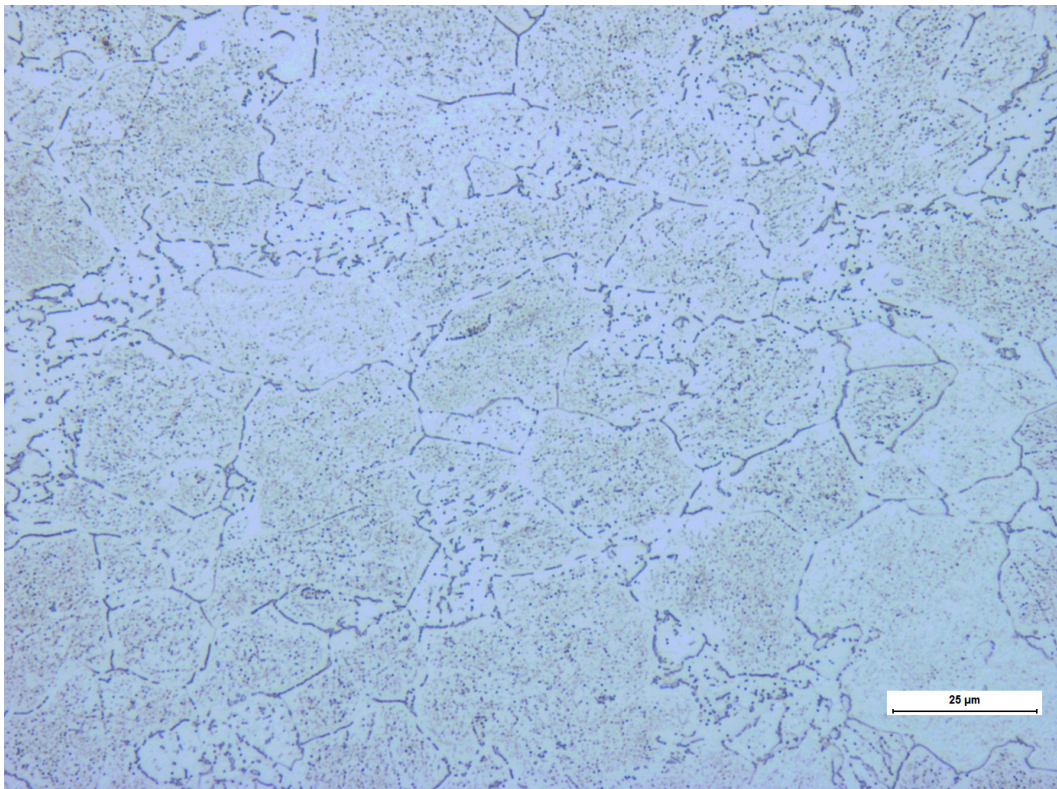


Figure 3 INSP-02 far from fracture. 500x. Damage class 0.

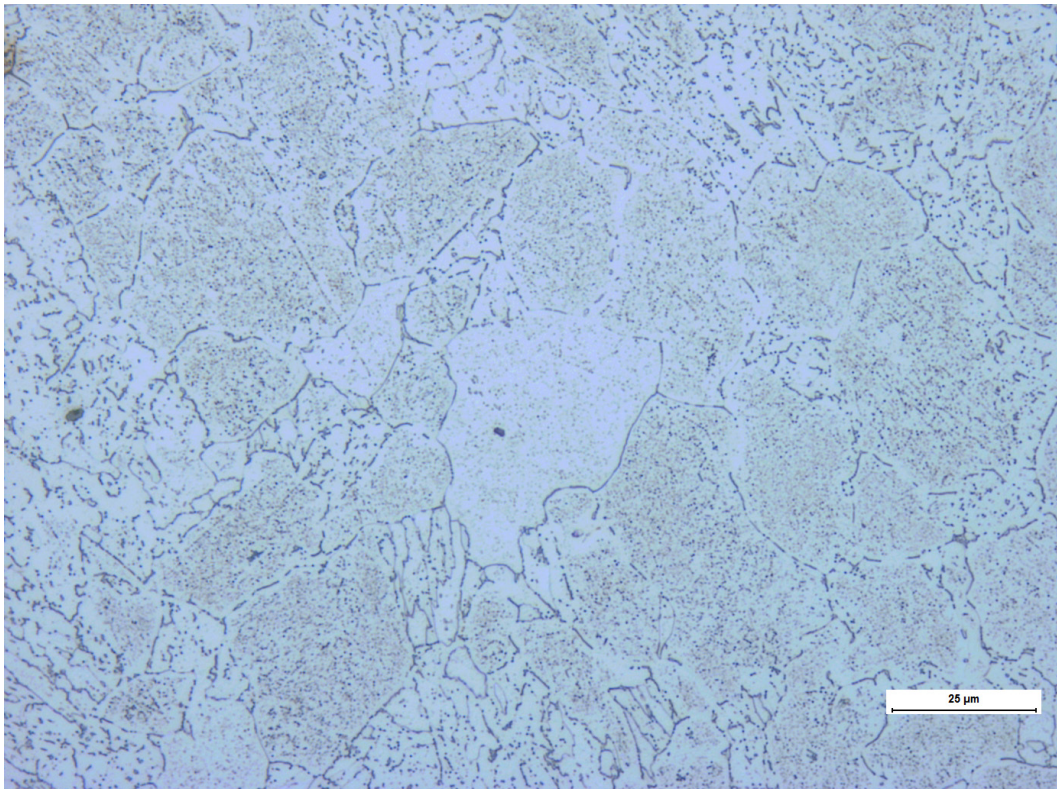


Figure 4 INSP-02 head of specimen. 500x. Damage class 0 or 1.

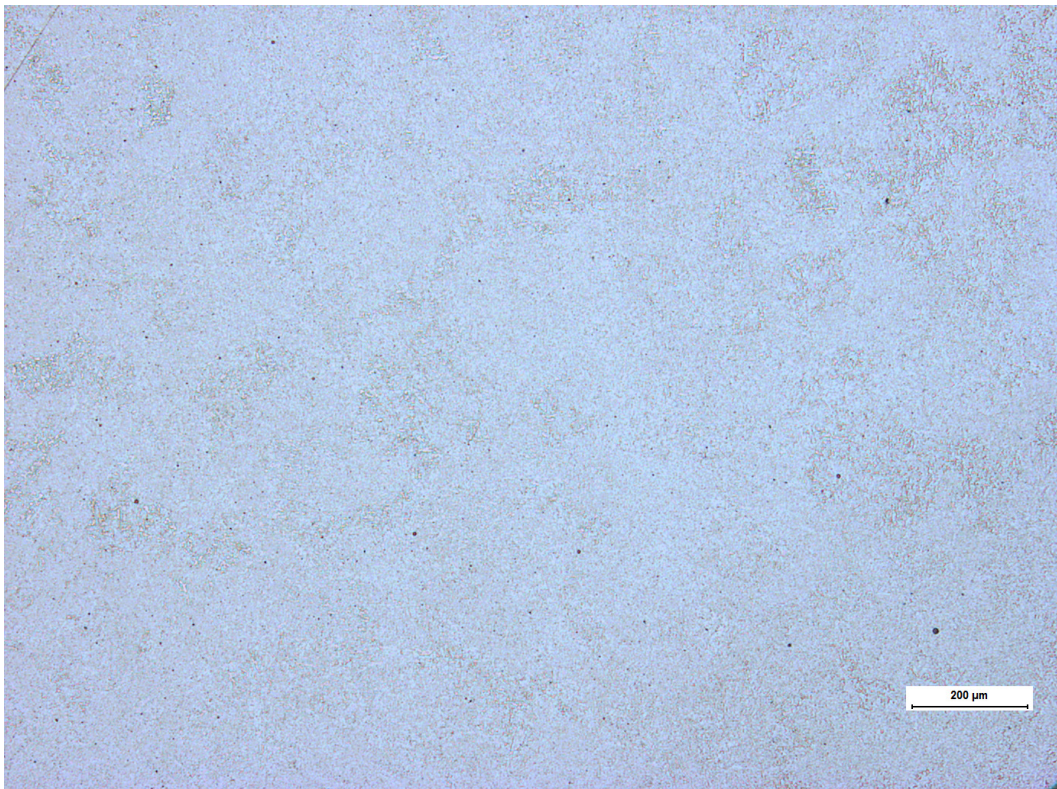


Figure 5 INSP-1-3 Middle of gauge length.50x.

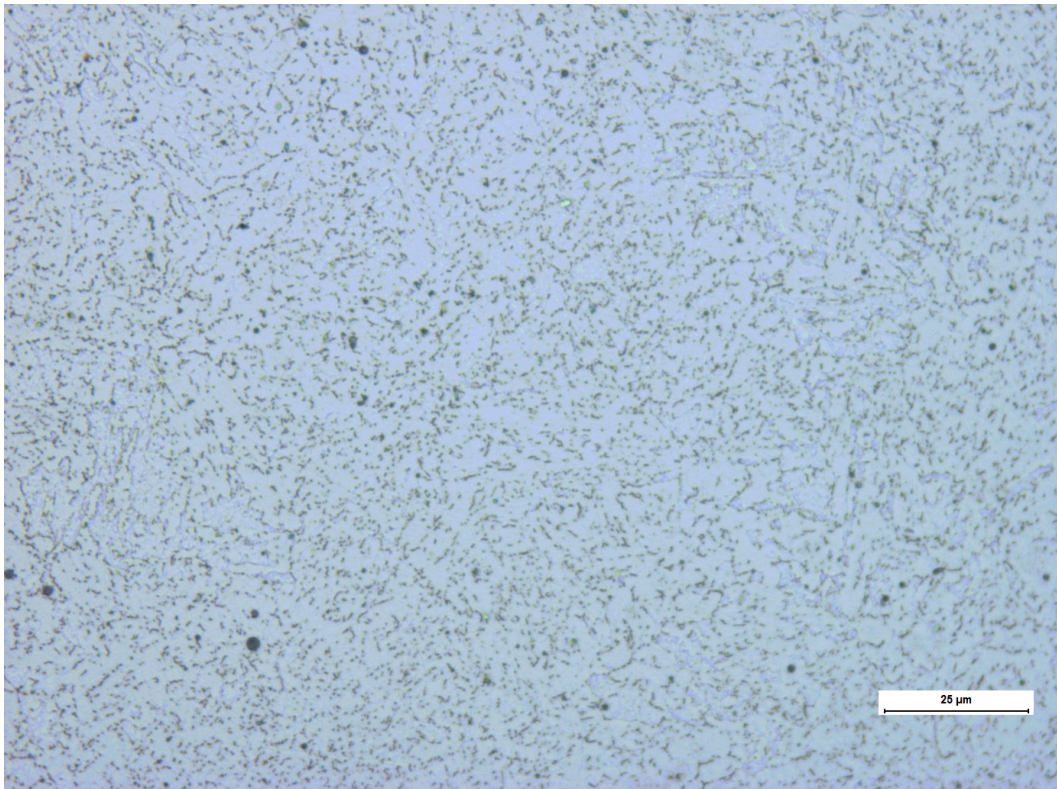


Figure 6 INSP-1-3 Middle of gauge length. Separate cavities class 2b. 500x.

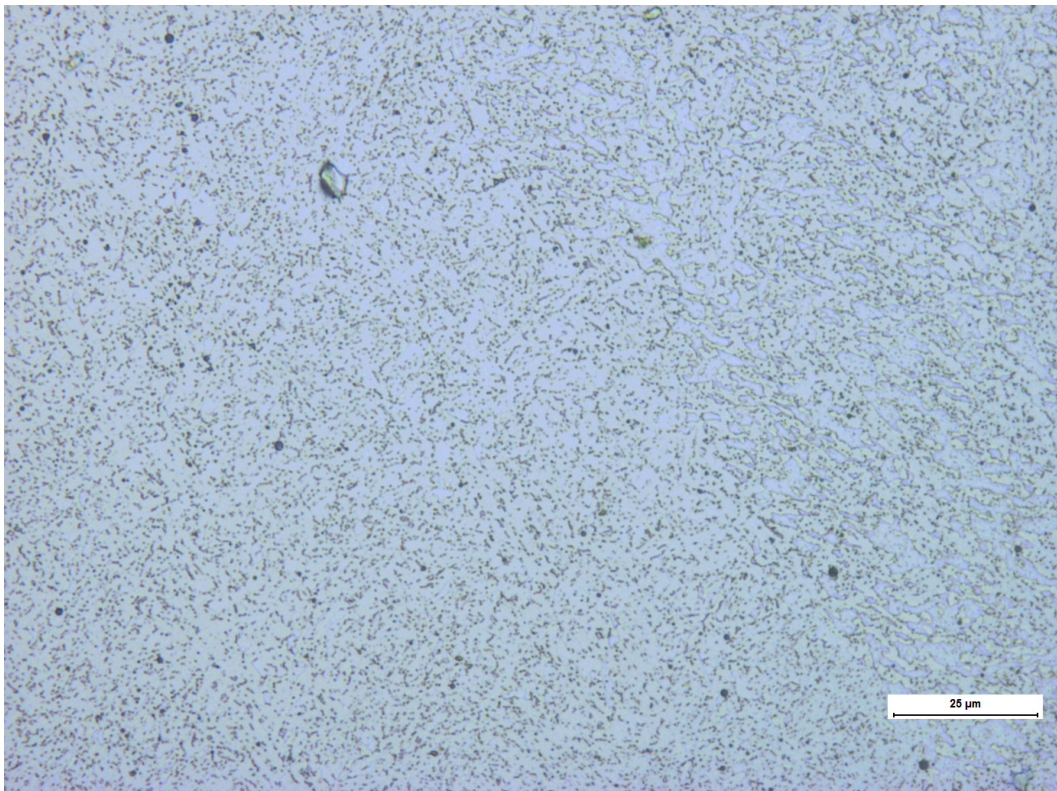


Figure 7 INSP-1-3 untested weld metal. Separate cavities class 2b. 500x.

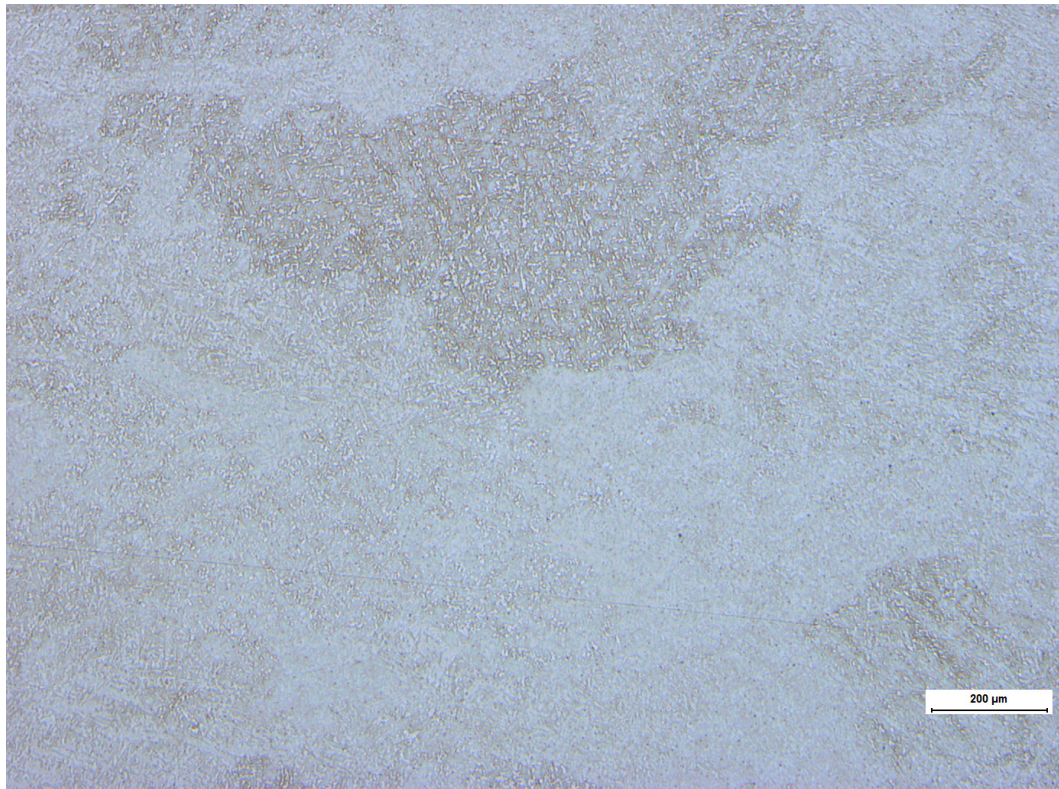


Figure 8 INSP10-2 Middle of gauge length.50x.

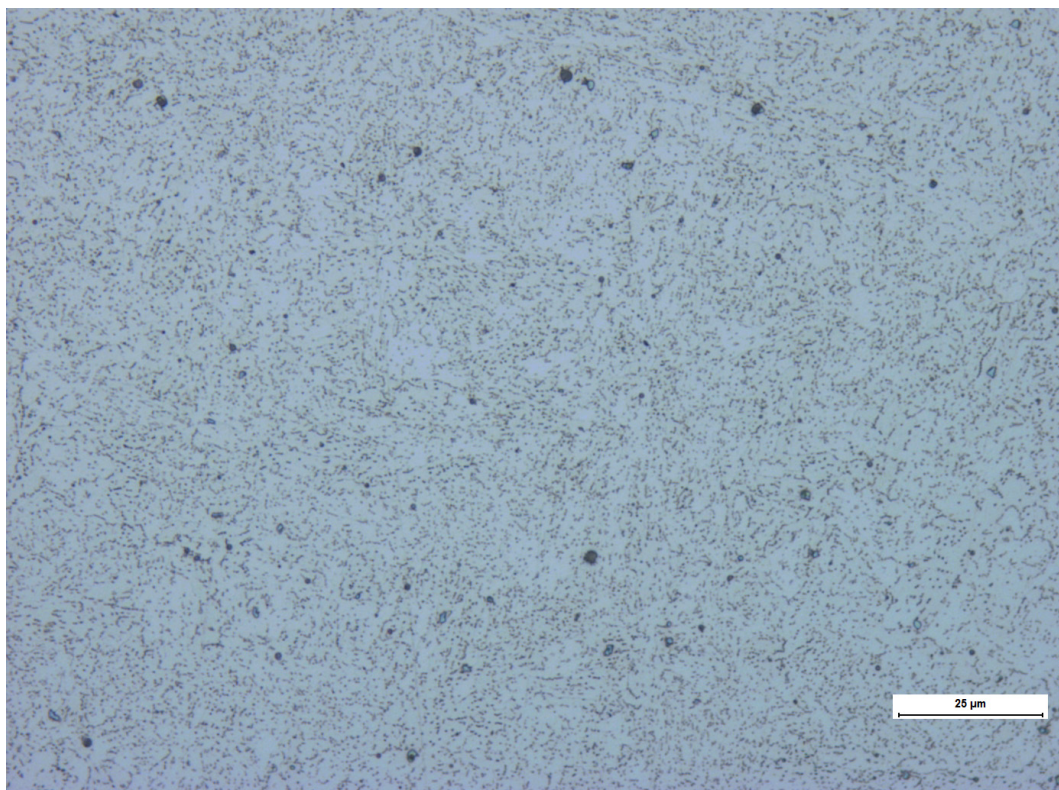


Figure 9 INSP10-2 Middle of gauge length. Separate cavities class 2b. 500x.

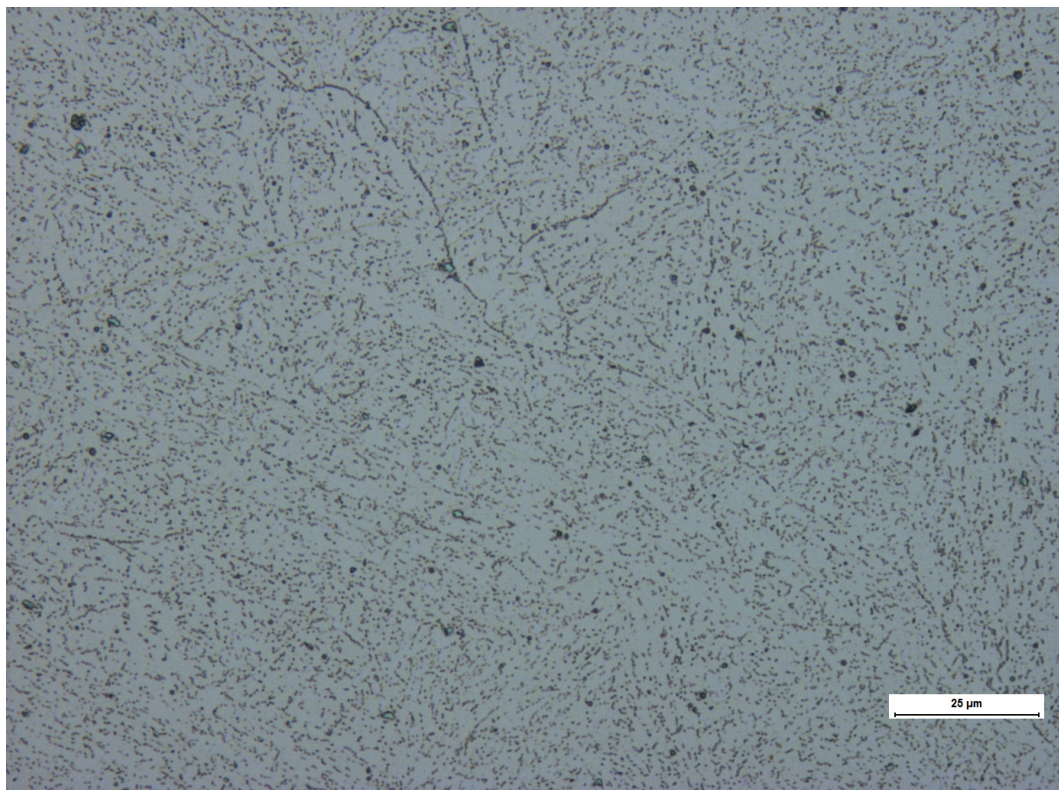


Figure 10 INSP10-2 untested weld metal. Separate cavities class 2b. 500x.

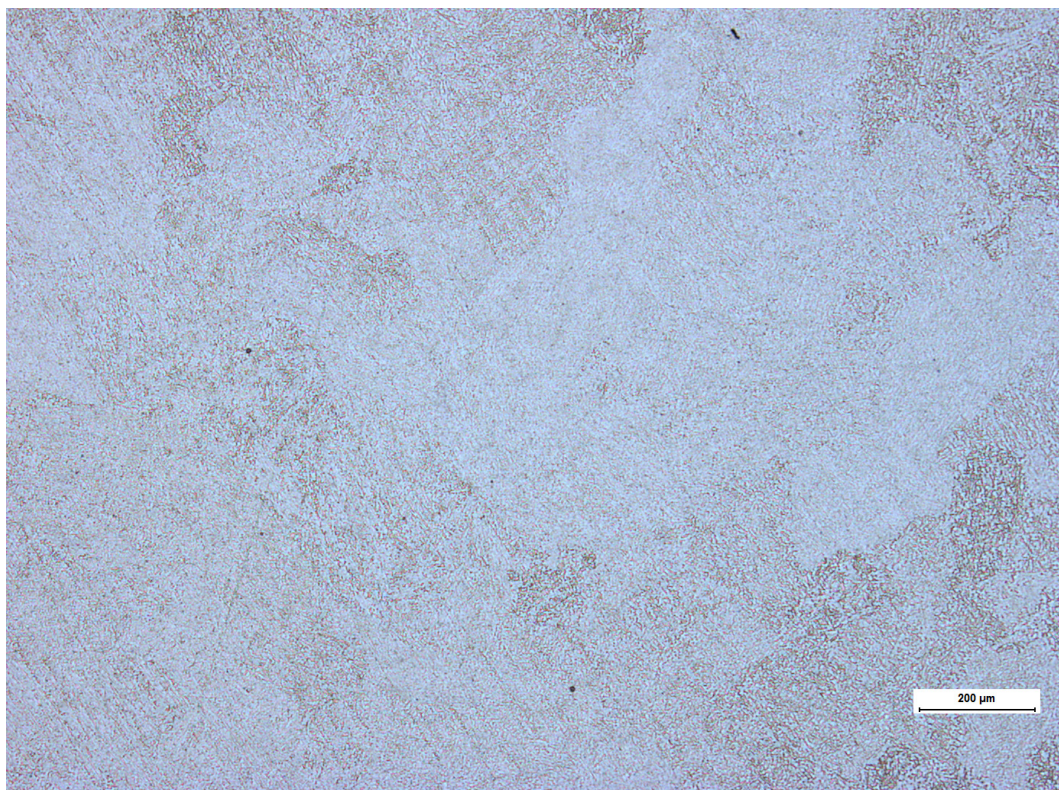


Figure 11 INSP-5-3 Middle of gauge length.50x.

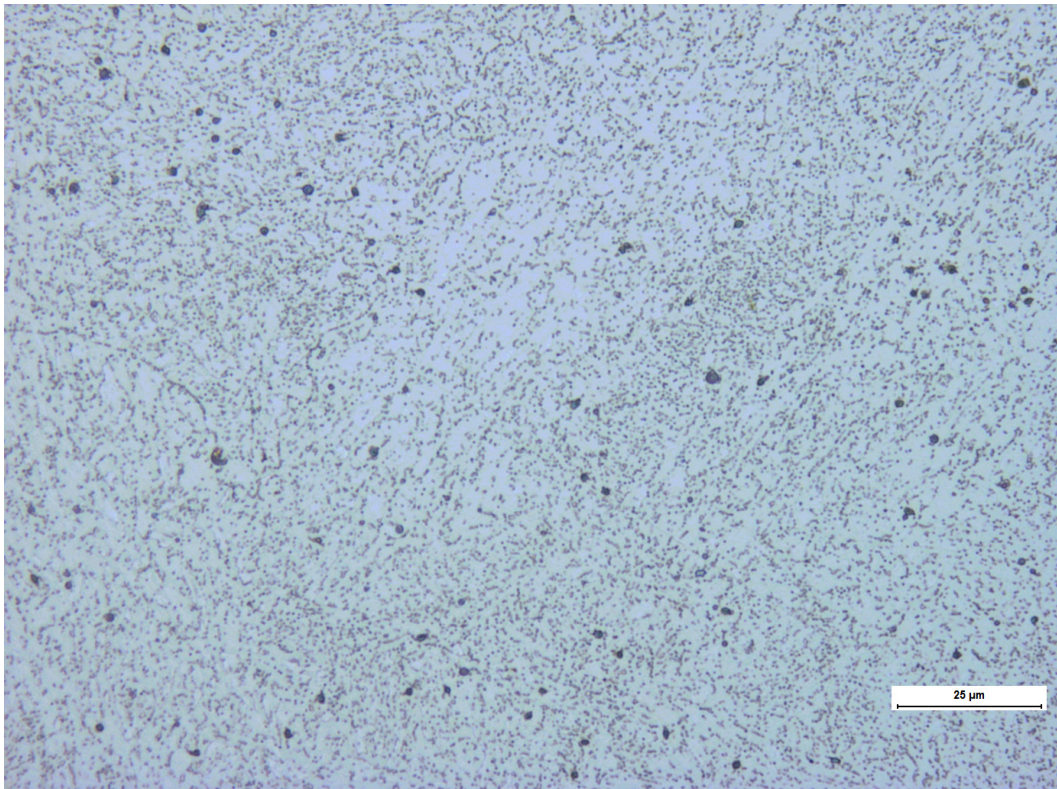


Figure 12 INSP-5-3 Middle of gauge length. Separate cavities class 2b. 500x.

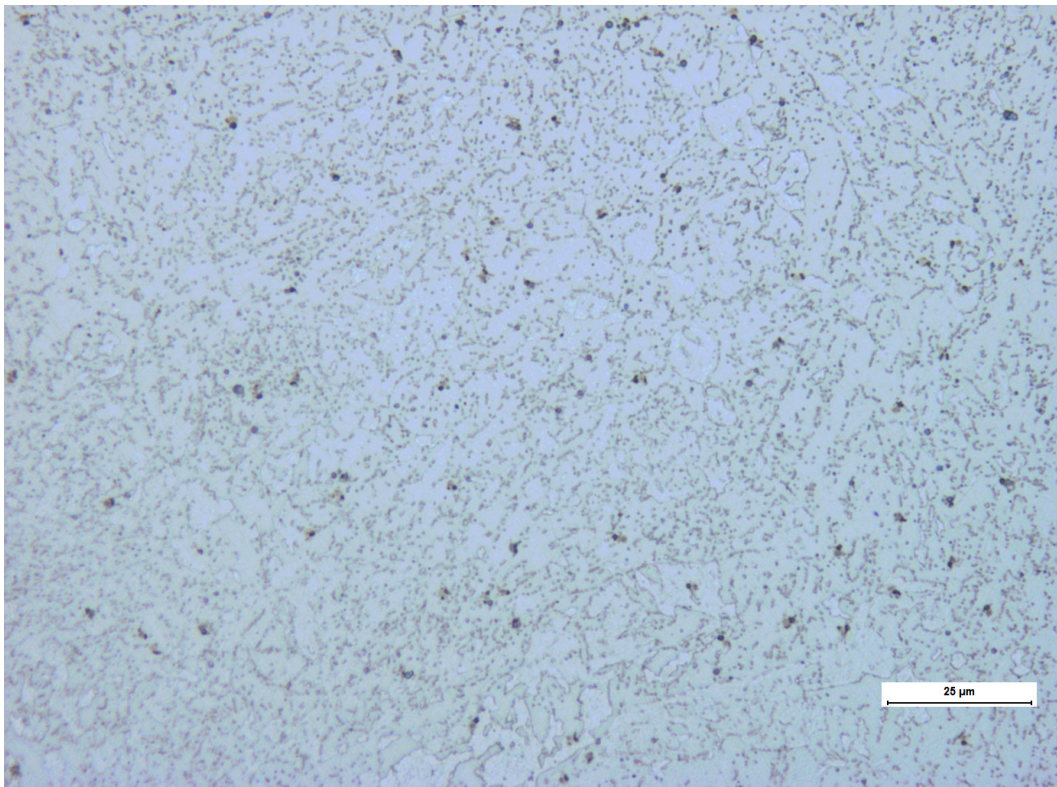


Figure 13 INSP-5-3 untested weld metal. Separate cavities class 2b. 500x.

VERIFICATION OF CREEP ANALYSES OF A STEAM PIPE SYSTEM

Här redovisas resultat från ett arbete som är ett fortsättningsprojekt av två tidigare studier kring livslängdsbedömning av ångledningssystem genom provning och analys.

Arbetet har gått ut på att verifiera provnings- och analysresultaten genom jämförelser med hur krypskador fördelat sig i komponenter som tagits ut från det analyserade systemet. För detta modellerades och analyserades hela ångsystemet i Heleneholmsverket.

En av slutsatserna från arbetet är att det är viktigt att inkludera primärkryp i en beräkningsmodell för livslängdsbedömning.

Energiforsk is the Swedish Energy Research Centre – an industrially owned body dedicated to meeting the common energy challenges faced by industries, authorities and society. Our vision is to be hub of Swedish energy research and our mission is to make the world of energy smarter!